

issn 2625-8129

An open-access journal by
the German Quaternary Association
Editor-in-chief: Henrik Rother



Vol. 5, 2024

DEUQUA Special Publications

Quaternary landscape dynamics in the Eastern Alps: from the highest peaks to the northern foreland basin – a guidebook to field trips

Guest editor: Bernhard Salcher



DEUQUA Special Publications

An open-access journal of the German Quaternary Association

Die Deutsche Quartärvereinigung [DEUQUA] e.V. ist ein Zusammenschluss deutschsprachiger Quartärwissenschaftler. Der Verein hat zum Ziel die Quartärwissenschaft zu fördern, sie in der Öffentlichkeit zu vertreten, den Kontakt zu angewandter Wissenschaft zu intensivieren sowie öffentliche und politische Gremien in quartärwissenschaftlichen Fragestellungen zu beraten. Desweiteren hat der Verein sich zur Aufgabe gemacht, die Kontaktpflege der Quartärforscher untereinander und zu verwandten Organisationen im In- und Ausland zu betreiben.

The German Quaternary Association [Deutsche Quartärvereinigung, DEUQUA e.V.] is the official union of German-speaking Quaternary scientists. The aim of the association is to support Quaternary science, to present it to the public, to intensify contacts to the applied sciences, and to provide advice to public and political authorities on issues related to Quaternary science. Furthermore, the association supports networking among Quaternary scientists and neighbouring disciplines at home and abroad.



Copernicus Publications
Bahnhofsallee 1e
37081 Göttingen
Germany

Phone: +49 551 90 03 39 0
Fax: +49 551 90 03 39 70

publications@copernicus.org
<http://publications.copernicus.org>



Printed in Germany.
Schaltungsdienst Lange o.H.G.

ISSN 2625-8129

Published by Copernicus GmbH [Copernicus Publications] on behalf of the German Quaternary Association [DEUQUA].



All DEUQUASP articles have been distributed under the Creative Commons Attribution 4.0 International License.

Image credits:

Top: Ibmer Moor peat bog north of Salzburg. Berchtesgaden Alps [Watzmann] in the background [Photo: B. Salcher]
Bottom left: Kitzsteinhorn, Hohe Tauern [Photo: I. Hartmeyer]
Bottom center: Loess-Paleosol outcrop near Göttweig/Danube [Photo: T. Sprafke]
Bottom right: Hoher Sonnblick, Hohe Tauern [Photo: J. Reitner]

<https://www.deuqua-special-publications.net>



Preface: Quaternary landscape dynamics in the Eastern Alps, from the highest peaks to the North Alpine Foreland – a guidebook to field trips

Bernhard Salcher

Department of Environment and Biodiversity, University of Salzburg, Salzburg, Austria

Correspondence: Bernhard Salcher (bernhard.salcher@plus.ac.at)

Relevant dates: Published: 9 September 2024

How to cite: Salcher, B.: Preface: Quaternary landscape dynamics in the Eastern Alps, from the highest peaks to the North Alpine Foreland – a guidebook to field trips, DEUQUA Spec. Pub., 5, 1–2, <https://doi.org/10.5194/deuquasp-5-1-2024>, 2024.

This volume has been compiled as a field companion to four Quaternary excursions offered at the Pangeo-DEUQUA 2024 conference held in Salzburg, Austria, from 23 to 27 September 2024 (Fig. 1). The conference motto is “converging disciplines”, and it is the first joint meeting of the Austrian Geological Society (ÖGG, Österreichische Geologische Gesellschaft) and the German Quaternary Association (DEUQUA, Deutsche Quartärvereinigung). The conference is hosted by the Geology Group, Department of Environment and Biodiversity at the Faculty of Natural and Life Sciences, Paris Lodron University of Salzburg. The city of Salzburg, located at the transition between the North Alpine Foreland (Molasse) basin and the high Alps, is a great starting point not only for classic geological excursions but also to explore a variety of Quaternary environments. The Quaternary excursions at Pangeo-DEUQUA 2024 visit a range of sites from high in the Alps to the perialpine lowlands, with a focus on key surface processes linked to the climatic extremes during the Quaternary, including the massive impact of anthropogenically induced climate change.

The contribution by Hartmeyer and Otto (2024, Fig. 1A) introduces the open-air lab at Kitzsteinhorn, Hohe Tauern range (Salzburg), and presents high-resolution data, which show the significant consequences of human-induced climate warming on glaciation, permafrost degradation and rock slope stability in the high Alps. The contribution by Reit-

ner and Steinbichler (2024, Fig. 1B) focuses on the deglaciation history and related processes in the Alps after the Last Glacial Maximum (LGM). The setting of this excursion to the Hüttwinkl Valley (upper part of the Rauris Valley), also in the Hohe Tauern, Salzburg, offers a unique sedimentary and morphological archive for determining the relative chronology of glacial, gravitational and fluvial processes. Salcher et al. (2024, Fig. 1C) present evidence on the erosional and depositional dynamics of a major piedmont glacier. The particularly well preserved landforms in the North Alpine Foreland record three glacial maxima that allow clear insights into the processes associated with periods of ice buildup to ice wastage as well as postglacial landscape evolution. The contribution by Sprafke et al. (2024, Fig. 1D) is dedicated to the famous loess–paleosol sequences around Krems at the Danube, Wachau region. These authors present recent paleoenvironmental data from key outcrops at sites at Paudorf, Göttweig and Krems (Schießstätte) which track the development of the regional climate back into the Early Pleistocene.

I thank all the authors for their informative and relevant contributions to this guidebook.

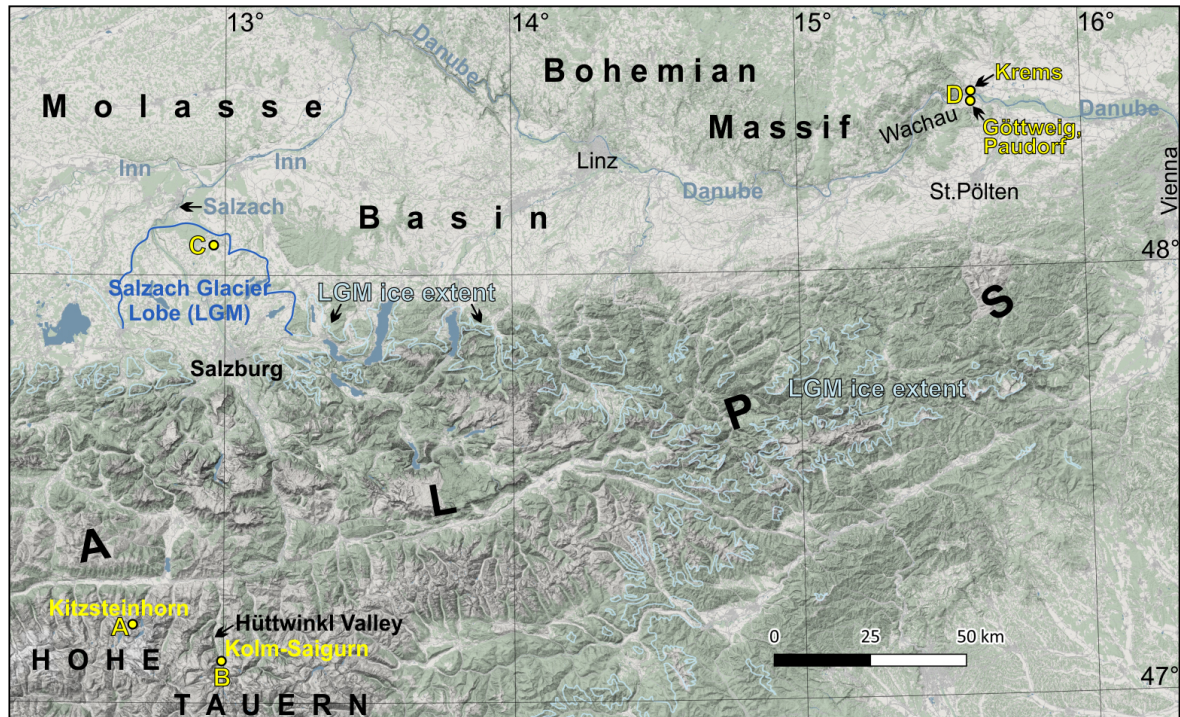


Figure 1. Quaternary excursions offered at Pangeo-DEUQUA 2024. (A) Kitzsteinhorn: Open-Air Lab (Hartmeyer and Otto, 2024, 23 September 2024), (B) Kolm-Saigurn: deglaciation history and mass movements since the LGM (Reitner and Steinbichler, 2024, 23 September 2024). (C) Salzach Glacier: dynamics of a major glacier lobe (Salcher et al., 2024, 26 September 2024). (D) Loess–paleosol sequences around Krens (Sprafke et al., 2024, 27 September 2024). Map data derived from <http://geoland.at> (last access: 4 June 2024; hillshade) and from ESA (EOX terrain layer, © ESA). LGM ice extent adapted from van Husen (1987).

Disclaimer. Publisher’s note: Copernicus Publications remains neutral with regard to jurisdictional claims made in the text, published maps, institutional affiliations, or any other geographical representation in this paper. While Copernicus Publications makes every effort to include appropriate place names, the final responsibility lies with the authors.

References

- Hartmeyer, I. and Otto, J.-C.: Rockfall, glacier recession and permafrost degradation: Long-term monitoring of climate change impacts at the Open-Air-Lab Kitzsteinhorn, Hohe Tauern, DEUQUA Spec. Pub., this volume, 2024.
- Reitner, J. M. and Steinbichler, M.: Glaciers and mass movements in the Hüttwinkl Valley (Hohe Tauern range): from the LGM until now, DEUQUA Spec. Pub., this volume, 2024.
- Salcher, B., Starnberger, R., Pollhammer, T., and Götz, J.: Sediment dynamics of a major piedmont glacier: the Salzach Glacier in the North Alpine Foreland, DEUQUA Spec. Pub., this volume, 2024.
- Sprafke, T., Peticzka, R., Thiel, C., and Terhorst, B.: Brunhes to burials – Loess region Krens, Lower Austria, DEUQUA Spec. Pub., this volume, 2024.
- van Husen, D.: Die Ostalpen in den Eiszeiten, Veröffentlichungen der Geologischen Bundesanstalt, Vienna, 2, 1–24, ISBN 3900312583, 1987.



Rockfall, glacier recession, and permafrost degradation: long-term monitoring of climate change impacts at the Open-Air-Lab Kitzsteinhorn, Hohe Tauern

Ingo Hartmeyer¹ and Jan-Christoph Otto²

¹GEORESEARCH Forschungsgesellschaft mbH, Wissenspark Salzburg-Urstein, Urstein 15, 5412 Puch bei Hallein, Austria

²Department of Environment and Biodiversity, Paris Lodron Universität Salzburg, Hellbrunnerstraße 34, 5020 Salzburg, Austria

Correspondence: Jan-Christoph Otto (jan-christoph.otto@plus.ac.at)

Relevant dates: Published: 9 September 2024

How to cite: Hartmeyer, I. and Otto, J.-C.: Rockfall, glacier recession, and permafrost degradation: long-term monitoring of climate change impacts at the Open-Air-Lab Kitzsteinhorn, Hohe Tauern, DEUQUA Spec. Pub., 5, 3–12, <https://doi.org/10.5194/deuquasp-5-3-2024>, 2024.

Abstract: Since 2010, comprehensive geoscientific monitoring has been established in the summit region of the Kitzsteinhorn (“Open-Air-Lab Kitzsteinhorn”), which focuses on the investigation of high-alpine climate change impacts in four monitoring domains: air temperature, glaciation, permafrost, and rock stability. Air and near-surface permafrost temperatures are currently rising with mean rates of almost $+0.1\text{ °C yr}^{-1}$. The thickness of the local cirque glacier is decreasing by more than 1 m yr^{-1} . Rockwall monitoring demonstrates that rockfall activity in freshly deglaciated rockwall sections has increased by 1 order of magnitude. The intensity of the observed processes is most likely unprecedented in recent human history. This emphasizes the importance of long-term monitoring efforts such as those carried out at the Kitzsteinhorn for improved geophysical understanding and for safe and sustainable infrastructure operation in high-alpine environments.

1 Introduction

Research activities in the summit region of the Kitzsteinhorn are driven by the particularly rapid progression of climate change in mountainous regions and its severe impact on geomorphic processes, natural hazard occurrence, and alpine infrastructure safety (Duvillard et al., 2021). In the past century alone, the average temperature in the Alpine region has increased by around 2 °C , which is twice as much as the global average increase during the same time period (Begert and Frei, 2018; Kotlarski et al., 2023).

Glacier recession represents the most visible consequence of this significant warming trend (WGMS, 2023). Less ob-

vious changes such as permafrost degradation (warming–thawing of permanently frozen ground) are more difficult to identify but have potentially serious consequences. A reduction in rock and slope stability, local subsidence, and increased rockfall activity are among the direct consequences of permafrost degradation (Gruber and Haeberli, 2007; Krautblatter et al., 2013).

However, due to buffering effects, the consequences of climate warming are often not immediately visible but rather emerge after significant lag times spanning years or even decades. Systemic long-term monitoring of the underlying processes, such as that conducted at the Kitzsteinhorn in the sense of an “open-air laboratory”, is therefore crucial for

a robust, quantitative understanding of high-alpine climate change and its impacts and for estimating future changes.

Since 2010, comprehensive geoscientific monitoring has been established in the summit region of the Kitzsteinhorn, studying the surface, subsurface, and atmosphere. Here we present excerpts of research findings, which center around the question of how glacier retreat and permafrost degradation alter rock stability and impact infrastructure safety. Results are summarized in four sections: air temperature (Sect. 3.1), glaciation (Sect. 3.2), permafrost (Sect. 3.3), and rock stability (Sect. 3.4).

2 Study area

The Kitzsteinhorn (3203 m a.s.l.) is located in the Hohe Tauern range, Salzburg, Austria (Fig. 1). Its summit pyramid belongs to the Bündner schist formation (Glockner Nappe) and is primarily composed of calcareous mica schist, with other rocks such as prasinite, amphibolite, phyllite, marble, and serpentinite also present to a lesser extent (Cornelius and Clar, 1935; Hoeck et al., 1994). Due to its high elevation (existence of glaciers and permafrost), distinct topography (isolated summit pyramid), and easy accessibility (cable car), the Kitzsteinhorn is exceptionally well suited for the long-term monitoring of high-alpine climate change impacts.

In addition to its excellent natural and infrastructural suitability, the Kitzsteinhorn represents one of the most diverse mountains in the entire Alps. It hosts Austria's oldest glacier ski area and has evolved into one of the countries most visited high-alpine tourist destinations, attracting around 1 million visitors per year. At the same time, large parts of the mountain are under strict nature protection (Nationalpark Hohe Tauern), while other parts are used for energy production by the Kaprun hydropower plant group. The coexistence of tourism, nature conservation, and energy production highlights the significant socio-economic and cultural impact of the Kitzsteinhorn and underscores the relevance of the research conducted here.

Systemic long-term observations in the Kitzsteinhorn summit region were initiated in 2010. Since then, unique and constantly expanding high-alpine research infrastructure has been established, aiming to identify and quantify changes related to climate warming. By combining atmospheric, surface, and subsurface measurements, slope stability-relevant variables are directly observed to identify potentially critical threshold values. Observation of rock instability can thus be directly related to the rapid warming of high-alpine environments. The high density of sensors and measuring instruments contributes to the laboratory character of the study site, and approaches include, among others, (i) borehole (30 m deep) temperature measurements, (ii) electrical resistivity surveys to capture ground thermal conditions, (iii) terrestrial laser scanning to quantify rockfall activity, (iv) UAV (unoccupied aerial vehicle) photogrammetry, (v) ground-

penetrating radar to document glacier retreat, (vi) geotechnical monitoring to register bedrock deformation (inclinometers, crackmeters, anchor load plates), and (vii) automatic weather stations to record atmospheric boundary conditions.

To increase the visibility of the research activities carried out at the Kitzsteinhorn, the Open-Air-Lab Kitzsteinhorn is associated with renowned national and international research networks and databases such as GTN-P (Global Terrestrial Network for Permafrost), VAO (Virtual Alpine Observatory), TUM-ALPHA (Research Center and Early Warning System for Alpine Natural Hazards), CCCA (Climate Change Centre Austria), and KryoMon.AT (Kryosphären Monitoring Österreich, translated as Cryospheric Monitoring Austria).

3 Monitoring results

3.1 Air temperature

Air temperature is recorded at three automatic weather stations located in the immediate vicinity (Fig. 2): (i) “Alpincenter” (2450 m a.s.l., 2.2 km N of the summit), (ii) “Kammerscharte” (2595 m a.s.l., 1.8 km NE of the summit), and (iii) “Gletscherplateau” (2920 m a.s.l., 0.6 km W of the summit). Temperature measurements started in 2008 at Alpincenter and in 2009 at Kammerscharte and Gletscherplateau.

The past year, 2023, was the hottest year on record at Gletscherplateau and the second-hottest year at Alpincenter and Kammerscharte. The annual average temperature was 0.7 °C above the recorded average since measurements began at Alpincenter (since 2008) and Kammerscharte (since 2009) and 0.9 °C above the average at Gletscherplateau (since 2009). Trend analyses for the period 2008/2009–2023 show a significant warming trend of +0.08 °C yr⁻¹ (+0.8 °C per decade) at all three Kitzsteinhorn weather stations. A comparison with the high-alpine reference weather station at “Sonnblick” (3106 m a.s.l.), located 25.7 km from the Kitzsteinhorn, shows a similar trend (+0.06 °C yr⁻¹) (GeoSphere Austria, 2024).

Long-term analyses dating back to 1887 with data from Sonnblick demonstrate a distinct acceleration in warming over the last few decades (Fig. 3). While warming from 1887–1980 was just +0.01 °C yr⁻¹, it was +0.04 °C yr⁻¹ in the period 1981–2023 and +0.06 °C yr⁻¹ in the period 2001–2023. These findings are in line with numerous other observations from the Alpine region, which have found significantly accelerated warming since the 1980s (European Environment Agency, 2009; Philipona, 2013).

3.2 Glaciation

Since 2016, the local cirque glaciers (Schmiedingerkees and Kammerkees) have been studied based on a total of 25 UAV (unoccupied aerial vehicle) surveys. As part of the surveys, the terrain surface was captured photogrammetrically and georeferenced using permanent ground control points.



Figure 1. (a) The summit pyramid of the Kitzsteinhorn hosts the long-term monitoring project “Open-Air-Lab Kitzsteinhorn”, which investigates the impacts of climate warming (e.g., permafrost degradation, glacier retreat) and their effect on rock stability. K, Kitzsteinhorn (3203 m a.s.l.); C, cable car top station (3030 m a.s.l.); S, Schmiedingerkees glacier; M, Maurerkees glacier; B, permafrost borehole; G, Großglockner (3797 m a.s.l.). (b) Location of the study site.

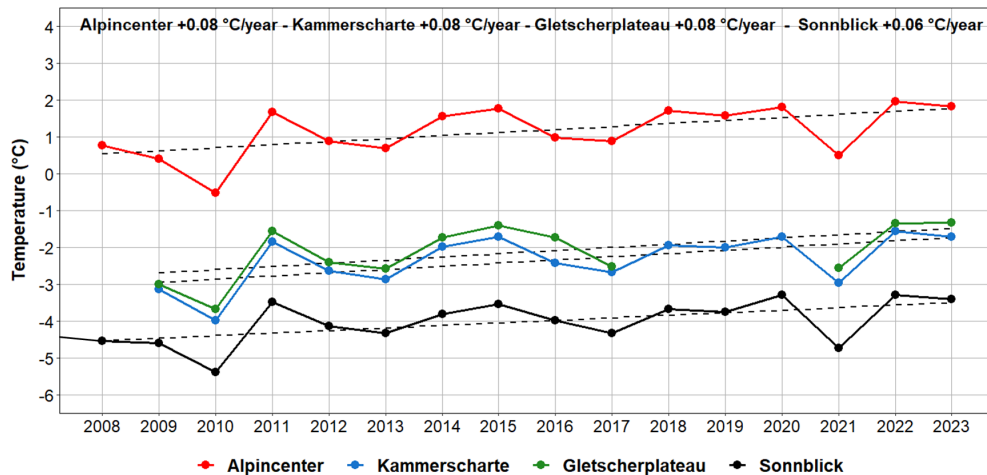


Figure 2. Mean annual air temperature and derived temperature trends for 2008–2023.

The subsequent analysis of overlapping image areas (“structure from motion”) allows the creation of high-resolution 3D point clouds and the reconstruction of area and volume changes to the glacier. The total area surveyed by UAV photogrammetry is approximately 6 km², and the ground sampling distance equals around 10 cm. Glacier changes before 2016 were assessed based on data available in historical databases (Fischer et al., 2015).

Between 1953 (first aerial survey) and 2023, the studied glacier area decreased from 2.17 to 0.71 km² (−1.46 km²) (Fig. 4). The glaciated area has therefore shrunk by

around 67% over the past 70 years. The greatest area loss (since 1953) was recorded in the Schmiedingerkees East section (−80%), followed by Schmiedingerkees West (−71%), Schmiedingerkees Central (−55%), and Kammerkees (−44%). High losses in the Schmiedingerkees East section are most likely related to the heterogeneous relief of the glacier forefield, which favors the formation of small glacier tongues prone to strong ablation. Extremely hot summers, such as the summer of 2022, had a significant impact on the recession of the studied glaciers. Between the UAV summer surveys of 2021 and 2022 alone, the glaciated area decreased

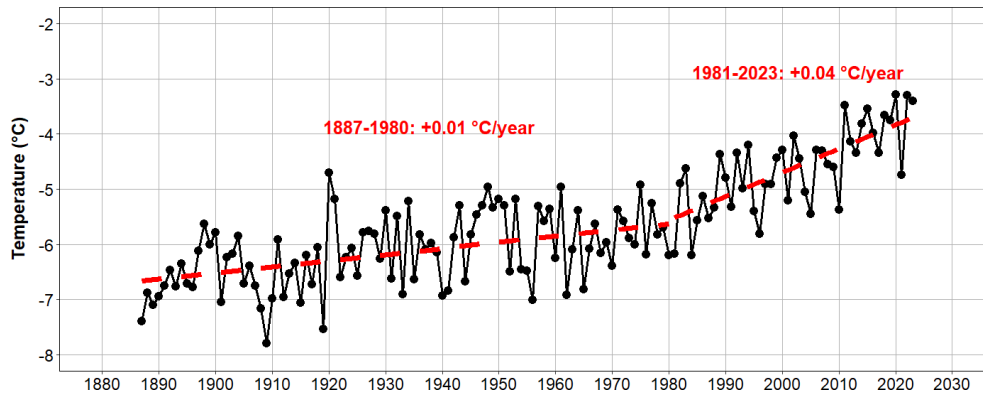


Figure 3. Long-term temperature increase (1887–2023) at weather station Sonnblick (3106 m a.s.l.), located 25 km from the Open-Air-Lab Kitzsteinhorn (data source: GeoSphere Austria, 2024).

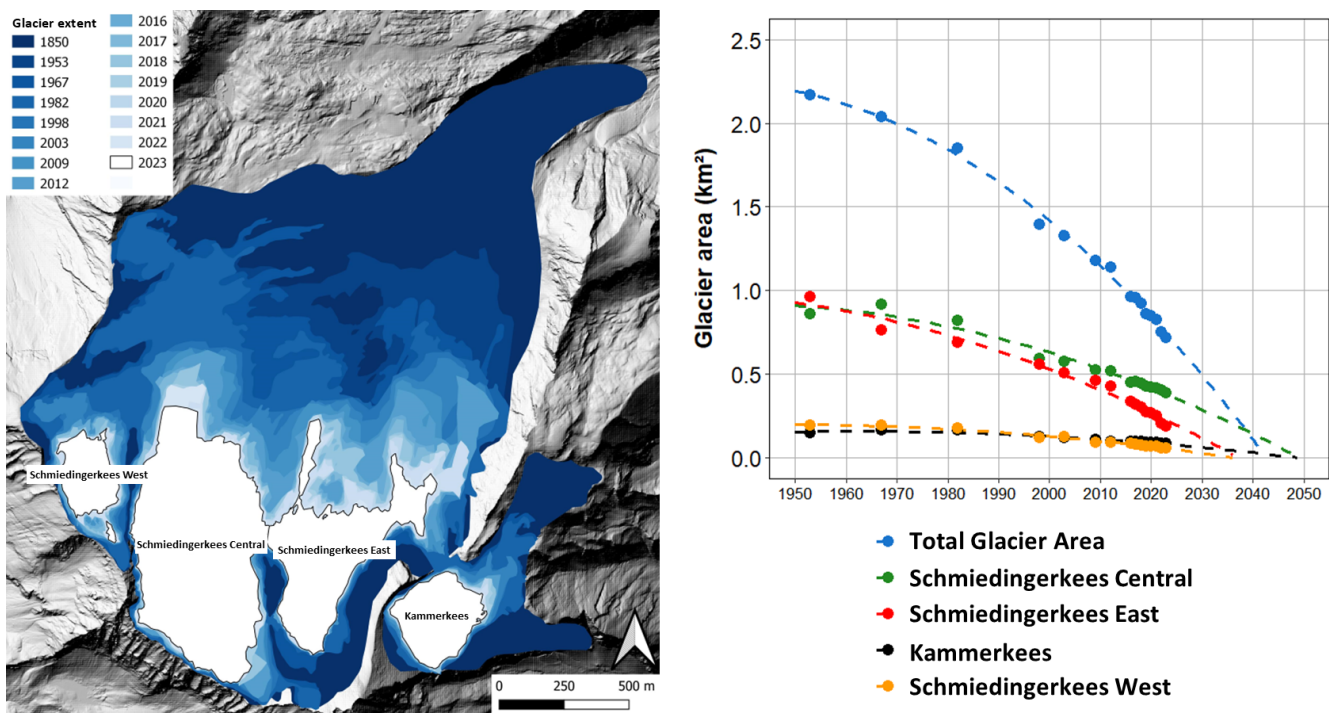


Figure 4. Loss of glacier area since 1850 at the Kitzsteinhorn (Schmedingerkees and Kammerkees) (1850 glacier extent from Fischer et al., 2015).

by over 9 %. This was the largest measured or reconstructed area loss within a single year since records began in 1953.

In accordance with the temperature measurements, the long-term glacier loss does not follow a linear trend but shows a clear acceleration (Fig. 4). In the last 14 years alone (2009–2023), the glacier area decreased by 37 %. Extrapolation of the area loss from the past 70 years to the future suggests that the investigated glacier could disappear in the 2040s. This trend might, however, slow down as the glacier retreats into shaded areas.

Combined analyses of airborne lidar data (2008), photogrammetry surveys (2016), and GPR (ground-penetrating

radar) ice thickness measurements (2016) demonstrate a glacier volume of $29.7 \times 10^6 \text{ m}^3$ for the Schmedingerkees Central and Schmedingerkees East sections for 2008. The most recent survey in September 2023 delivered a glacier volume of only $16.0 \times 10^6 \text{ m}^3$, representing a decrease of $13.7 \times 10^6 \text{ m}^3$ in the last 15 years, which equals a loss of 46.1 %. From 2008–2023 the average thickness of the investigated glacier areas decreased by 1.1 m yr^{-1} (Fig. 5).

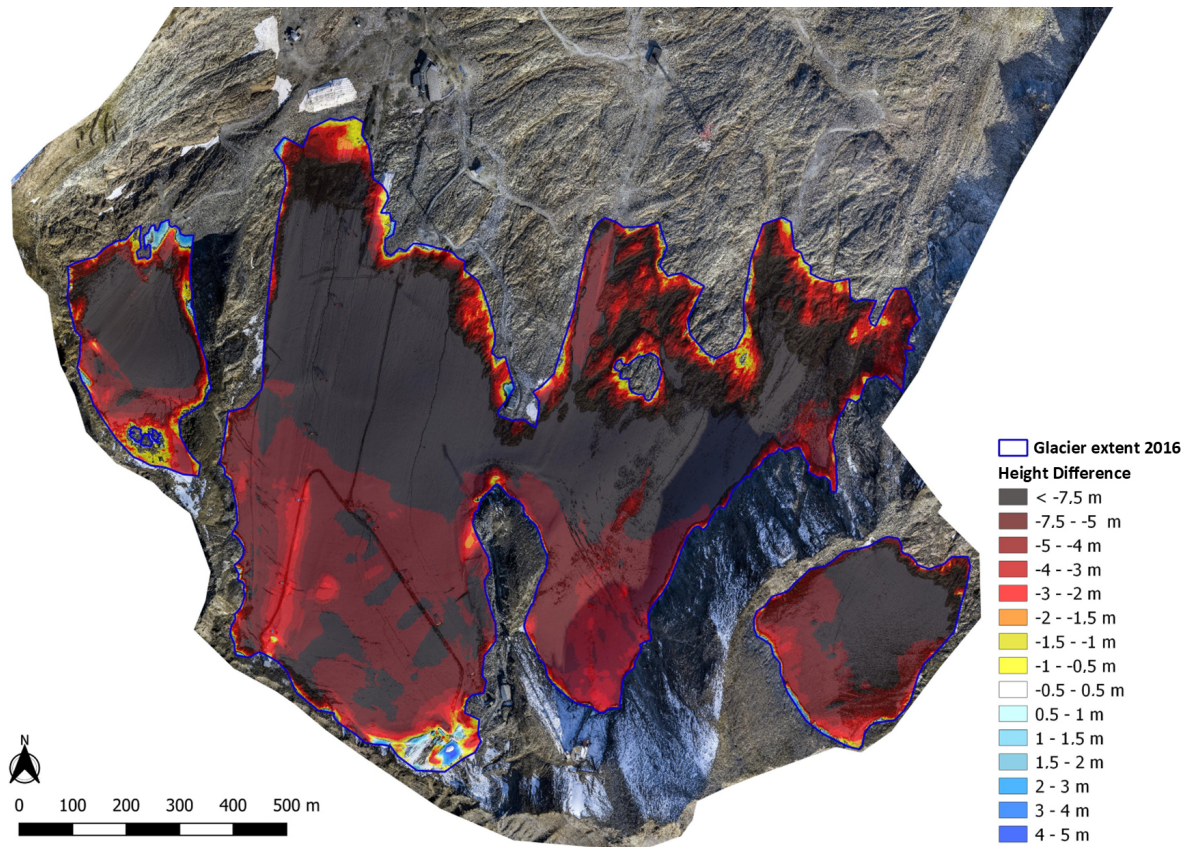


Figure 5. Total surface lowering of the cirque glaciers at the Kitzsteinhorn between 2016 and 2023.

3.3 Permafrost

In Austria, direct permafrost temperature measurements, i.e., measurements in deep boreholes, are restricted to two sites – Hoher Sonnblick and the Kitzsteinhorn. This scarcity of sites with direct measurements underlines the importance of the data acquired at Sonnblick and the Kitzsteinhorn for the understanding of current and future permafrost evolution in Austria and the Eastern Alps. At the Open-Air-Lab Kitzsteinhorn, seven deep boreholes collect data on permafrost temperatures at different depths. In this contribution, we focus on the longest time series available at the Kitzsteinhorn, recorded at borehole B2, located around 50 m below the cable car top station. The 30 m deep borehole B2 was drilled perpendicular to the north-facing rock slope, which has a mean gradient of about 45°. Borehole B2 is considered to be undisturbed by anthropogenic impacts such as the cable car top station. Temperature measurement inside the borehole is carried out with high-quality thermistors with an accuracy of ± 0.03 °C (Platinum Resistance Temperature Detector L220, 1/10 B, Heraeus Sensor Technology®) at 12 depths (0.1, 0.5, 1, 2, 3, 5, 7, 10, 15, 20, 25, 30 m). Inside the borehole, the thermistors are mechanically coupled to brass segments which are integrated into the PVC casing that protects the borehole from water entry. Due to the high thermal

conductivity of the brass segments ($\sim 110 \text{ W m}^{-1} \text{ K}^{-1}$), this specifically designed solution enables excellent thermal coupling between the temperature sensors and the surrounding bedrock, allowing reliable measurements of small temperature changes.

The temperature record from borehole B2 covers 8 full years (2016–2023). Ground thermal conditions of the near-surface regions are characterized by strong diurnal and seasonal fluctuations related to atmospheric temperature changes. With increasing depth, fluctuations are damped, indicating a reduced impact of external conditions on the ground temperature. At 15 m depth, ground temperature varies by just a few tens of a degree over a year. The depth of zero annual amplitude, which represents the depth at which seasonal fluctuations can no longer be observed, is situated at around 20 m. Slow, conduction-dominated heat propagation leads to significant lag times between ground surface warming and cooling and changes at depth. Temperature variations take around half a year to arrive at a depth of 10 m (PERMOS, 2023).

In the summer season, the uppermost layer of the subsurface thaws. This so-called active layer is usually initiated in June and reaches its maximum thickness between the end of August and mid-September. Subsequent seasonal cooling

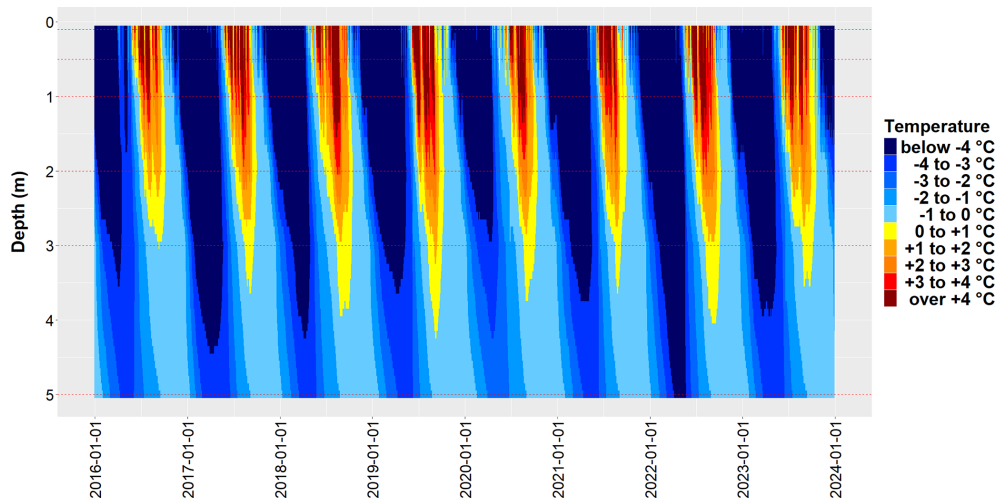


Figure 6. The 8-year bedrock temperature record measured at permafrost borehole B2 within the first 5 m (2016–2023). Meter indications refer to the maximum thickness of the permafrost active layer in each summer. Sensor depths are indicated by dotted red lines. Linear interpolation at 0.1 m depth increments was used to model ground temperature between sensors.

then leads to a complete refreezing of the active layer, which usually takes about 1 month and is completed in October. The multi-year (2016–2023) active layer evolution is illustrated in Fig. 6. From 2016–2019 a growth trend was observed for four consecutive summers. In the summer of 2019, the active layer thickness reached its highest value (4.2 m) of the entire observation period. In the two following summer periods (2020, 2021), the active layer thickness reached 3.7 and 3.6 m, respectively. During the extremely hot summer of 2022, the active layer thickness reached “only” 4.0 m. This is most likely related to the cold preceding winter period. Significant subsurface cooling could not be completely offset by the ensuing hot summer.

Regression analyses carried out for the full 8-year observation period (2016–2023) demonstrate a clear warming trend (Fig. 7). Warming is significantly more pronounced for near-surface regions (e.g., 2, 3 m) and is in agreement with recent air temperature rise (refer to Sect. 3.1). With increasing borehole depth, the observed warming trend is attenuated considerably to only a few hundredths of a degree per year (e.g., 15, 30 m). Ground temperature at large depth thus reacts with significant delay to atmospheric warming. These findings are consistent with previous modeling studies that found significant lag times between climate warming and thermal response at depth (e.g., Noetzi et al., 2007). Lag times have important implications for our understanding of the response time of temperature-induced destabilization at depth.

3.4 Rock stability

Rock stability at the Open-Air-Lab Kitzsteinhorn is monitored based on a combination of remote sensing techniques and in situ geotechnical monitoring. Here we present the re-

sults of a 12-year remote sensing survey and introduce the implemented geotechnical monitoring.

Since August 2011, four rock faces in the study area have been systematically examined annually using high-resolution terrestrial laser scanning to identify rockfall source areas (Hartmeyer et al., 2020a, b). Laser scanning is an active 3D imaging method well-suited to identifying surface change in steep bedrock. The studied rock faces comprise a surface area of around 230 000 m² and are located immediately adjacent to the Schmiedingerkees glacier.

Laser scanning of the four examined rockwalls (Fig. 8) is carried out during snow-free periods (end of August/beginning of September) at least once a year. The laser-scanning survey conducted at the Kitzsteinhorn is among the most extensive high-altitude rockfall monitoring campaigns in the world in terms of observation duration and level of detail, allowing precise quantification of rockfall activity following glacier retreat.

During the 12-year laser-scanning campaign (August 2011 to August 2023), 799 rockfall source areas (which are here referred to as “rockfalls” to improve readability) with a total volume of 3340 m³ were identified. The majority of the registered rockfalls had small volumes. Exactly 84 % of the identified events were smaller than 1 m³, and only six events (0.8 %) were larger than 100 m³. The largest event recorded had a volume of 879.4 m³. The magnitude–frequency distribution of the rockfalls identified at the Kitzsteinhorn follows a pronounced power law function over 4 orders of magnitude.

Rockfall activity was highest in the Kitzsteinhorn north face, where the terrain gradient follows cleavage dip (calcareous mica schist) and facilitates large dip-slope failures of cubic rock bodies. Rockfall activity in the Kitzsteinhorn north face (71.5 m³ ha⁻¹ yr⁻¹) was almost 6 times higher than the mean value over all sites (12.2 m³ ha⁻¹ yr⁻¹).

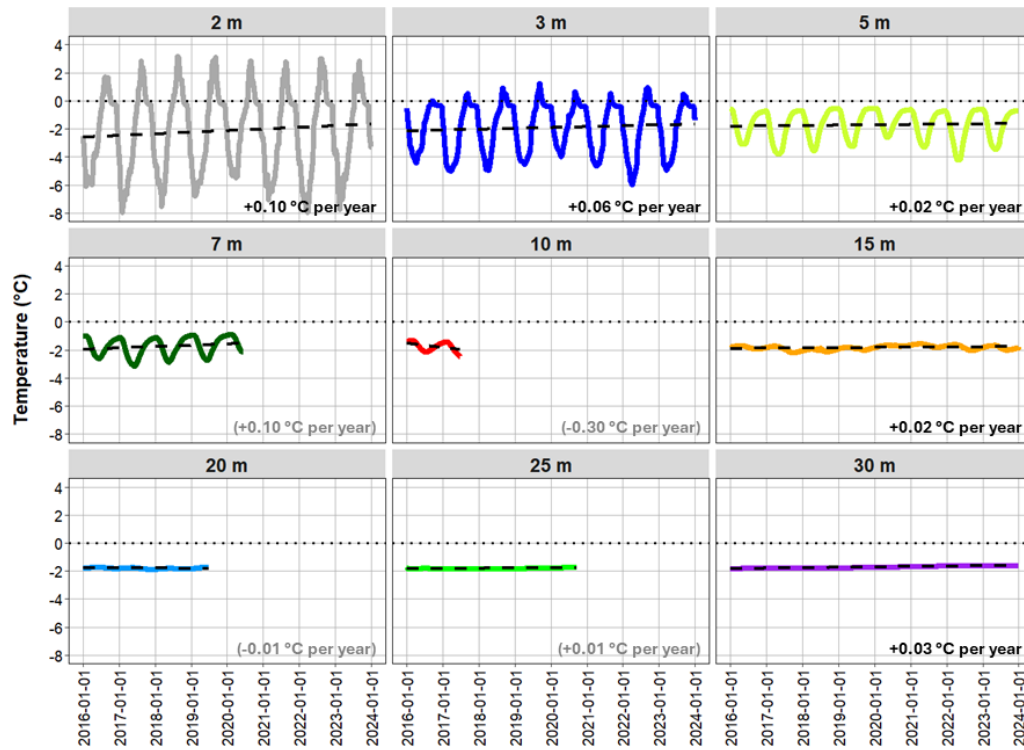


Figure 7. Temperature data and regression analysis for permafrost borehole B2 at different depths (2016–2023). Warming is evident for all (completely) recorded depths and is significantly more pronounced in near-surface regions. Permanent sensor failure occurred after lightning strikes at 7 m (14 June 2020), 10 m (24 June 2017), 20 m (1 July 2019), and 25 m (16 September 2020).



Figure 8. Rockwalls surveyed with terrestrial laser scanning at the Kitzsteinhorn (C, cable car top station).

A significant increase in rockfall activity close to the glacier surface (base of the rockwall) was observed for all the rockwalls studied (Fig. 9). More than 60 % of the total rockfall volume originated from source areas located less than 10 m above the current glacier surface. Rockfall activity in these “proximal” areas is 9.8 times higher than in areas located more than 10 m above the current glacier surface. The mean annual rockwall retreat rate equaled 5.36 mm yr^{-1} in

proximal regions and only 0.55 mm in distal regions located more than 10 m above the glacier.

The highly active rockwall areas near the glacier surface primarily involve regions that have been exposed in recent years or decades due to downwasting of the adjacent Schmiedingerkees glacier. Freshly exposed rock surfaces are therefore considered particularly unstable. The loss of glacial shielding leads to strong seasonal fluctuations in rock tem-

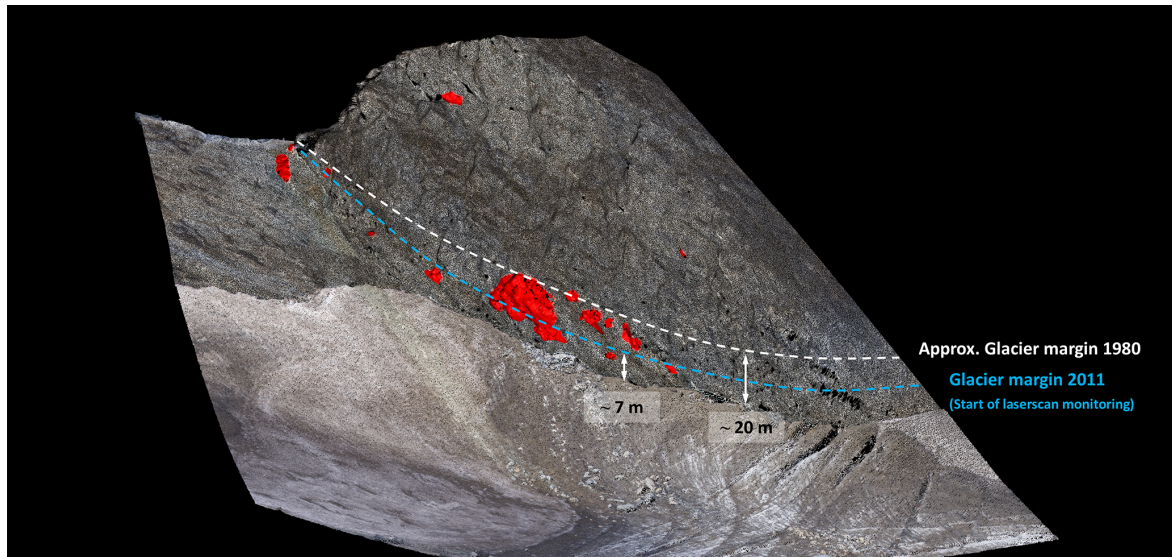


Figure 9. Rockfall source areas ($> 0.5 \text{ m}^3$) identified in the east face of the Magnetköpfel (2011–2023). For all rockwalls, significantly increased rockfall activity has been found in freshly deglaciated rockwall sections.

peratures, melting of ground ice, and increased water infiltration – resulting in massively increased destabilization.

To identify and study minimal ground movement (displacement, deformation), a complementary network of geotechnical monitoring devices has been established in the surroundings of the cable car top station, which consists of the following components: (i) deep borehole deformation measurements with two biaxial inclinometer chains, (ii) inclination measurements at four building foundations with triaxial tiltmeters, (iii) bedrock stress measurements at three rock anchor heads with hydraulic anchor load cells, (iv) cleft aperture measurements with four crackmeters, and (v) pore water pressure measurements with piezometers in three deep boreholes. All instruments are connected via a wireless sensor network (Fig. 10). Data are acquired every 60 min and then transmitted via a central gateway to a web application. Pre-defined alarms enable targeted and fully automatic notification (via email and SMS) in the event of threshold exceedance or data failure. Due to the hourly data collection, rapid information and warning for the recipients is ensured (near real time).

High precision of the measurement devices used enables the identification of movements in the sub-millimeter range, thus forming the basis for the early detection of stability-relevant changes. The integration of the measuring instruments within a wireless sensor network (communication via LoRa radio communication) reduces susceptibility to lightning strike damage and significantly contributes to the robustness and efficient maintainability of the system.

4 Highlights

- Air temperature monitoring at three local weather stations shows a considerable warming trend of $+0.08 \text{ }^\circ\text{C yr}^{-1}$ ($+0.8 \text{ }^\circ\text{C}$ per decade) over the last 15 years. Historical climate data from nearby weather stations (Hoher Sonnblick) demonstrate significantly accelerated warming since the 1980s.
- Over the last 70 years (1953–2023), the area of the Schmiedingerkees glacier has decreased from 2.17 to 0.71 km^2 (-67%). Area loss does not follow a linear trend but shows a clear acceleration. Extrapolation of the observed area loss suggests that the investigated glacier could disappear in the 2040s. UAV-based photogrammetry measurements show that the mean thickness of the Schmiedingerkees has reduced by more than 1 m yr^{-1} .
- Permafrost temperature measurement in a 30 m borehole (2016–2023) demonstrates a clear warming trend. Significant warming ($\sim +0.1 \text{ }^\circ\text{C}$) has been registered for near-surface regions (e.g., $2, 3 \text{ m}$), which is in agreement with recent air temperature rise. With increasing borehole depth, the observed warming trend is attenuated considerably to only a few hundredths of a degree per year (e.g., $15, 30 \text{ m}$). The maximum depth of the permafrost active layer varies around 4 m .
- Based on 12-year rockwall monitoring with terrestrial laser scanning (2011–2023), 799 rockfall source areas with a total volume of 3340 m^3 were identified. For all studied rockwalls, a significant intensification of rockfall activity was registered close to the glacier surface,

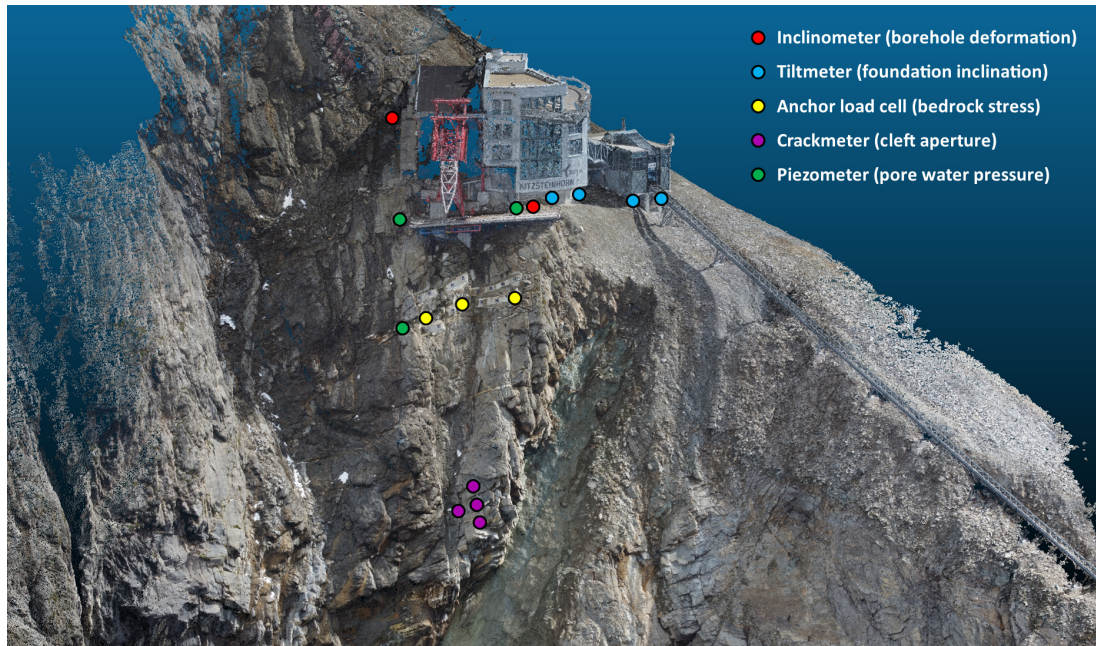


Figure 10. Geotechnical monitoring in the immediate vicinity of the cable car top station.

i.e., in freshly deglaciated rockwall sections. Rockfall activity in these proximal areas is ca. 10 times higher than in distal areas located more than 10 m above the current glacier surface (not or only marginally affected by current glacier retreat). Mean annual rockwall retreat equaled 5.36 mm yr^{-1} in proximal regions and only 0.55 mm in distal regions.

Data availability. All data sets are available upon request. Borehole temperature data are available via GTN-P (the Global Terrestrial Network for Permafrost) at <http://gtnpdatabase.org/boreholes/view/1120/> (Hartmeyer, 2024). Rockfall data (2011–2017) are available under the following DOI: <https://doi.org/10.14459/2020mp1540134> (Krautblatter, 2020).

Author contributions. IH: conceptualization, data curation, formal analysis, investigation, project administration, visualization, writing – original draft preparation. JCO: supervision, writing – review and editing.

Competing interests. The contact author has declared that neither of the authors has any competing interests.

Disclaimer. Publisher’s note: Copernicus Publications remains neutral with regard to jurisdictional claims made in the text, published maps, institutional affiliations, or any other geographical representation in this paper. While Copernicus Publications makes ev-

ery effort to include appropriate place names, the final responsibility lies with the authors.

Acknowledgements. We thank Bernhard Salcher for constructive comments on an earlier version of the paper. Funding and support by the Gletscherbahnen Kaprun AG are gratefully acknowledged.

Financial support. This research has been supported by the Gletscherbahnen Kaprun AG, the Austrian Research Promotion Agency (FFG), and the Austrian Academy of Sciences (ÖAW).

References

- Begert, M. and Frei, C.: Long-term area-mean temperature series for Switzerland – Combining homogenized station data and high resolution grid data, *Int. J. Climatol.*, 38, 2792–2807, <https://doi.org/10.1002/joc.5460>, 2018.
- Cornelius, H. and Clar, E.: Erläuterungen zur geologischen Karte des Glocknergebietes, Geologische Bundesanstalt, Vienna, 32 pp., 1935.
- Duvillard, P.-A., Ravel, L., Schoeneich, P., Deline, P., Marcer, M., and Magnin, F.: Qualitative risk assessment and strategies for infrastructure on permafrost in the French Alps, *Cold Reg. Sci. Technol.*, 189, 103311, <https://doi.org/10.1016/j.coldregions.2021.103311>, 2021.
- European Environment Agency: Regional climate change and adaptation: the Alps facing the challenge of changing water resources, Office for Official Publications of the European Communities, Luxembourg, <https://doi.org/10.2800/12552>, 2009.

- Fischer, A., Seiser, B., Stocker Waldhuber, M., Mitterer, C., and Abermann, J.: Tracing glacier changes in Austria from the Little Ice Age to the present using a lidar-based high-resolution glacier inventory in Austria, *The Cryosphere*, 9, 753–766, <https://doi.org/10.5194/tc-9-753-2015>, 2015.
- GeoSphere Austria: <https://data.hub.geosphere.at> (last access: 1 June 2024), 2024.
- Gruber, S. and Haeberli, W.: Permafrost in steep bedrock slopes and its temperature-related destabilization following climate change, *J. Geophys. Res.*, 112, F02S18, <https://doi.org/10.1029/2006JF000547>, 2007.
- Hartmeyer, I.: Kitzsteinhorn 2, GTN-P – Global Terrestrial Network for Permafrost [data set], <http://gtnpdatabase.org/boreholes/view/1120/>, last access: 6 August 2024.
- Hartmeyer, I., Delleske, R., Keuschnig, M., Krautblatter, M., Lang, A., Schrott, L., and Otto, J.-C.: Current glacier recession causes significant rockfall increase: the immediate paraglacial response of deglaciating cirque walls, *Earth Surf. Dynam.*, 8, 729–751, <https://doi.org/10.5194/esurf-8-729-2020>, 2020a.
- Hartmeyer, I., Keuschnig, M., Delleske, R., Krautblatter, M., Lang, A., Schrott, L., Prasicsek, G., and Otto, J.-C.: A 6-year lidar survey reveals enhanced rockwall retreat and modified rockfall magnitudes/frequencies in deglaciating cirques, *Earth Surf. Dynam.*, 8, 753–768, <https://doi.org/10.5194/esurf-8-753-2020>, 2020b.
- Hoeck, V., Pestal, G., Brandmaier, P., Clar, E., Cornelius, H., Frank, W., Matl, H., Neumayr, P., Petrakakis, K., Stadlmann, T., and Steyrer, H.: Geologische Karte der Republik Österreich, Blatt 153 Großglockner, Geologische Bundesanstalt, Vienna, <https://doi.org/10.24341/tethys.70>, 1994.
- Kotlarski, S., Gobiet, A., Morin, S., Olefs, M., Rajczak, J., and Samacoïts, R.: 21st Century alpine climate change, *Clim. Dynam.*, 60, 65–86, <https://doi.org/10.1007/s00382-022-06303-3>, 2023.
- Krautblatter, M.: Rockfall Source Areas, Kitzsteinhorn, Austria (2011–2017), TUM Technical University Munich [data set], <https://doi.org/10.14459/2020mp1540134>, 2020.
- Krautblatter, M., Funk, D., and Günzel, F. K.: Why permafrost rocks become unstable: a rock-ice-mechanical model in time and space, *Earth Surf. Proc. Land.*, 38, 876–887, <https://doi.org/10.1002/esp.3374>, 2013.
- Noetzli, J., Gruber, S., Kohl, T., Salzmann, N., and Haeberli, W.: Three-dimensional distribution and evolution of permafrost temperatures in idealized high-mountain topography, *J. Geophys. Res.*, 112, F02S13, <https://doi.org/10.1029/2006JF000545>, 2007.
- PERMOS: Swiss Permafrost Bulletin 2022, edited by: Noetzli, J. and Pellet, C., Swiss Permafrost Monitoring Network (PERMOS), No. 4, 23 pp., 2023.
- Philipona, R.: Greenhouse warming and solar brightening in and around the Alps, *Int. J. Climatol.*, 33, 1530–1537, <https://doi.org/10.1002/joc.3531>, 2013.
- WGMS: Global Glacier Change Bulletin No. 5 (2020–2021), edited by: Zemp, M., Gärtner-Roer, I., Nussbaumer, S. U., Welty, E. Z., Dussailant, I., and Bannwart, J., ISC(WDS)/IUGG(IACS)/UNEP/UNESCO/WMO, World Glacier Monitoring Service, Zurich, Switzerland, 134 pp., <https://doi.org/10.5904/wgms-fog-2023-09>, 2023.



Glaciers and mass movements in the Hüttwinkl Valley (Hohe Tauern range): from the Last Glacial Maximum (LGM) until now

Jürgen M. Reitner and Mathias Steinbichler

Department of Geological Mapping, GeoSphere Austria, 1190 Vienna, Austria

Correspondence: Jürgen M. Reitner (juergen.reitner@geosphere.at)

Relevant dates: Published: 9 September 2024

How to cite: Reitner, J. M. and Steinbichler, M.: Glaciers and mass movements in the Hüttwinkl Valley (Hohe Tauern range): from the Last Glacial Maximum (LGM) until now, *DEUQUA Spec. Pub.*, 5, 13–30, <https://doi.org/10.5194/deuquasp-5-13-2024>, 2024.

Abstract: The Hüttwinkl Valley, the uppermost section of the Rauris Valley, offers a unique sedimentary and morphological archive to study the development of the landscape in a high-Alpine valley since the Last Glacial Maximum (LGM). Glacial extents of the past, especially during the Younger Dryas (12.8–11.7 ka) and the Little Ice Age, as well as the present-day massive glacier retreat, are clearly recorded. On the other hand, the effects of different mass movements on valley development are evident. The field trip begins in Kolm-Saigurn, where the Durchgangswald landslide occurred in the Bølling–Allerød interstadial (14.7–12.9 ka). In the Younger Dryas (12.9–11.7 ka) glaciers overflowed parts of the Durchgangswald landslide deposit followed by the Lenzanger landslide (Preboreal, Early Holocene). North of Kolm-Saigurn, the Bucheben landslide (Early Holocene) and the Lechnerhäusel landslide (Middle Holocene) showed first a rockslide phase followed by a rock avalanche (sturzstrom), which led to the formation of toma in the distal area. All landslides detached from the western flank of the valley, whereas the eastern slopes are predominantly characterized by slow, deep-seated gravitational slope deformation (DSGSD). The most recent significant mass wasting was caused by rockfalls and catastrophic debris flows.

1 Introduction

The Hüttwinkl Valley, the upper part of the Rauris Valley, drained by the creek Hüttwinkl Ache, is one of the most outstanding valleys of the Eastern Alps regarding the impact of different types of mass movements on landscape development. In addition, moraines and glacially shaped landforms in the forefield of rapidly decaying glaciers result in a picturesque scenery. The aim of the field trip is to show this unique sedimentary and morphological archive and demonstrate how the chronology of the contributing glacial, gravitational and fluvial processes have been deciphered so far. We present partly preliminary research performed in the course

of the geological survey for the geological map sheet ÖK 154 Rauris.

This contribution provides a short overview of the morphological and geological setting (Sect. 2; Figs. 1, 2, 3), followed by a brief summary of the landscape development known so far with a special focus on mass movements and valley floor development (Sect. 3). A more detailed description of the sites will be given in the following chapters in order of their appearance during the field trip. It starts with the first location at Kolm-Saigurn (A in Figs. 1, 2; Sect. 4; Figs. 4, 5, 6, 7, 8) followed by the description of the landslides north of Bodenhaus (Sect. 5), including the Lechnerhäusel landslide (B in Figs. 1, 2; Figs. 9, 10) and the Bucheben

landslide (Figs. 11, 12). Finally, the various cases of deep-seated gravitational slope deformation (DSGSD; term used in the sense of Dramis and Sorriso-Valvo, 1994, and Agliardi et al., 2001) on the eastern valley flank, which are evident throughout the field trip, will be discussed in Sect. 6 (Fig. 12).

Last Glacial Maximum (LGM) is used in the sense of the Würmian Pleniglacial and covers the time span of 29 to ca. 19 ka (see Reitner, 2022; van Husen and Reitner, 2022, with further references). The subdivision of the Würmian or Alpine Lateglacial (ca. 19–11.7 ka) into glacial stadial follows the suggestion by Reitner et al. (2016). Holocene stages and subepochs are classified according to Walker et al. (2018).

2 General overview and geological setting

2.1 Topographical conditions and highlights

The catchment of the Hüttwinkl Valley (valley of the Hüttwinkl Ache creek) reaches from the highest and most prominent peaks (Hocharn 3254 m, Hoher Sonnblick 3106 m) to the confluence with the Seidlwinkl Ache at the village of Wörth (part of the community of Rauris) and thus to the onset of the Rauriser Ache creek (Figs. 1, 2, 3). The uppermost cirques of the catchment are still glaciated with the most prominent glaciers (called “Kees” in the local dialect) of Goldbergkees and Pilatuskees below the Hoher Sonnblick peak and Hocharnkees and Krumlkees below the Hocharn peak. The glaciological monitoring of the Goldbergkees started already in the year 1896 (Penck, 1897), which allowed us to document the effect of climate change on the glacier size in great detail since then (Böhm et al., 2007; Auer et al., 2010; Hansche et al., 2023)

Such an early scientific investigation was enabled by the last attempts of gold mining lasting some centuries (Gruber, 2004). In 1886, Ignaz Rojacher, the last gold mining entrepreneur and open-minded adventurer, constructed the, by that time, highest meteorological observatory on the summit of the Hoher Sonnblick (Böhm et al., 2011). This Sonnblick Observatory, now run by GeoSphere Austria, is an outstanding research infrastructure for studying high-atmospheric processes and climate change.

2.2 Geological framework

The Hüttwinkl Valley is located in the eastern part of the so-called “Tauern Window”. The Tauern Window exposes the lower-plate Penninic and Sub-Penninic superunits that were buried during the Alpine subduction and collision below the upper-plate Austroalpine Superunit (Schmid et al., 2004). With its size of 160 × 30 km, it is the biggest of the intra-Alpine tectonic windows. In addition to preserved thrust contacts, the limits of the Tauern Window are to the west and east the Brenner and Katschberg normal faults, to the north

the Salzachtal–Ennstal fault zone, and to the southeast the Mölltal fault zone. The northern part of the Hüttwinkl Valley is mainly built up by Penninic rocks and consists of Jurassic to Cretaceous oceanic meta-sediments as well as mafic and ultramafic rocks deriving from an oceanic lithosphere. The southern part of the Hüttwinkl Valley on the other hand consists of rocks of the Sub-Penninic Superunit and is built up by pre-Variscan crystalline complexes, Carboniferous orthogneiss and Carboniferous to Cretaceous meta-sediment formations (Pestal et al., 2005; Schuster et al., 2014). The lithological information is used to understand prominent landscape-forming events like the Durchgangswald landslide, as, e.g., the lithological succession of the scarp area of the landslide is preserved in the landslide deposits. Furthermore, the main glaciers of the Hüttwinkl Valley (Goldbergkees and Pilatuskees) are located more or less in areas where the border between the Penninic to Sub-Penninic superunits crops out. Hence, the finding of sub-rounded to rounded “Zentralgneis” (carboniferous orthogneiss; see Fig. 1) components in glacial sediments downstream of the bedrock is indicative of transport during Lateglacial and Holocene advances and retreats (Bichler et al., 2016; Pestal et al., 2005).

3 Landscape evolution of the Hüttwinkl Valley since the Last Glacial Maximum (LGM) and before

Descriptions and explanations of the landscape of the Hüttwinkl Valley in the context of bedrock geology, glacial shaping and mass movements have been provided by Hottinger (1935), Exner (1957) and von Poschinger (1986). Especially the pronounced valley asymmetry (see Fig. 2) consisting of a more gentle slope on the eastern flank (average 20°; according to Fellner, 1993) and a steeper western flank (average 35°; based on Fellner, 1993) leads to different explanations. Hottinger (1935), who for the first time discovered the large landslide deposits of Kolm-Saigurn, Lechnerhäusl and Bucheben descending from the steep western flank, explained the overall morphology with the general trend of the main planar fabric (foliation, schistosity): the gentle slopes on the true right flank follow the dip towards west and show slow mass movements. In contrast, the steep true left flank where the scarp of the landslides is located is made up of bas-set edges. Exner (1957) mapped large areas affected by mass movements on the eastern flank from Fröstlberg southward to east of Bodenhaus, which can be classified in modern terminology as DSGSDs. However, he regarded most DSGSDs to be of interglacial (= pre-LGM) age, as large areas are covered by an LGM till some meters thick (see Figs. 9, 11). Already von Poschinger (1986) showed that Hottinger’s (1935) explanation of the morphological asymmetry appears to be oversimplified, as the main planar fabric (foliation, schistosity) shows for large areas (approx. from the Kruml Valley and Lechnerhäusl northward) a gentle northward dip. His results as well as those of Fellner (1993) show the importance of the

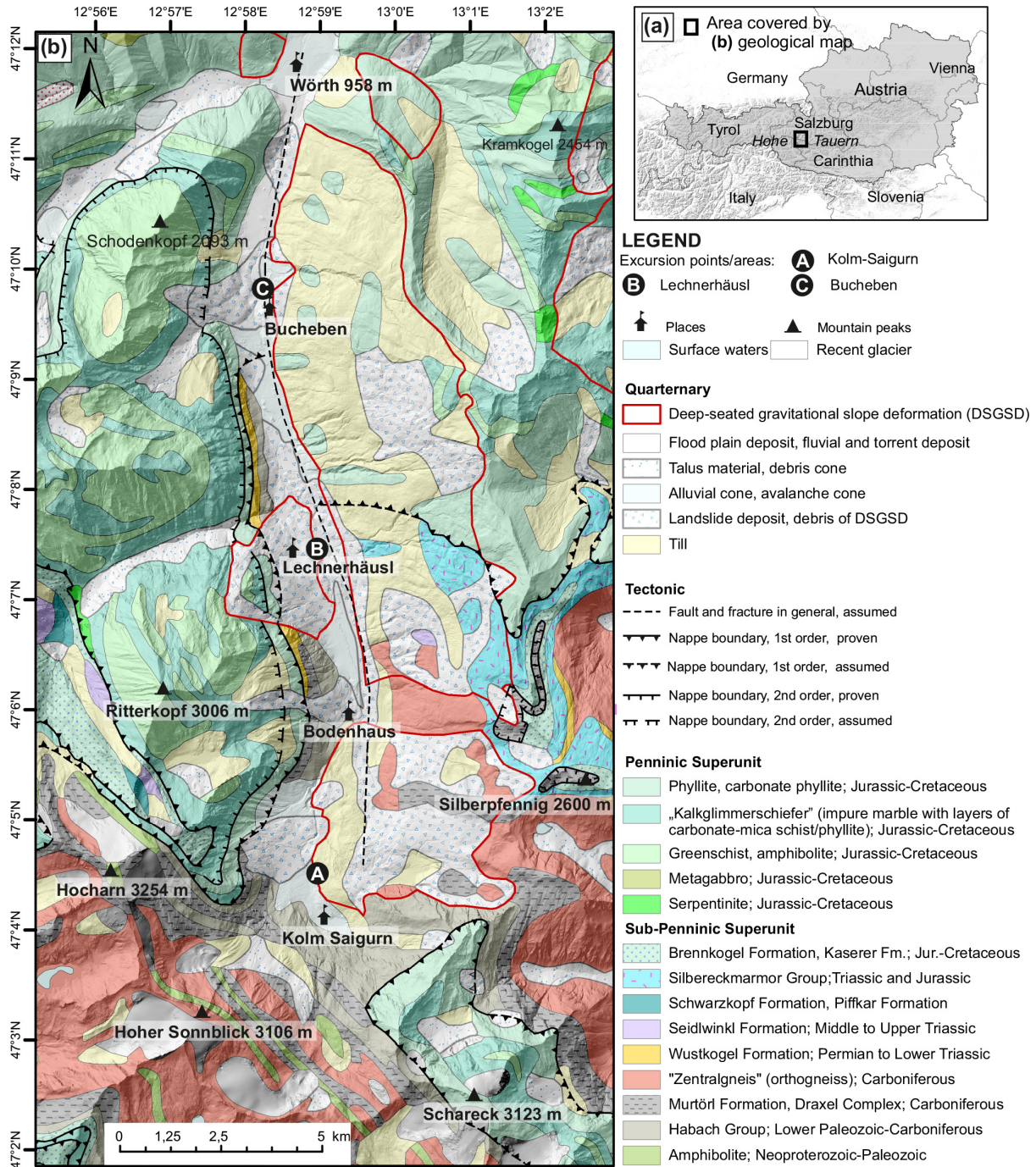


Figure 1. (a) Location of the Hüttwinkl Valley in the Province of Salzburg, in the Hohe Tauern mountain group (Eastern Alps) is marked. (b) Geological overview based on Pestal et al. (2005) with the main sites of the field trip (A – Kolm-Saigurn; B – Lechnerhäusl landslide; C – Bucheben landslide) indicated. Sources: Hillshade – Geoland Basemap (<http://geoland.at>, last access: 10 June 2024); Geology: Geologische Bundesanstalt Österreich (2022).

joint orientation together with that of the main planar fabric (foliation, schistosity) as a relevant cause for the formation of DSGSDs and hence the valley morphology.

Based on the existing reconstruction of the LGM ice extent (van Husen, 1987), the Hüttwinkl Valley was part of the large

network of valley glaciers with an ice surface along the valley axes between 2800 and 2300 m a.s.l. (see Fig. 3). However, well-developed trimlines of the LGM have not been found in the Hüttwinkl Valley due to comparable weak lithologies like different types of schists, which are not able to preserve the

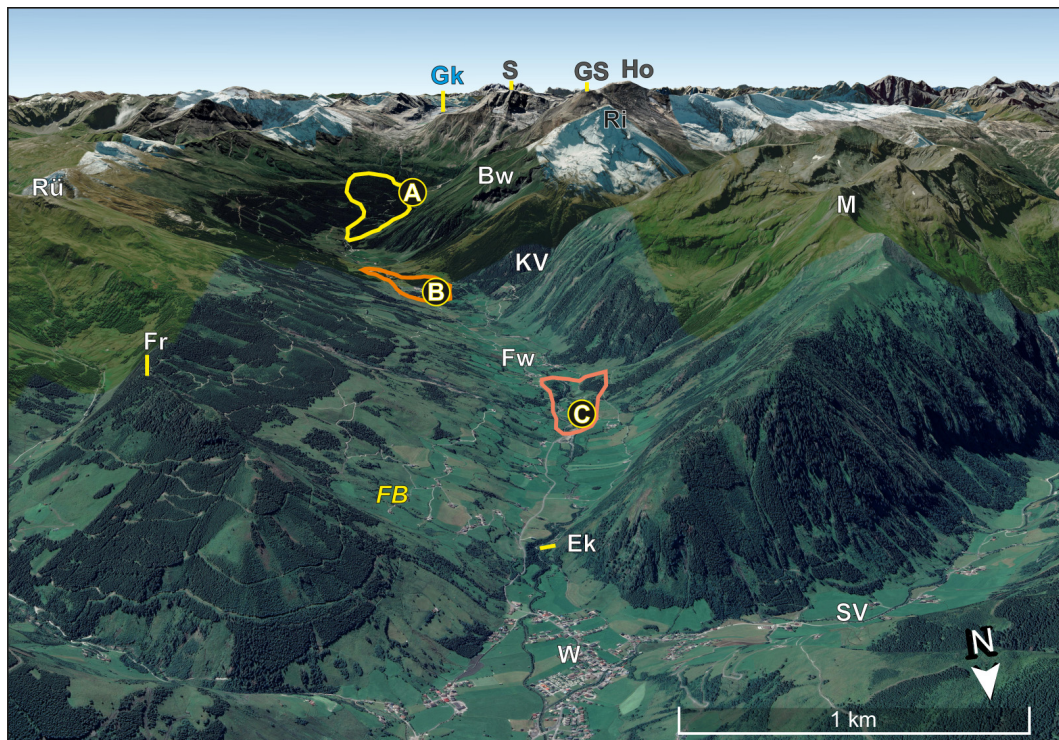


Figure 2. View of the Hüttwinkl Valley towards the south showing the valley asymmetry with steep west-facing slopes and more gentle slope on the east-facing side. Important sites are indicated. Field trip locations are plotted on a Google Earth image (with black circle, © Google Earth 2024); A – Kolm-Saigurn; B – Lechnerhäusl landslide; C – Bucheben landslide. Further locations: Bw – Bocksteinwand rock wall; Ek – Einödskapelle (1012 m); FB – Fröstlberg slope; Fr – Fröstlberg (1823 m); Fw – Frohnwirt (1074 m); Grieswies-Schwarzkogel (3116 m); Ho – Hocharn (3254 m); KV – Kruml Valley; M – Mitterkarkopf (2404 m); Ri – Ritterkopf (3006 m); Rü – Rührkübel (2482 m); S – Hoher Sonnblick (3106 m); SV – Seidlwinkl Valley.

record of glacial erosion (compare with Penck and Brückner, 1909). In addition, different types of mass movements altered the subglacial landscape shaped during the LGM. In total, glacial shaping had a limited influence on the valley morphology as indicated by the valley asymmetry (von Poschinger, 1986). The most prominent legacy of the LGM exists with an extensive cover by subglacial tills on the eastern flank (compare with Exner, 1957; Figs. 9, 11).

Delta foreset beds consisting of sandy to gravelly clinoforms and silty glaciolacustrine deposits are present in some areas from the valley floor up to ca. 1600 m a.s.l. (Figs. 3, 9, 10e). Such deposits were formed in ephemeral ice-dammed lakes at the margin of rapidly downmelting glaciers during the phase of ice decay in the early Lateglacial (Reitner, 2007; Reitner et al., 2016), when the LGM ice masses of the Eastern Alps collapsed between 19 and 18 ka (Klasen et al., 2007; Wirsig et al., 2016).

Latero-frontal moraines of the following Gschnitz stadial (17–16 ka; Ivy-Ochs et al., 2023a, with references), which represents the last glacier advance before the Bølling–Allerød Interstadial (14.7–12.9 ka), are missing in the Hüttwinkl Valley in contrast to quite frequent documented instances in the Hohe Tauern mountain range elsewhere (see

van Husen and Reitner, 2022). Direct removal or coverage by catastrophic landslides and the infill of landslide-dammed lakes resulting in drowned landscapes most likely erased all landforms of the Gschnitz paleoglaciers.

No time markers for the (re-)activation of the DSGSDs after the LGM have been identified so far (von Poschinger, 1986). Evidence from Kolm-Saigurn (see below) indicates an onset of such DSGSDs before the Bølling–Allerød Interstadial (14.7–12.9 ka).

According to ^{10}Be surface exposure dating, the Durchgangswald landslide (Bichler et al., 2016; Figs. 3, 4, 5, 6, 7, 8) happened around 13 ka at the end of the Bølling–Allerød Interstadial (14.7–12.9 ka). Von Poschinger (1986) could show that the emplacement of the $400 \times 10^6 \text{ m}^3$ large landslide mass (Bichler et al., 2016) at the toe of the eastern slope most likely stopped the further development of a previously formed DSGSD (at Durchgangriegel; Fig. 12b).

During the Younger Dryas (YD; 12.9–11.7 ka), the last climatic deterioration of the Würmian Lateglacial, the cirque glaciers showed the prominent re-advance of the Egesen stadial. The precursors of Goldberger and Pilatuskees merged together at Kolm-Saigurn and overflowed parts of the Durchgangswald landslide deposit. A series of recessional moraines

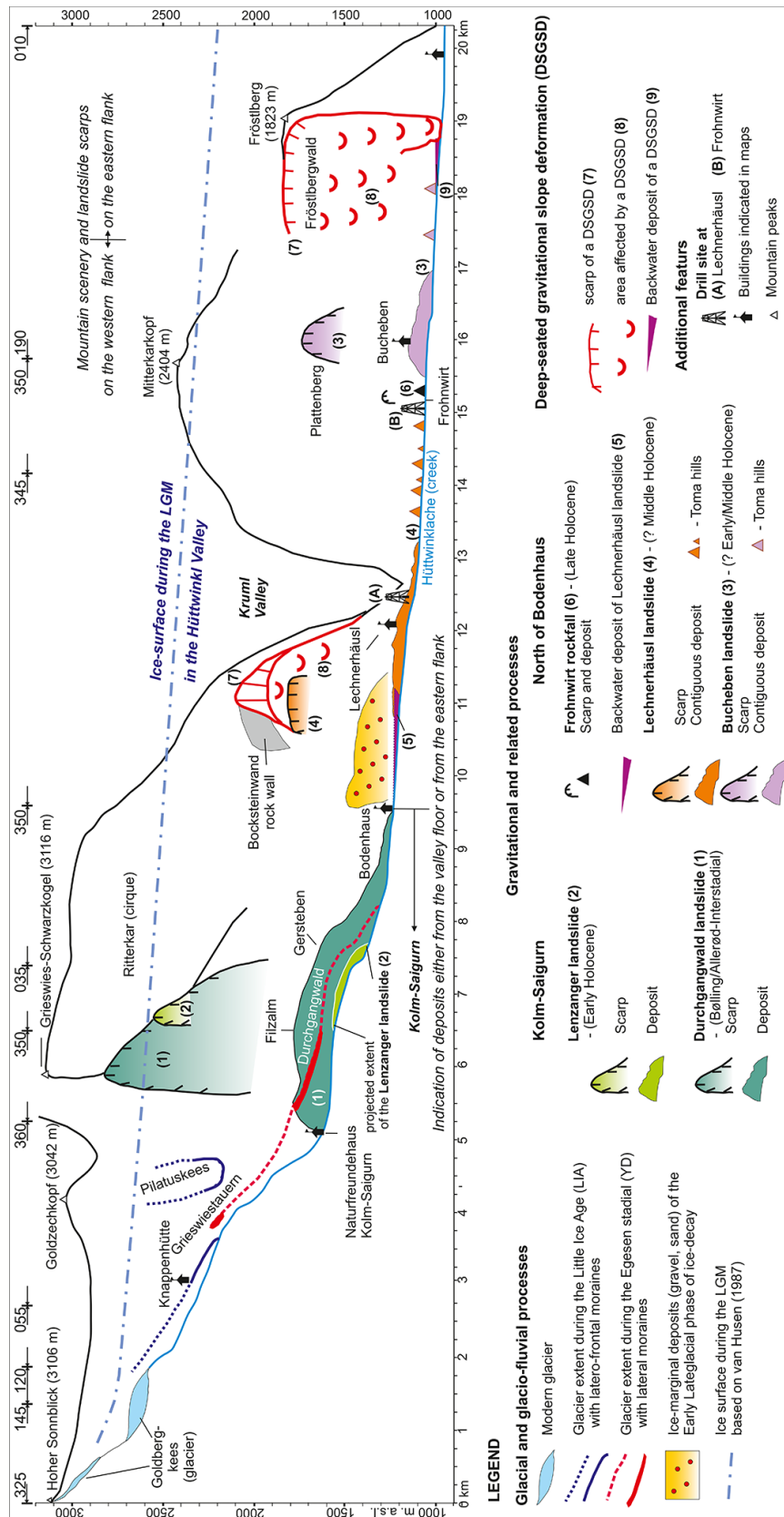


Figure 3. Section along the Hüttwinkl Valley from the Hoher Sonnblick peak to the confluence with the Seidlwinkl Ache creek showing main elements for understanding the landscape evolution.

show the further development during the Egesen stadial before the onset of the Holocene. Latero-frontal moraines of the Egesen stadial are quite frequent in the Hüttwinkl catchment and show in many cases the last glacier occupation of present-day non-glaciated cirques. In the older literature (e.g., Exner, 1957), such moraines are attributed to the Daun stadial, which is now included in the term Egesen stadial (see Reitner et al., 2016).

At Kolm-Saigurn, the Early Holocene Lenzanger landslide (^{10}Be age of ca. 11 ka; Preboreal; Bichler et al., 2016; Figs. 3, 4, 6) covered the subglacial till of the Egesen stadial, which finally resulted in a unique sequence of superpositions where a YD till is part of a sequence from the Bølling–Allerød Interstadial to the early Holocene (compare also with Ivy-Ochs et al., 2023b).

Down-valley of Bodenhaus, where the most distal parts of the Durchgangswald landslide are evident (Figs. 4, 9), the chronology of mass movements (landslides and DSGSDs) can be constrained only relatively.

The Bucheben landslide (Figs. 3, 11) occurred most likely at the end of the Early Holocene (Greenlandian; 11.7–8.3 ka), based on the ^{14}C -dated drilling results in the backwater area (drill site B). As the toma hills of the Bucheben landslides lay on top of the backwater terrace level of the Fröstlberg DSGSD, the latter must be older.

The Lechnerhäusl landslide (Figs. 3, 9) happened after the Bucheben landslide as its toma hills were deposited on the valley floor level formed in the backwater area of the Bucheben landslide. A dated base of a peat drilled at a mire within the landslide area at Lechnerhäusl (drill site A) indicates a landslide event during the Middle Holocene (Northgrippian; 8.3–4.2 ka). The damming of the Hüttwinkl creek resulted as well in the formation and infill of a lake, which most likely drowned the most distal deposits of the Durchgangswald landslide south of Bodenhaus (Bichler et al., 2016).

Smaller rockfall events happened of course afterwards but had no impact on the development of the valley floor. The only exception is the small rockfall deposit at Frohnwirt (Fig. 3, 11), which may have led to a short-lasting disturbance of the river gradient in the Late Holocene (Meghalayan; 4.2–0 ka).

Catastrophic debris flows of mostly limited extent occur frequently. The disintegrated rock of the DSGSD slopes (Fig. 13c), as well as tills, provides sufficient debris for such catastrophic events (Baur et al., 1992), as demonstrated by the last event on 28 August 2023 (Fig. 5e).

4 Kolm-Saigurn

At Kolm-Saigurn (Figs. 1, 3, 4, 5, 6) three well-distinguishable geological and geomorphological units allow a reconstruction of gravitational and glacial processes and

the establishment of chronology (Bichler et al., 2016). These units are, in chronological order,

1. the Durchgangswald landslide
2. the tills and moraines of the Kolm-Saigurn glacier system
3. the Lenzanger landslide.

During the field trip, the morphological and sedimentary expression of all three units will be presented.

4.1 The Durchgangswald landslide

The ^{10}Be surface exposure dating and geological reconstructions (Bichler et al., 2016) showed that the Durchgang landslide occurred at 13.0 ± 1.1 ka in an ice-free environment at the end of the Bølling–Allerød Interstadial, just before the onset of the Younger Dryas. The 0.4 km^3 landslide mass (Figs. 4, 5, 7, 8) detached from the glacially oversteepened eastern flank of the Grieswies-Schwarzkogel (3116 m) and covers an area of ca. 3.9 km^2 . By comparing the lithological succession at the flank consisting of westward-dipping garnet mica schist, “Kalkglimmerschiefer” (meaning impure marble with layers of carbonate–mica schist and phyllite) and biotite mica schist, with the similar but rotated succession of the landslide deposit east of the Hüttwinkl creek, the detachment and movement occurred along one distinct displacement plane as proposed by Hottinger (1935) and von Poschinger (1986). The upper part of the plane has an inclination of $40\text{--}50^\circ$ and is thus less steep than the $70\text{--}80^\circ$ joints in the scarp area (Fig. 8), indicating a new formation of the plane (von Poschinger, 1986). Outcrops of the landslide deposit and the geological evidence of the water tunnel running through the mass (see also Dirnberger and Hilberg, 2020; Fig. 12) document a slightly rotated, i.e., steeper, dip with more or less the same dip direction, indicating a rotational component of the movement. The rugged surface of the landslide (Fig. 6) consists of clast-supported boulder-sized scree made up of angular to subangular, sometimes house-sized Kalkglimmerschiefer blocks. The forested area is also characterized by a large number of small standing water and waterlogged areas (see also hydrogeological investigations by Dirnberger and Hilberg, 2020), which leads to the local name “Rauriser Urwald” (primeval forest of Rauris or “Rauris virgin forest”).

The northern sector of the landslide comprises compressional structures, as evident in the field and on the DEM. These morphological features indicate a fast, dynamic flow in the sense of a rock avalanche (sturzstrom) for the most distal and down-valley part of the landslide mass, towards the Bodenhaus (K7) location. Such a change in the landslide kinematics might have been enabled by the successive increase in fragmentation with transport distance towards the distal part and by a supposed pre-existing step in the bedrock in the valley (at K8), leading to a steeper gradient in this area. The

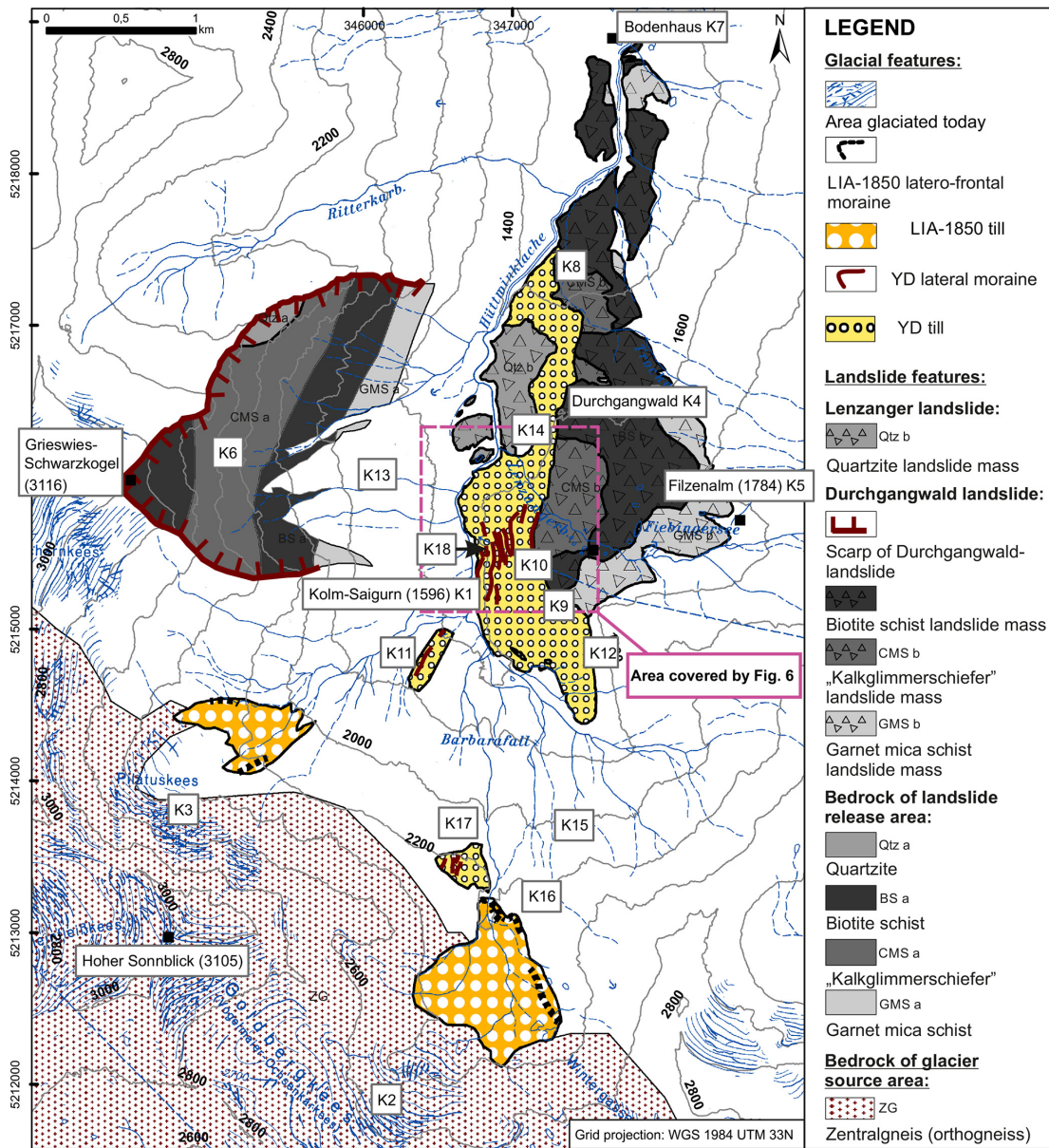


Figure 4. Simplified topographical and geological overview of the study area, showing the most important features of the study area. Topographical features referred in this study are marked on the map as (K). Numbers given on contour lines and next to topographical names indicate elevation in meters above sea level (m a.s.l.; modified after Bichler et al., 2016). The extent of Fig. 6 is indicated.

calculated Fahrböschung (meaning travel angle; Heim, 1932) for the main sliding part is an 11 to 12° angle with a run-out length of ~ 4.1 km. Including the rock avalanche leads to a run-out length of around 5.6 km and a travel angle of ~ 14°. However, the latter number has to be considered an upper limit, as the most distal part of the rock avalanche is covered by backwater sediments derived from the Lechnerhäusl landslide (Sect. 5.1; Figs. 3, 9). Altogether, the Durchgangswald landslide resulted in the blocking of the Hüttwinklache creek in the area of Kolm-Saigurn (K1) and of the creeks at the

Filzenalm (K5), with lakes and bogs subsequently forming at its margin (Fig. 7).

4.2 The Kolm-Saigurn glacier system

At the onset of the Younger Dryas (YD), glaciers re-advanced into the valley head of both the Pilatuskees (K3) and Goldbergkees (K2) (Fig. 7). During this prominent glacier advance the western part of the Durchgangswald landslide got overridden, as proven by a cover of consolidated, massive and matrix-supported diamict with occasional striated clasts, a subglacial till typical of a temperate glacier

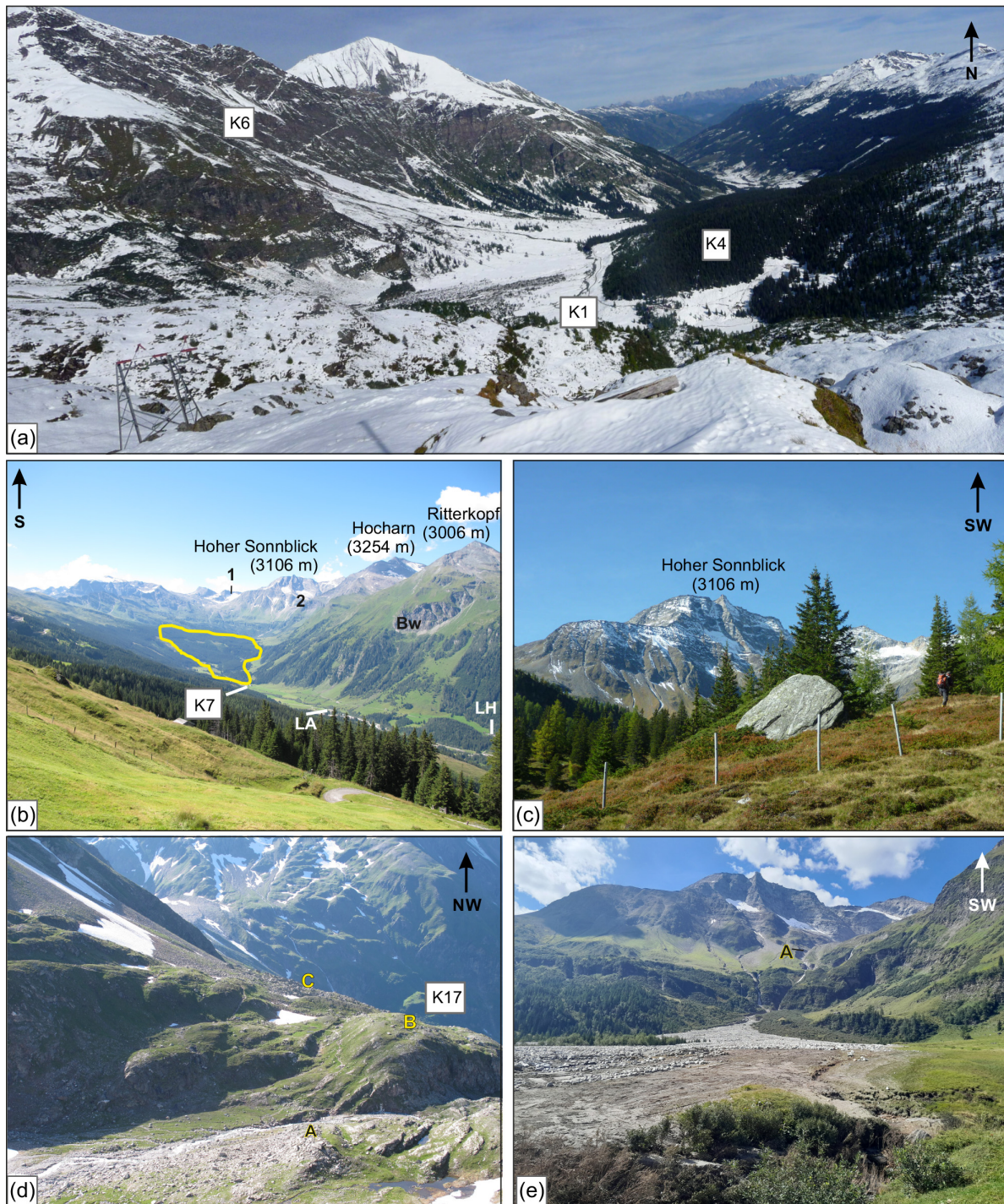


Figure 5. Photographs of the Kolm-Saigurn area ((a), (c), (d) are modified after Bichler et al., 2016). Locations are marked according to Fig. 4. (a) View from K17 towards the north. The scarp area of the Durchgangswald landslide (K6) and its main mass (K4) onlapping on the opposite valley side is visible. (b) View towards the south of the whole study area. Note the still glaciated areas of the Goldbergkees (1) and Pilatuskees (2) in the background. The extent of the landslide area is highlighted in yellow. LH – location of Lechnerhäusl inn; LA – quarry north of Lohningeralm (see Fig. 9). (c) Most distal part of the Durchgangswald landslide, at the Filzenalm (K5). The boulder in the photograph is a ^{10}Be -dated boulder from Bichler et al. (2016). (d) View at the forefield of the LIA-1850 terminal moraine of the Goldbergkees. A is terminal moraine; B is plateau of K17 with several dated boulders and dated quartz veins in polished bedrock; C is four lateral moraine ridges at K17 belonging to the Kolm-Saigurn glacier system of Younger Dryas (YD) age. (e) View at the LIA moraine (A) of Pilatuskees, which was partly mobilized in the course of the heavy rain event on 28 August 2023. Debris flow deposits in the foreground (image by Marc Ostermann).

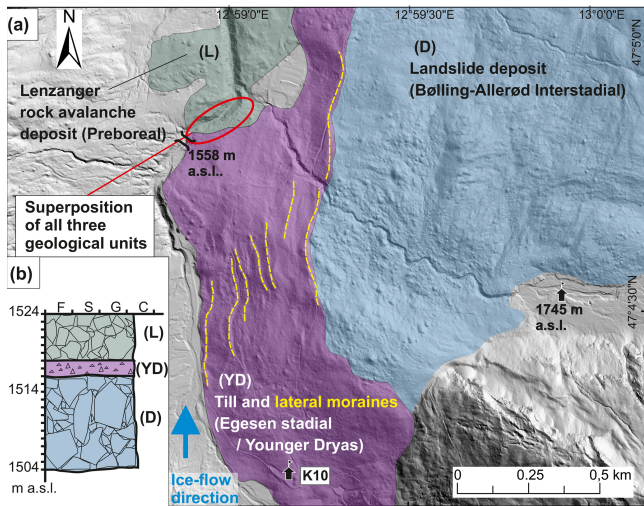


Figure 6. (a) Hillshade image showing the morphological contrast between the rugged terrain of the interstadial Durchgangswald rockslide deposit (D) and the subglacially smoothed landscape with multiple latero-frontal moraines formed during the Egesen stadial (YD; location indicated by Fig. 4). The youngest rock avalanche event (Lenzanger (L)) is evident in the northwest. K10 – Ammererhof. (DEM provided by the government of Salzburg Province.) (b) The site with the superposition of all three units (inset stratigraphic profile) is indicated (modified after Ivy-Oches et al., 2023b, and Bichler et al., 2016).

(Fig. 4). Zentralgneis and Kalkglimmerschiefer dominate the clast lithology. On the slope north of the Ammererhof (K10), a series of nine parallel latero-frontal moraines, mostly with Zentralgneis boulders on top, can be mapped, with the highest marking the border to the un-topped Durchgangswald landslide deposits (Fig. 6). Based on the morphological and sedimentary features, the maximum extent of the YD advance and the recessional phase with glacier stillstands and stabilization can be reconstructed. However, no end moraine exists anymore at the maximum position south of Bodenhaus, most likely due to fluvial action, which eroded also big parts of the glacial evidence on the true left flank.

The most remarkable succession of four lateral moraines of YD age occurs on a plateau at 2250–2200 m (K17) in the forefield of the Little Ice Age (LIA) – moraines of the Goldbergkees (K16) and thus high above the field trip route (Fig. 4d). Their position and altitude allow an approximation on the paleo-equilibrium-line altitude (ELA) during the YD maximum based on the maximum elevation of lateral moraine approach (Lichtenecker, 1938).

The age model of the YD Kolm-Saigurn glacier system is based on the superposition of the ¹⁰Be-dated Durchgangswald landslide and the ¹⁰Be exposure dates of eight boulder samples and two bedrock samples (for details see Bichler et al., 2016). The ¹⁴C-dated base of a peat formed after the glacier advance of Melcherböden with an age of 11.35–11.20

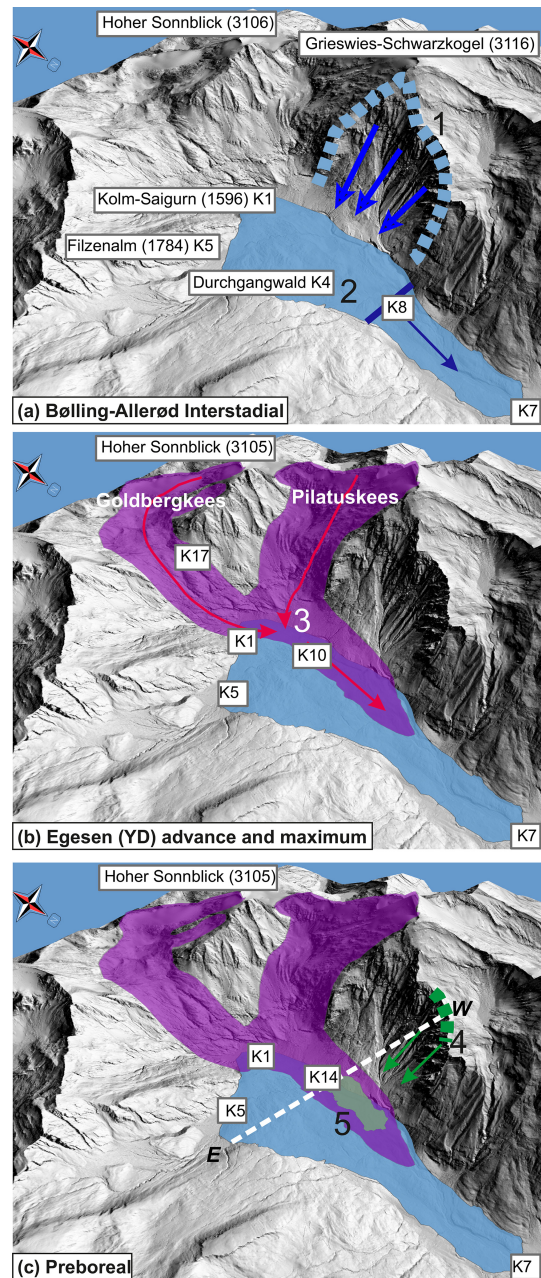


Figure 7. Visualization of the extent, origin and movement direction of the Durchgangswald landslide (a), the Kolm-Saigurn glacier system (b) and the Lenzanger landslide (c). (a) 1 is the scarp of the Durchgangswald landslide; 2 is the border at the Gersteben step (K8) where the kinematics of the landslide changed from sliding to dynamic flow in the sense of a rock-avalanche and the flow direction changed from east to north. (b) 3 is the confluence of the Goldbergkees and Pilatuskees in Kolm-Saigurn. (c) 4 is the supposed scarp area of Lenzanger landslide; 5 is the Lenzanger landslide mass. The dashed line marks the approximate location of the cross-section in Fig. 8. Locations (K) as indicated in Fig. 4: K1 – Kolm-Saigurn Naturfreundehaus; K5 – Filzenalm; K7 – Bodenhaus; K10 – Ammererhof; K14 – Lenzanger; K17 – plateau in the forefield of Goldbergkees. (Figure modified after Bichler et al., 2016; DEM provided by the government of Salzburg Province.)

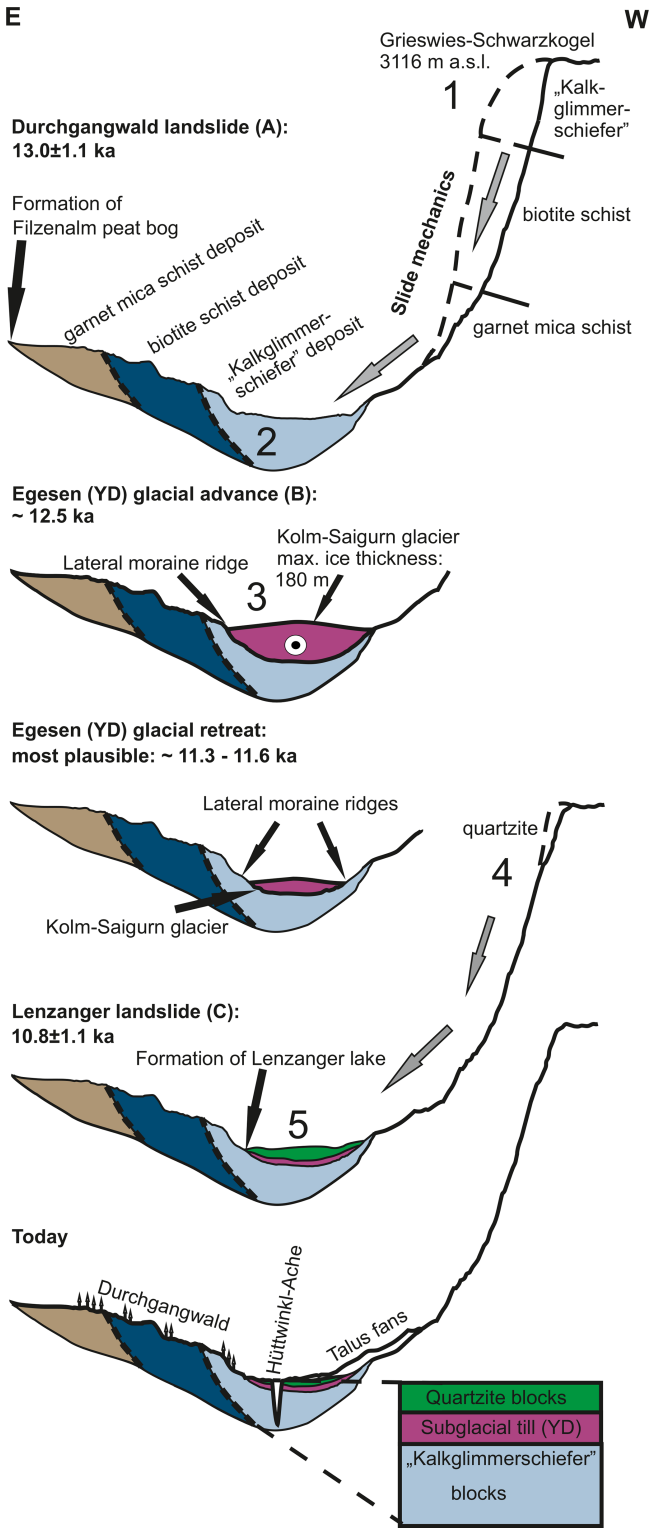


Figure 8. Generalized landscape evolution sketch, indicated in Fig. 7. Numbers and letters are according to Fig. 7. Features are not to scale. (Figure modified after Bichler et al., 2016.)

ka cal BP provides the upper age constraint of the YD glacier advance.

4.3 The Lenzanger landslide

Around the Grieswiesalm (K13) and Lenzanger (K14) area, the till cover is topped by a clast-supported scree with angular quartzite boulders reaching a size of up to 10 m diameter (Figs. 4, 6; Bichler et al., 2016). The surface morphology is characterized by a series of curved ridges, indicating a flow-like movement. The quartzite blocks cover an overall surface area of around 0.3 km². The source of these blocks has been interpreted to document a landslide or, more precisely, a rock avalanche, originating from the western valley flank, similar to the Durchgangswald landslide but much smaller in scale. The stratigraphical succession (Figs. 1, 3, 6) and the preservation of typical rock avalanche features indicate that this rapid mass movement happened in an ice-free environment after the YD glacier advance and retreat. This conclusion is supported by the ¹⁰Be ages of two boulders giving a mean age of 10.8 ± 1.1 ka which falls into the Preboreal (Early Holocene).

4.4 Debris flow event of 28 August 2023

In the course of the field trip, we will see the legacy of a very recent debris flow event which devastated the valley floor of Kolm-Saigurn (Fig. 5e). On 28 August 2023, a massive debris flow mobilized some 100 000 m³ of Pilatuskees LIA moraine triggered by a heavy rain event (unpublished data provided by Melina Frießenbichler, Daniel Binder, Bernhard Hynek, Anton Neureiter, Georg Pistotnik, Marc Ostermann, Gernot Weyss). The debris flow is part of a process cascade that has even reached Rauris about 16 km downstream.

5 Landslides north of Bodenhaus

5.1 Lechnerhäusl landslide

The investigation of the Lechnerhäusl landslide event has not been performed in such detail as that of Kolm-Saigurn. Hottinger (1935) provided a brief description of the scarp and the extent of the deposits. Exner (1957) assumed a Gschnitz moraine within the area of the landslide, whereas von Poschinger (1986) described the lithology of the deposits. Abele (1974) named the landslide Bocksteinwand–Lechnerhäusl as he, like Exner (1957), regarded the rock wall of Bocksteinwand as the head scarp. However, such a release area seems to be unlikely according to the map of Hellerschmidt-Alber (1998). Taking into account his results and the modern DEM, the assumed extent of the scarp is displayed in Fig. 9. The lithological units in the surrounding stable areas show a shallow to moderate dip from the southwest to northwest.

An extensive scarp below the Bocksteinwand represents the release area of a large DSGSD which resulted in a downward movement of a rock mass consisting of Kalkglimmerschiefer, prasinite, dark phyllite and so-called “phengite

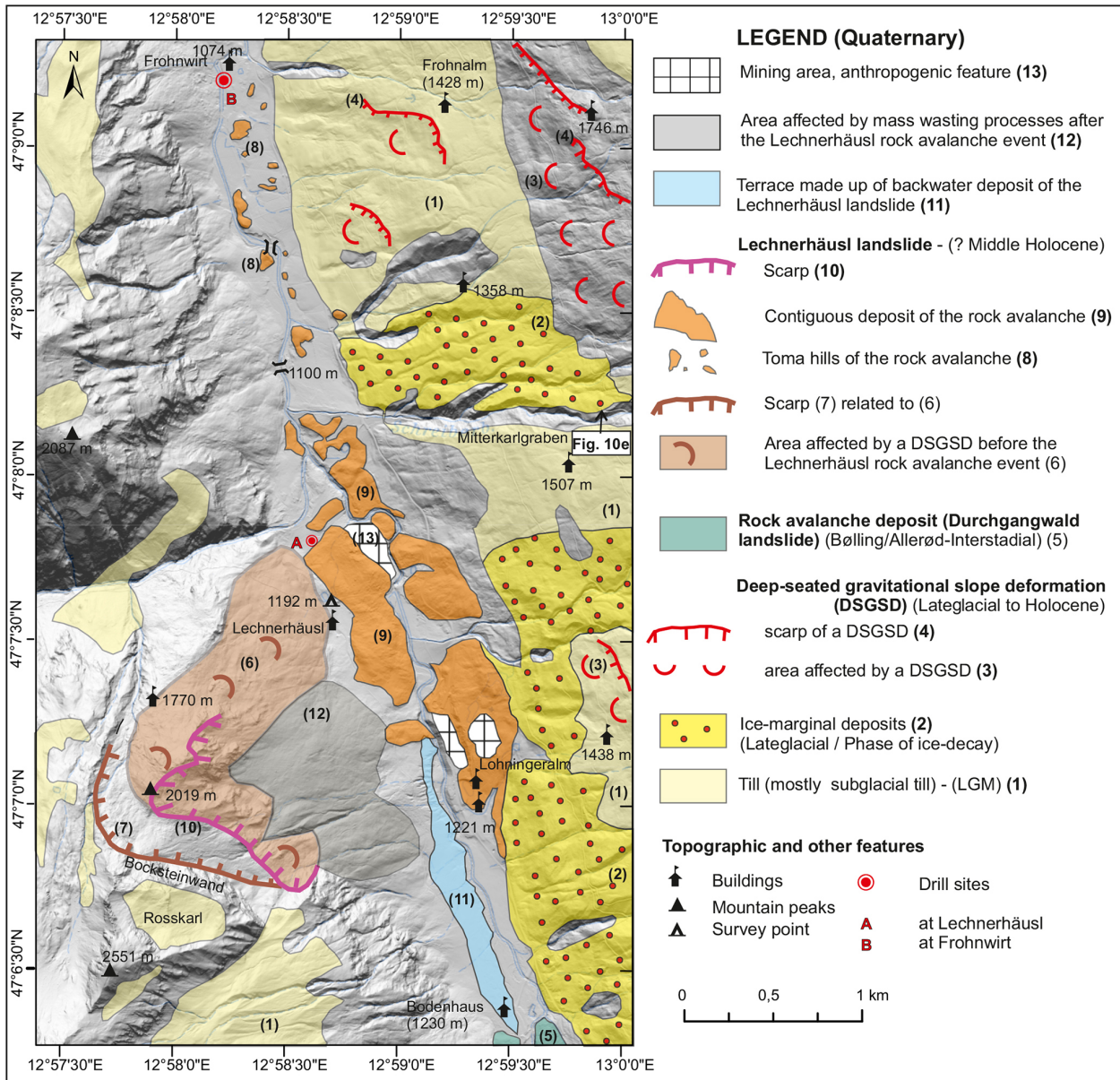


Figure 9. Simplified geological map of the Lechnerhäusl landslide and surrounding. The extent of the till cover is partly based on Griesmeier (2021). Source: Hillshade – Geoland Basemap (<http://geoland.at>).

gneiss” of the Wustkogel Formation. Eventually the scarp of the Lechnerhäusl landslide developed on the southern part of the rock mass affected by the DSGSD (Figs. 9, 10a).

More or less contiguous bodies of landslide deposits can be mapped east of Lechnerhäusl and on the opposite (eastern) valley flank from Lohningeralm northward. In general, a lithological succession from west to east with Kalkglimmerschiefer, dark phyllites and quartzite, phengite gneiss, and prasinite with dark phyllite occurs within the landslide debris (von Poschinger, 1986). Large angular boulders of Kalkglimmerschiefer are characteristic east of Lechnerhäusl. Quarries for natural stone slabs northeast of Lechnerhäusl and north

of Lohningeralm expose phengite gneiss. The original set of discontinuities (joints, foliation, schistosity, faults) is still discernible, but the dip shows a strong variation, and features typical of dynamic fragmentation (in the sense of McSaveney and Davies, 2006) like jigsaw clasts (see Dufresne et al., 2016) are present (Fig. 10b, c).

Isolated hills, so-called toma, occasionally sitting on the toe of the eastern flank but mostly on top of the flat valley floor represent the distal part of the landslide (Figs. 9, 10d). Those toma with a height of a few meters consist mostly of Kalkglimmerschiefer but also of prasinite, dark phyllite and phengite gneiss (Wustkogel Formation).

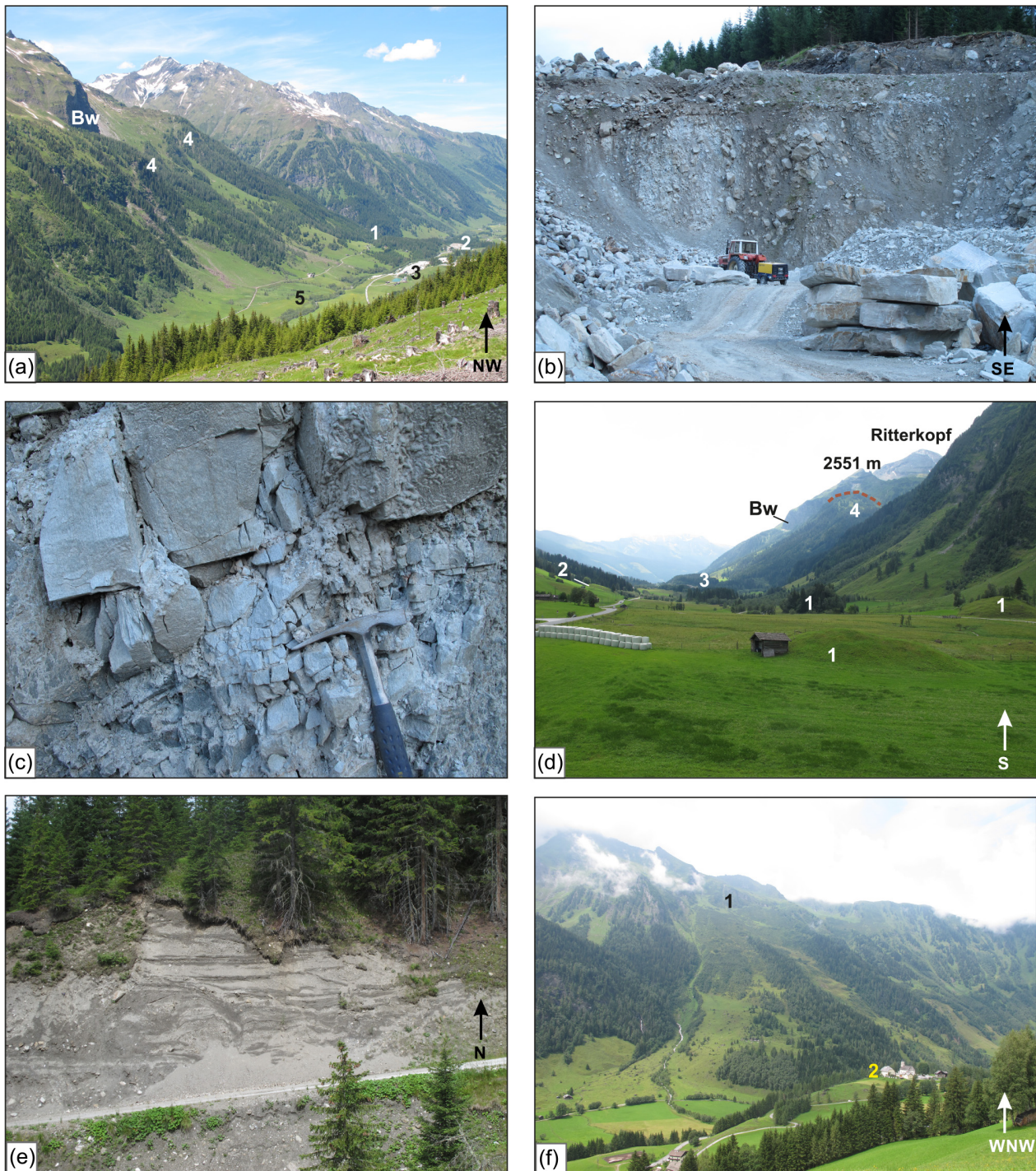


Figure 10. (a) View at the Lechnerhäusl landslide from the eastern valley flank. The landslide deposit at Lechnerhäusl (1) and the quarries in the landslide deposit (2 – northeast of Lechnerhäusl; 3 – north of Lohningeralm) are evident. The run of the supposed scarp (4) below the Bocksteinwand (Bw) rock wall) is less clear in contrast to the backwater terrace of the Lechnerhäusl landslide (5). (b) Landslide deposit at the quarry northeast of Lechnerhäusl (no. 2 in (a)). Vertically dipping of strongly fragmented phengite gneiss. (c) Detail of a strongly fragmented phengite gneiss showing fractures which were caused by dynamic fragmentation resulting in the formation of jigsaw-clasts. (d) View to the south with small hills, so-called toma (1), made up of Lechnerhäusl rock avalanche deposits. Their position is mostly on the valley floor. In one case (2) such a deposit was deposited at the toe of a slope. (3) – Quarry northeast of Lechnerhäusl. (4) – scarp of the DSGSD which was formed before the Lechnerhäusl-landslide. Bw – Bocksteinwand rock wall. (e) Delta foresets structures indicating synsedimentary deformation typical of ice-marginal deposits of the early Lateglacial phase of ice decay (Mitterkarlgraben in 1575 m a.s.l., indicated in Fig. 9). (f) View at the scarp (1) and landslide deposit (2) of Bucheben (with chapel of Bucheben).

A preliminary kinematic analysis based on field evidence indicates that an initial rockslide with a newly formed plane hit the opposite valley flank. Increasing dynamic fragmentation soon led to the transformation into a typical rock avalanche as indicated by the depositional features and the toma hills. The latter “surfing” on top of the valley floor which was formed in the backwater of the Bucheben landslide.

No calculation of the volume detached during the landslide has been performed so far. Abele (1974) estimated the area at 3 km² and calculated the travel length (5.5 km) and the Fahrböschung (12.5°) based on a proposed scarp detachment from the Bocksteinwand. We reconstructed a contiguous landslide area of 1.5 km², which did not include the areas below the scarp which were affected by slope processes after the landslide event. Depending on the assumed highest scarp, the travel length varies between 4.7–5.2 km, resulting in a Fahrböschung from 8.4 to 10.2°.

According to the situation along the Hüttwinkl valley, the Lechnerhäusl landslide is younger than the landslides of Durchgangswald and Bucheben. A drill core at the mire northeast of Lechnerhäusl (drill site A; Figs. 3, 9) consisted of sandy material ca. 4.7 m below the surface containing a small amount of mostly undefinable plant material. The ¹⁴C dating provided an age of ca. 5.3–5.0 ka cal BP indicating that the Lechnerhäusl landslide most likely occurred in the Middle Holocene (8.3–4.2 ka). Such a quite young age fits well to the morphological evidence, as the perturbation of the river gradient of the Hüttwinkl creek in this flat area is still prominent (Fig. 3).

In the course of the field trip, we will make a short walk to the former upper mining area east of Lohningeralm where we see landslide deposits and adjoining ice-marginal deposits. From this point, we get an excellent overview of the Lechnerhäusl scarp area, the backwater area and the distal part of Durchgangswald landslide.

5.2 Bucheben

Again, Hottinger (1935) described the Bucheben landslide (Figs. 10f, 11) for the first time. Fellner (1993; unpublished report) made a brief structural analysis of the scarp area with a special focus on present-day block stability. The scarp is developed in Kalkglimmerschiefer and prasinite, which have a dip of 10–15° from west to north (Dieter Fellner, unpublished report). Joints dipping 40–50° towards the east are regarded as the most efficient for the release of the rock mass on the glacially oversteepened slope.

Morphological features indicate a relatively younger rockslide/rock flow (no. 8 in Fig. 11) just below the scarp area which did partly override the Bucheben landslide deposits. The latter can be mapped as two contiguous bodies on both sides of the Hüttwinkl creek. The chapel of Bucheben (1144 m) sits on the eastern landslide mass. The surface is covered by angular boulders made up of predominantly prasinite but also of Kalkglimmerschiefer. Toma hills can be

traced 2 km north of Bucheben on top of a valley fill, which was formed before the landslide event as a result of mass movement action before (see Sect. 6).

Like in the case of Lechnerhäusl, an initial rockslide transformed into a rock avalanche whose distal parts disintegrated and moved as isolated toma (no. 5 in Fig. 11). Abele (1974) reconstructed a landslide area of > 1 km², a travel length of 2.2 km and a Fahrböschung of 25°. According to our reconstructions, we get a contiguous landslide area of 1.5 km², a travel length of 3.4–3.6 km and a Fahrböschung of 16–17°.

The Bucheben landslide is relatively older than the Lechnerhäusl landslide. A 13.5 m deep drill core at site B (Figs. 3, 11), 500 m upstream of the southernmost landslide deposits and ca. 200 m upstream of the quite small rockfall deposits of Frohnwirt (made up of Kalkglimmerschiefer boulder), helps to constrain the age. ¹⁴C dating of wood samples from the lower sandy layer (13.5–8.5 m below the surface), partly rich in organic material, provided ages of ca. 8.6–8.4 ka cal BP for 11.8 m below the surface and ca. 8.2–8.0 ka cal BP for 8.7 m below the surface. This fine-grained layer is topped by coarse gravel followed by a fining-upward sequence with sand and finally silt (4.4–2 m). The ¹⁴C dating of wood gave an age of ca. 2.3–2.0 ka cal BP. In the absence of further age constraints, we regard the lower fine-grained deposits to be a result of the damming by the Bucheben landslide which happened before 8.6–8.4 ka at the end of the Early Holocene. According to this hypothesis, the Frohnwirt rockfall caused the formation of the upper backwater deposits and thus occurred in the Late Holocene just before 2.3–2.2 ka.

During the field trip we will stop at Bucheben (1144 m) and study the scarp and deposits of the Bucheben landslide as well as the surrounding landscape (backwater areas, DS-GSDs, etc.).

6 Deep-seated gravitational slope deformation (DSGSD) and related deposits

Exner (1957) emphasized mass movements in his geological map of Gastein. There he differentiated between “im Schichtverband abgerutschte Gesteinsmassen” (in the sense of displaced rock masses with a still recognizable set of discontinuities) and “abgerutschte Gesteinsmassen und Bergsturz-Blockwerk” (displaced rock masses and landslide boulders). The first term is covered by what we call “area affected by DSGSD” (see Steinbichler et al., 2019). Exner’s (1957) second term has the disadvantage of not discriminating between deposits of catastrophic landslide (e.g., Bucheben) and totally disintegrated rock masses at, e.g., the toe of DSGSDs (see also the geological map in Fig. 1 which follows the same classification). Exner (1957) realized that displaced rock masses with a moderate disintegration exist below an extensive cover of subglacial till some meters thick on the lower parts of the eastern slopes. Thus, he re-

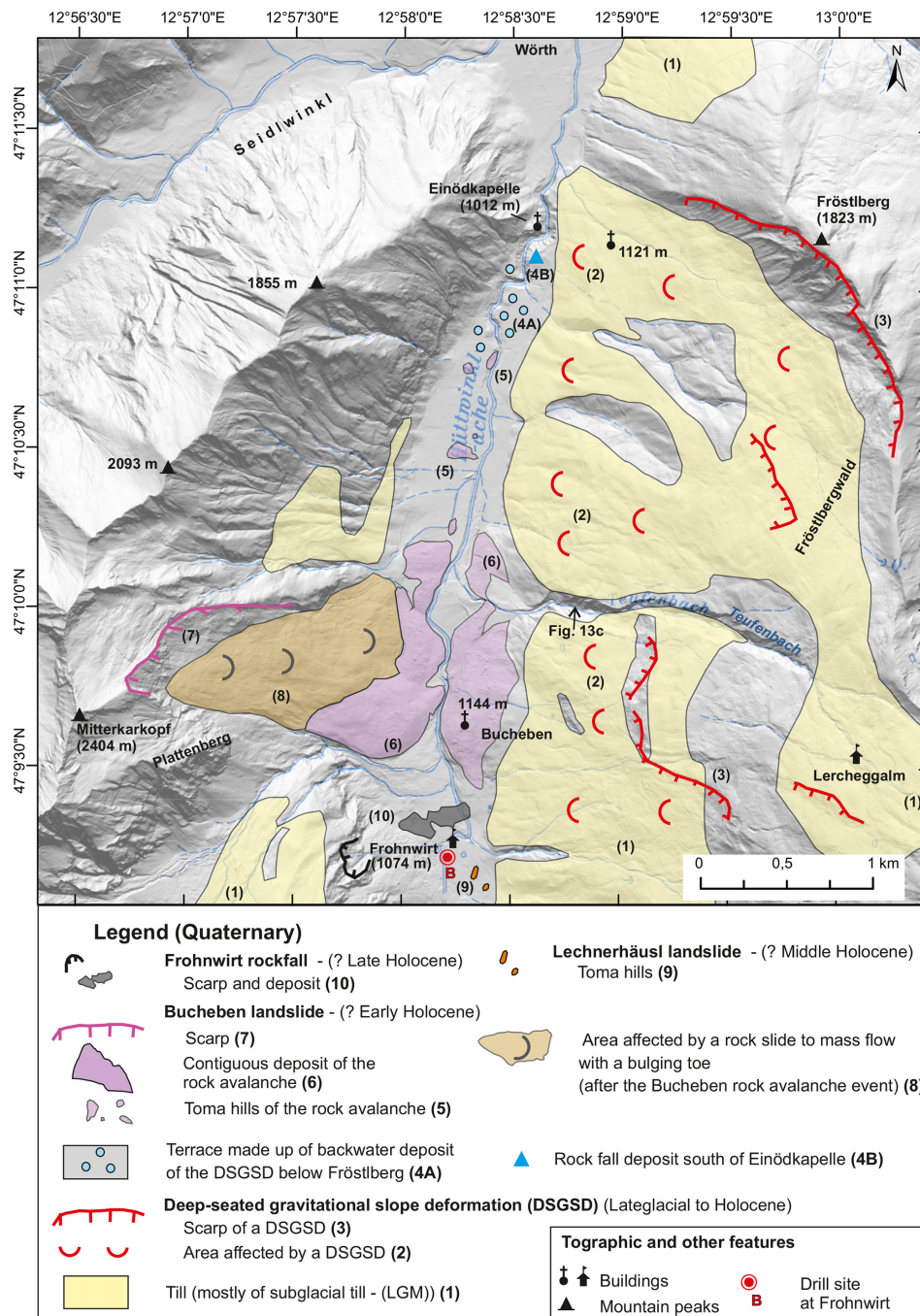


Figure 11. Simplified geological map of the Bucheben landslide and surrounding. The extent of the till cover is mostly based on Griesmeier (2021). Source: Hillshade – Geoland Basemap (<http://geoland.at>).

garded those slope deformations as having formed during an interglacial (in the sense of pre-LGM).

Von Poschinger (1986) made kinematic analyses of the slopes of the eastern flank between Kolm-Saigurn and the Lechnerhäusl landslide deposits based on the set of discontinuities (joints, foliation, schistosity, faults). He showed that only a combination of the westward-dipping main planar fabric and suitable joints enabled the creeping (meaning

slow displacement) slope deformation along distinct sliding planes (Fig. 12). On the other hand, he as well realized that the lower parts of the slopes show only slight to moderate indications of slope deformation compared to the upper parts (Fig. 12a). The primary movements, which affected an area of 16 km² and an estimated total volume of 0.8 to 2.4 km³, probably do not take place along a single defined slide plane but rather along many sliding horizons that cannot be pre-

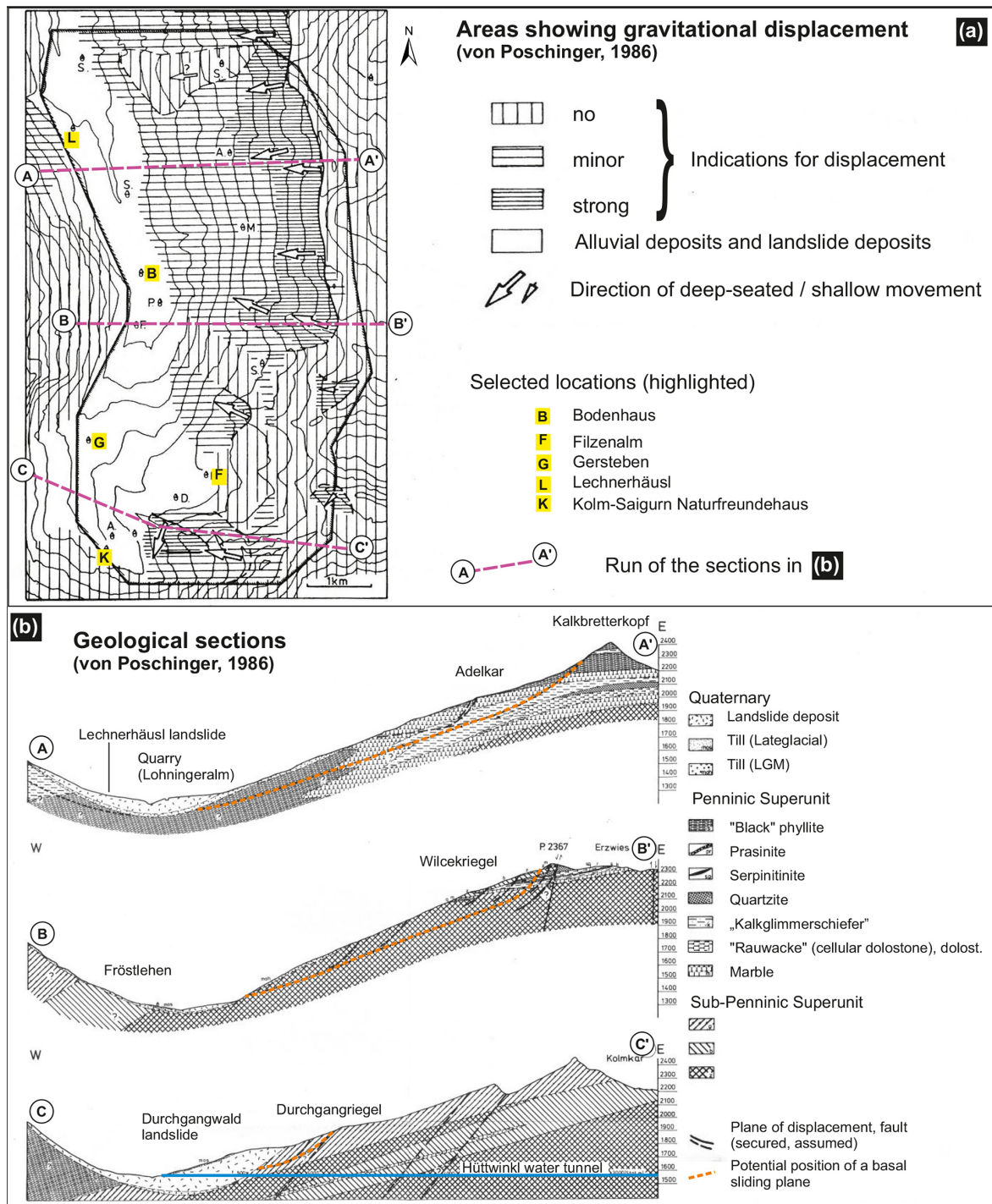


Figure 12. (a) Area showing gravitational displacement (after von Poschinger, 1986; terminology translated). **(b)** Geological sections after von Poschinger (1986). Location of the sections is indicated in (a). Translation of the legend.

cisely defined. During this process, the rock is broken up into sometimes huge rock slabs with a size of up to some square kilometers. The movements of the valley flank, which can also be classified as a “Talzuschub” (“valley closure”; a bulging toe of a slope due to slope deformation; see Stein-

bichler et al., 2019), probably began before the LGM and are still continuing today, at least in part. According to von Poschinger (1986), there is currently no risk of the right flank of the upper Hüttwinkl transitioning from (slow) creeping to (accelerated) sliding processes.

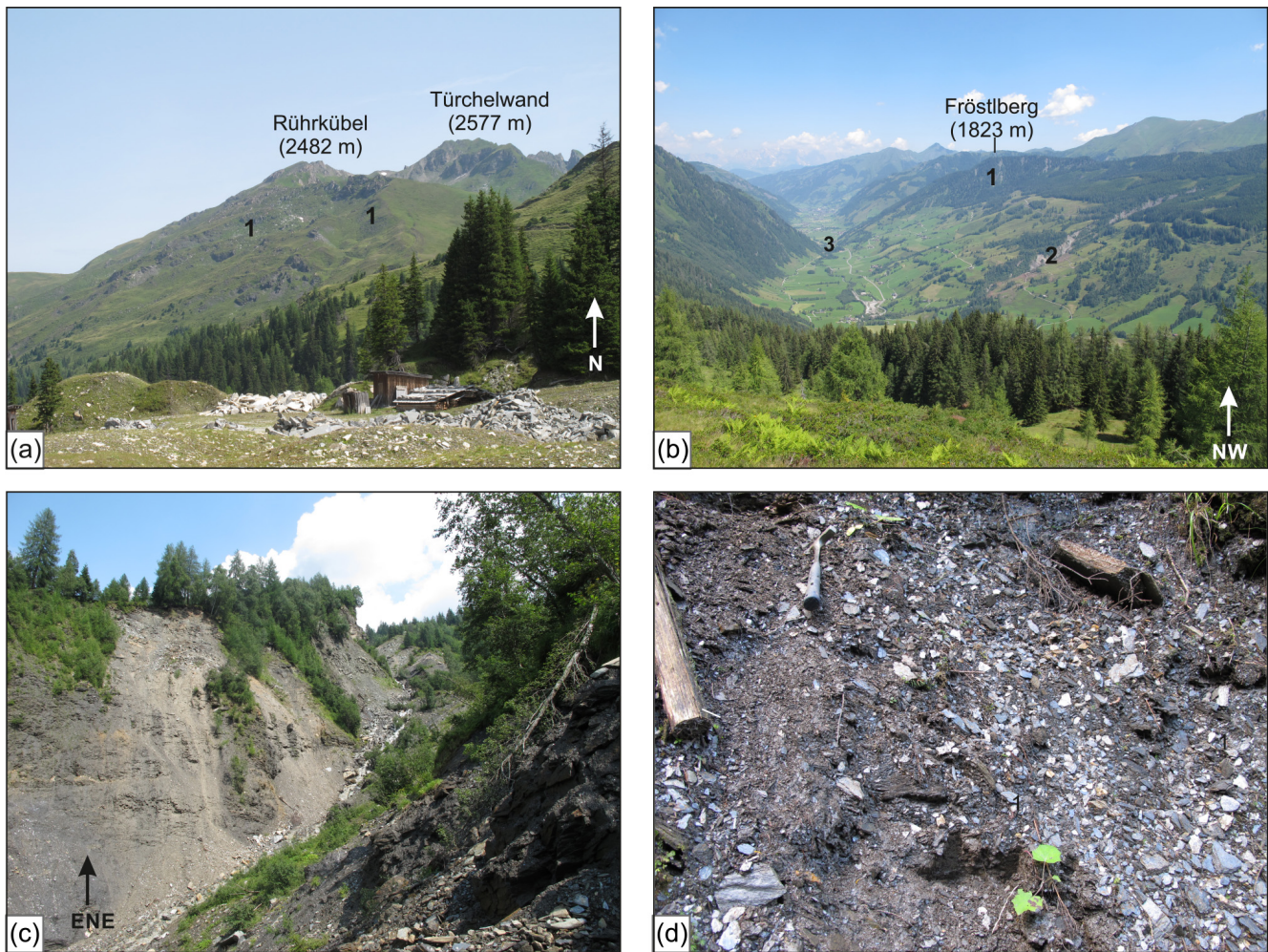


Figure 13. Slopes affected by DSGSDs: **(a)** View from Adelkaralm marble quarry to the western slope of Rührkübel (location in Fig. 2) consisting mostly of Kalkglimmerschiefer and prasinite. Multiple scarps (1) are evident. **(b)** View from the Felderalm at the scarp of Fröstlberg (1). The flanks of the Teufenbach eroded into disintegrated DSGSDs slopes is evident (2 – site of **(c)**). **(c)** Flanks along the Teufenbach in ca. 1200 m a.s.l. (site 2 in **(b)**) eroded in DSGSDs. Disintegrated and tilted dark phyllite (“Schwarzphyllit”). **(d)** Further disintegration of dark phyllite due to DSGSD. The schistosity is still recognizable in the lower part (dip 260/20) but the material is extremely weak and shows a transformation to loose debris (hammer for scale).

Fellner (1993; unpublished report), who investigated the eastern flank north of von Poschinger’s study area, emphasized the influence of the abundantly occurring, mechanically weak dark phyllite (Fig. 13c, d) as a condition for the DSGSDs beside the importance of the general dip of the main planar fabric. He classified the DSGSDs as “gleitender Talzuschub” (“valley closure” due to sliding). Mountain rupture phenomena like scarps and tension gaps as well as vertical movements of large rock slabs with the size of a square kilometer with vertical offsets of more than 140 m characterize the uppermost slope areas of the eastern flank. Due to the morphological clarity and freshness of the observed mass movement phenomena and the fact that the numerous tension gaps hardly show any backfilling, Fellner (1993) concludes that there are ongoing movements. Based on the case

of the Teufenbach torrent (northeast of Bucheben in Fig. 11; Fig. 13b, c), Baur et al. (1992) emphasize that disintegrated rock masses at the toe of a Talzuschub (DSGSD) are a major source for catastrophic debris flows.

The formation of the backwater deposits south of Einöd-kapelle (1012 m), which show an onlap on the toe of the Fröstlberg slope (Figs. 11, 13), is of importance for understanding the development of the lower Hüttwinkl Valley (Figs. 2, 3). The Hüttwinkl creek has already incised into this deposit (Figs. 3, 11) and is now already incising into bedrock, but the slightly raised level is still evident upstream. Moreover the backwater level existed already when the Bucheben landslide (Sect. 5.2) occurred, enabling the emplacement of the toma at this valley floor level. Currently there are some options which might have caused this situa-

tion. (1) The Fröstlberg ridge is a prominent scarp (Fig. 13a) where the outlines of the displaced mass (in the sense of a DSGSD) below are easily detectable. Like in the cases of DSGSD discussed above, the lower part is covered by till and missing any strong indication of mass movement activity. However, a till cover can be preserved if sliding is the main process. (2) There are clast-supported boulders of up to more than 100 m³ in size (4B in Fig. 11), mainly Kalkglimmerschiefer but also occasionally prasinite. Their source area must be on the western side but not from immediately above the deposit. This sediment could potentially document the most distal part of the Bucheben rock avalanche and/or the product of a larger rockfall from the western side with a so far not identified scarp. (3) There might have been a “valley closure” due to a DSGSD from Fröstlberg and/or a rockfall deposit, maybe also with the contribution of a debris-flowed fan from the east, up to the Early Holocene. Such a situation resulted in a slight shift in the river, leading to the formation of an epigenetic valley formed in bedrock which preserved the toe of the Fröstlberg DSGSD from further erosion and hence permanent reactivation.

Data availability. Additional data are available from the authors upon reasonable request.

Author contributions. JMR and MS conceptualized the field trip and the article together. JMR wrote the major part and made most figures. Geological framework and Fig. 1 are a contribution of MS.

Competing interests. The contact author has declared that neither of the authors has any competing interests.

Disclaimer. Publisher’s note: Copernicus Publications remains neutral with regard to jurisdictional claims made in the text, published maps, institutional affiliations, or any other geographical representation in this paper. While Copernicus Publications makes every effort to include appropriate place names, the final responsibility lies with the authors.

Acknowledgements. The authors thank the following persons for their helpful contributions: Benjamin Huet (on bedrock geology), Michael Lotter (on mass movements), Alfred Gruber (on design of figures) and Marc Ostermann (on the debris flow event of August 2023). Thomas Zwack and Wolfgang Jaritz provided data of the drill core at Frohnwirt (site B). The authors highly appreciate the commitment of the editors of this *DEUQUA Special Publications* field guide, Bernhard Salcher and Henrik Rother.

We dedicate this work to the memory of two great explorers of the Hohe Tauern mountain range, who inspired us in our research and passed away far too soon: Reinhard Böhm (climate researcher; 1948–2012) and Gerhard Pestal (geologist; 1958–2014).

References

- Abele, G.: Bergstürze in den Alpen, ihre Verbreitung, Morphologie und Folgeerscheinungen, *Wissenschaftliche Alpenvereinshefte*, 25, 230, https://bibliothek.alpenverein.de/webOPAC/01_Alpenvereins-Publikationen/06_wiss._Alpenvereinshefte/AV-HeftNr.025.pdf (last access: 10 June 2024), 1974.
- Agliardi, F., Crosta, G., and Zanchi, A.: Structural constraints on deep-seated slope deformation kinematics, *Eng. Geol.*, 59, 83–102, [https://doi.org/10.1016/S0013-7952\(00\)00066-1](https://doi.org/10.1016/S0013-7952(00)00066-1), 2001.
- Auer, I., Pretenthaler, F., Böhm, R., and Proske, H. (Eds.): *Zwei Alpentäler im Klimawandel*, in: *Alpine Space — Man & Environment*, Vol. 11, Innsbruck University Press, Innsbruck, Austria, 199 pp., ISBN 978-3-902719-44-72010, https://www.uibk.ac.at/iup/buch_pdfs/alpine_space_vol.11.pdf (last access: 10 June 2024), 2010.
- Baur, M., Edmaier, B., and Spaun, G.: Talzuschübe als Geschieberherde für Murgangereignisse in Saalbach und Rauris (Land Salzburg), in: *Internat. Symp. INTERPRAEVENT 1992*, 29 June–3 July 1992, Bern, Switzerland, Verlag Forschungsgesellschaft für vorbeugende Hochwasserbekämpfung, Klagenfurt, 165–180, ISBN 3-901164-03-0, 1992.
- Bichler, M. G., Reindl, M., Reitner, J. M., Drescher-Schneider, R., Wirsig, C., Christl, M., Hajdas, I., and Ivy-Ochs, S.: Landslide deposits as stratigraphical markers for a sequence-based glacial stratigraphy: a case study of a Younger Dryas system in the Eastern Alps, *Boreas*, 45, 537–551, <https://doi.org/10.1111/bor.12173>, 2016.
- Böhm, R., Schöner, W., Auer, I., Hynek, B., Kroisleitner, C., and Weyss, G.: *Gletscher im Klimawandel, Vom Eis der Polargebiete zum Goldbergkees*, Zentralanstalt für Meteorologie und Geodynamik, Morava, 112 pp., ISBN 978-3-200-01013-0, 2007.
- Böhm, R., Auer, I., and Schöner, W.: *Labor über den Wolken – die Geschichte des Sonnblick Observatoriums, Böhlau, Wien-Köln, Weimar*, 380 pp., ISBN 978-3-205-78723-5, 2011.
- Dirnberger, D. and Hilberg, S.: *Hydrogeologie im Tauernfenster – Fallbeispiel Rauristal*, Salzburg, *Grundwasser*, 25, 31–41, <https://doi.org/10.1007/s00767-019-00442-x>, 2020.
- Dramis, F. and Sorriso-Valvo, M.: Deep-seated gravitational slope deformations, related landslides and tectonics, *Eng. Geol.*, 38, 231–243, [https://doi.org/10.1016/0013-7952\(94\)90040-X](https://doi.org/10.1016/0013-7952(94)90040-X), 1994.
- Dufresne, A., Bösmeier, A., and Prager, C.: Sedimentology of rock avalanche deposits – case study and review, *Earth-Sci. Rev.*, 163, 234–259, <https://doi.org/10.1016/j.earscirev.2016.10.002>, 2016.
- Exner, C.: *Erläuterungen zur Geologischen Karte der Umgebung von Gastein*, Verlag der Geologischen Bundesanstalt, Wien, 168 pp., 1957.
- Fellner, D.: Massenbewegungen im Bereich Bucheben im Hüttwinkeltal bei Rauris (Salzburg, Österreich), *Jahrbuch der Geologischen Bundesanstalt*, 136, 307–313, 1993.
- Geologische Bundesanstalt Österreich: *Geodaten – Bundesland Salzburg (1 : 200 000)*, Tethys RDR, Geologische Bundesanstalt (GBA), Wien, <https://doi.org/10.24341/tethys.190>, 2022.
- Griesmeier, G.: *Zusammenstellung ausgewählter Archivunterlagen der Geologischen Bundesanstalt 1 : 50 000 – 154 Rauris*, Vienna, 2021.
- Gruber, F.: *Das Raurisertal: Gold – Bergbaugeschichte*, Eigenverlag, Marktgemeinde Rauris, 256 pp., 2004.

- Hansche, I., Fischer, A., Greiling, M., Hartl, L., Hartmeyer, I., Helfricht, K., Hynek, B., Jank, N., Kainz, M., Kaufmann, V., Kellerer-Pirklbauer, A., Lieb, G. K., Mayer, C., Neureiter, A., Prinz, R., Reingruber, K., Reisenhofer, S., Riedl, C., Seiser, B., Stocker-Waldhuber, M., Strudl, M., Zagel, B., Zechmeister, T., and Schöner, W.: KryoMon.AT – Kryosphären Monitoring Österreich, 2021/22 Kryosphärenbericht No. 1, Österreich, Bundesministerium Klimaschutz, Umwelt, Energie, Mobilität, Innovation und Technologie, 204 pp., <https://doi.org/10.25364/402.2023.1>, 2023.
- Heim, A.: Bergsturz und Menschenleben, Beiblatt zur Vierteljahrsschrift der Naturforschenden Gesellschaft in Zürich, 20, 1–218, 1932.
- Hellerschmidt-Alber, J.: Bericht 1997 Über geologische Aufnahmen im Penninikum des Hüttwinkeltales auf Blatt 154 Rauris, Jahrbuch der Geologischen Bundesanstalt, 141, 297–302, 1998.
- Hottinger, A.: Geologie der Gebirge zwischen der Sonnblick-Hochalm-Gruppe und dem Salzachtal in den östlichen Hohen Tauern, PhD thesis, Eidgenössische Technische Hochschule Zürich, 123 pp., <https://www.research-collection.ethz.ch/bitstream/handle/20.500.11850/134235/eth-20951-02.pdf?sequence=2> (last access: 10 June 2024), 1935.
- Ivy-Ochs, S., Monegato, G., and Reitner, J. M.: Chapter 20 – The Alps: glacial landforms during the deglaciation (18.9–14.6 ka), in: *European Glacial Landscapes – The Last Deglaciation*, edited by: Palacios, D., Hughes, P. D., García-Ruiz, J. M., and Andrés, N., Elsevier, 175–183, <https://doi.org/10.1016/B978-0-323-91899-2.00005-X>, 2023a.
- Ivy-Ochs, S., Monegato, G., and Reitner, J. M.: Chapter 55 – The Alps: glacial landforms from the Younger Dryas Stadial, in: *European Glacial Landscapes – The Last Deglaciation*, edited by: Palacios, D., Hughes, P. D., García-Ruiz, J. M., and Andrés, N., Elsevier, 525–539, <https://doi.org/10.1016/B978-0-323-91899-2.00058-9>, 2023b.
- Klasen, N., Fiebig, M., Preusser, F., Reitner, J. M., and Radtke, U.: Luminescence dating of proglacial sediments from the Eastern Alps, *Quatern. Int.*, 164, 21–32, <https://doi.org/10.1016/j.quaint.2006.12.003>, 2007.
- Lichtenecker, N.: Die gegenwärtige und die eiszeitliche Schneegrenze in den Ostalpen, in: *Verhandlungen der III Internationalen Quartär-Konferenz, INQUA, Vienna, Austria, September 1936*, edited by: Göttinger, G., Geologische Landesanstalt, Vienna, Austria, 141–147, 1938.
- McSaveney, M. J. and Davies, T. R. H.: Inferences from the morphology and internal structure of rockslides and rock avalanches rapid rock mass flow with dynamic fragmentation, in: *Landslides from Massive Rock Slope Failure*, edited by: Evans, G. E., Mugnozza, G. S., Storm, A., and Hermanns, R. L., Springer, Dordrecht, 285–304, https://doi.org/10.1007/978-1-4020-4037-5_16, 2006.
- Penck, A.: Gletscherstudien im Sonnblickgebiete, *Zeitschrift des Deutschen und Österreichischen Alpenvereins*, 1897, 52–71, 1897.
- Penck, A. and Brückner, E.: *Die Alpen im Eiszeitalter. 1. Band: Die Eiszeiten in den nördlichen Ostalpen*, Tauchnitz, Leipzig, 393 pp., 1909.
- Pestal, G., Hejl, E., Braunstingl, R., Egger, H., Linner, M., Mandl, G. W., Moser, M., Reitner, J., Rupp, C., Schuster, R., and van Husen, D.: *Geologische Karte von Salzburg 1 : 200 000*, Geologische Bundesanstalt, Wien, 2005.
- Reitner, J. M.: Glacial dynamics at the beginning of Termination I in the Eastern Alps and their stratigraphic implications, *Quatern. Int.*, 164–165, 64–84, <https://doi.org/10.1016/j.quaint.2006.12.016>, 2007.
- Reitner, J. M.: The Imprint of Quaternary Processes on the Austrian Landscape, in: *Landscapes and Landforms of Austria*, edited by: Embleton-Hamann, C., Springer International Publishing, Cham, 47–72, https://doi.org/10.1007/978-3-030-92815-5_3, 2022.
- Reitner, J. M., Ivy-Ochs, S., Drescher-Schneider, R., Hajdas, I., and Linner, M.: Reconsidering the current stratigraphy of the Alpine Lateglacial: Implications of the sedimentary and morphological record of the Lienz area (Tyrol/Austria), *E&G Quaternary Sci. J.*, 65, 113–144, <https://doi.org/10.3285/eg.65.2.02>, 2016.
- Schmid, S. M., Fügenschuh, B., Kissling, E., and Schuster, R.: Tectonic map and overall architecture of the Alpine orogen, *Eclogae Geol. Helv.*, 97, 93–117, <https://doi.org/10.1007/s00015-004-1113-x>, 2004.
- Schuster, R., Daurer, A., Krenmayr, H. G., Linner, M., Mandl, G. W., Pestal, G., and Reitner, J. M.: *Rocky Austria. Geology of Austria – brief and colourful*, Geological Survey of Austria, Vienna, 80 pp., ISBN 978-3-85316-078-7, 2014.
- Steinbichler, M., Reitner, J., Lotter, M., and Steinbichler, A.: *Begriffskataloge der Geologischen Landesaufnahme für Quartär und Massenbewegungen in Österreich*, Jahrbuch der Geologischen Bundesanstalt, 159, 5–49, 2019.
- van Husen, D.: *Die Ostalpen in den Eiszeiten*, Veröffentlichungen der Geologischen Bundesanstalt, Vienna, 2, 1–24, ISBN 978-3-900312-58-9, 1987.
- van Husen, D. and Reitner, J. M.: Quaternary System, in: *The lithostratigraphic units of Austria: Cenozoic Era(them)*, edited by: Piller, W. E., *Abhandlungen der Geologische Bundesanstalt, Vienna*, 76, 240–267, ISBN 978-3-903252-14-1, 2022.
- von Poschinger, A.: *Instabile Talflanken in Kristallingesteinen und ihre geologischen Ursachen, dargestellt am Beispiel des oberen Hüttwinkeltales (Land Salzburg, Österreich)*, PhD thesis, Technische Universität München, 170 pp., 1986.
- Walker, M., Head, M. J., Berkelhammer, M., Björck, S., Cheng, H., Cwynar, L., Fisher, D., Gkinis V., Long, A., Lowe, J., Newnham, R., Rasmussen, S. O., and Weiss, H.: Formal ratification of the subdivision of the Holocene Series/Epoch (Quaternary System/Period): two new Global Boundary Stratotype Sections and Points (GSSPs) and three new stages/subseries, *Episodes* 2018, 41, 213–223, <https://doi.org/10.18814/epiuiugs/2018/018016>, 2018.
- Wirsig, C., Zasadni, J., Christl, M., Akçar, N., and Ivy-Ochs, S.: Dating the onset of LGM ice surface lowering in the High Alps, *Quaternary Sci. Rev.*, 143, 37–50, <https://doi.org/10.1016/j.quascirev.2016.05.001>, 2016.



Sediment dynamics of a major piedmont glacier: the Salzach Glacier in the North Alpine Foreland

Bernhard Salcher¹, Reinhard Starnberger², Thomas Pollhammer¹, and Joachim Götz³

¹Department of Environment & Biodiversity, Paris Lodron University of Salzburg, Salzburg, Austria

²Institute of Geology, University of Innsbruck, Innsbruck, Austria

³Geography Department, University of Bayreuth, Bayreuth, Germany

Correspondence: Bernhard Salcher (bernhard.salcher@plus.ac.at)

Relevant dates: Published: 9 September 2024

How to cite: Salcher, B., Starnberger, R., Pollhammer, T., and Götz, J.: Sediment dynamics of a major piedmont glacier: the Salzach Glacier in the North Alpine Foreland, *DEUQUA Spec. Pub.*, 5, 31–39, <https://doi.org/10.5194/deuquasp-5-31-2024>, 2024.

Abstract: The foreland basins of the European Alps were repeatedly covered by major piedmont glaciers during Quaternary glacial maxima. The Salzach Glacier was the easternmost of a series of large Pleistocene piedmont glaciers entering the North Alpine Foreland through major Alpine valleys. It covered an area of more than 1000 km² during at least four glacial maxima. The slightly elevated molasse bedrock provides a high potential for preservation of glacial landforms and offers an ideal setting to explore the erosional and depositional dynamics of a major glacier piedmont lobe. This field excursion guide leads to some selected key sites representing deposits of glacial advance, relative equilibrium, and ice lobe collapse.

1 Introduction

Quaternary landforms in the foreland basins of the European Alps record the impact of significant depositional and erosional processes associated with the dynamics of major piedmont glaciers. In the region between the Rhine Graben and the Bohemian Massif, individual glaciers along the mountain range reached areal extents comparable e.g. to the modern Malaspina piedmont glacier (Alaska Range). Between the Rhine Graben and the Bohemian Massif, at least four glaciation events with relatively similar spatial extents are indicated from landforms and terminal moraines. These periods are locally referred to as (from oldest to youngest) Günz, Mindel, Riss, and Würm (Penck and Brückner, 1909). Numerical age calculations for landforms that formed during the most recent two events suggest a close correlation with the global maximum of the last (Last Glacial Maximum, LGM)

and penultimate (Penultimate Glacial Maximum, PGM) periods of glaciation (e.g. Ivy-Ochs et al., 2022a, b). Landforms and outwash deposits related to the older two glacial maxima, Günz and Mindel, have so far not been successfully dated but are assumed to fall in the time periods of Marine Isotope Stage (MIS) 16 and 12 respectively (e.g. Raymo, 1997; van Husen and Reitner, 2011, 2022).

The Bavarian and Austrian parts of the Alpine Molasse basin provide particularly good conditions for glacial landform preservation. Glacial deposits sit on (glacially) flattened and slightly elevated molasse bedrock and host only small, low-order catchments with a low potential for fluvial erosion. Major fluvial processes are focused along the Alpine Danube tributaries (e.g. Salzach), which have also been partly overdeepened by the glaciers. Furthermore, there was sufficient space for the full development of the piedmont major lobes. This, in combination with slightly decreasing

extensions of glacier lobes during successive glacial maxima, offers the opportunity to explore landforms of three glacial maxima that predate the LGM.

This field excursion guide presents visits to glacial features which record the erosional and depositional dynamics associated with the advance and meltdown of a major glacial piedmont lobe, the Salzach Glacier (Fig. 1). The sequence of stops will provide insights into the temporal succession of processes, from ice build-up through maximum ice expansion and ice wastage at the onset of global climate relaxation, and finally analyses the effects of postglacial landscape dynamics in a deglaciated foreland region.

2 Stop 1: Döstling gravel pit – the advancing period of the Salzach Glacier lobe (Fig. 2)

The Döstling gravel pit is situated at the eastern slope of the Salzach valley and allows for insights into ca. 30 m thick glacial and glaciofluvial deposits. Deposition of coarse-grained fluvial sediments (upper and lower channel unit) is interpreted as originating from a bedload-dominated stream but regularly providing flow depths large enough for effective sorting (e.g. cross-bedded strata). The interfingering of the fluvial succession (*lower unit*) with the heavily consolidated basal till on top indicates that these sediments were deposited in the forefield of the advancing Salzach Glacier and later overridden by the ice. Rare occurrence of laminated fines within basal till may point to uncoupling of the ice from the bed, giving rise to melt-out till formation (Fig. 2e). The position of fluvial deposits relatively high up the valley suggests significant filling of the Salzach valley during these periods. Derived optically stimulated luminescence ages (Salcher et al., 2015) indicate that sediments of the lower unit (and thus the interfingered basal till) were deposited during the penultimate glaciation (Riss glaciation) and left uneroded by the LGM glacier. Ages exceeding the LGM are in principle agreement with the weathering intensity (e.g. Fig. 2g). Absolute ages are thus far not available from the *upper channel unit*. Thus, it is not clear whether the upper channel unit capped by *basal till* reflects an oscillation of the PGM glacier or glacial outwash of the advancing stage of the subsequent glaciation (LGM). The LGM glaciation might, however, have at least provided the modification of the glaciofluvial sediments into streamlined bedforms (Fig. 2b; Weinberger, 1952; Salcher et al., 2010).

3 Stop 2: Pfaffinger gravel pit – maximum position of the LGM glacier and evidence for the glacial series (Fig. 3)

This outcrop is situated within fluvial outwash closely related to the terminal moraine of the most extensive advance of the Salzach Glacier during the LGM (Fig. 3b). The terminal moraine of the penultimate glacial maximum (PGM,

Riss) can be recognised just north of the outcrop at an altitude of around 500 m a.s.l (above sea level). The outcrop shows a succession of three coarse-grained, massive units (Fig. 3a). These units consisting of non-channelised horizontal bedload sheets are considered to represent deposits of shallow flash floods relating to the upper flow regime (Miall, 1977; Todd, 1989). Supercritical sheetfloods are typical of alluvial fans (Nemec and Postma, 1993; Blair and McPherson, 1994) e.g. associated with a glacier, such as ice contact fans (Fig. 2b) or ramps (Benn and Evens, 1998; Krzyszkowski and Zielinski, 2002). The *lowest sheetflood unit* is separated from the *middle sheetflood unit* by a ca. 3–4 m thick layer of basal till. While there is a clear unconformity between the basal till and the middle sheetflood unit above, the transition from the lower sheetflood unit to the basal till is indistinct and marked by gravel sheets intercalated within the till (similar to the situation observed at “Döstling”; Stop 1, Fig. 2). The sequence refers to ice proximity and glacier coverage. The depositional context and luminescence ages suggest that these sediments were deposited during the penultimate glaciation (Riss, MIS 6). If not eroded, the top decimetres of the middle sheetflood unit may appear altered into a brownish–dark-reddish paleosol. It may also form distinct wedge-shaped structures (up to ca. 3 m) referring to periglacial features (i.e. ice wedge casts; see Salcher et al., 2015). The intensively weathered paleosol might have been mainly formed during the Riss–Würm interglacial period (Eemian). Just below the paleosol, sediment may locally appear cemented to conglomerates of decimetres in diameter. The absence of any weathering of the upper sheetflood unit agrees with the derived LGM age.

4 Stop 3: fluvial outwash and postglacial incision (Fig. 4)

Stop 3 (Ach) is located vis-à-vis Burghausen Castle. The position shows the altitudinal contrast in streamflow elevation of the Salzach River between full-glacial and interglacial (present) conditions (ca. 100 m). Numerous terrace steps nicely mark the successive incision of the river during deglaciation (Termination I; Fig. 4). Glacier retreat and associated fluvial incision must have been extraordinary rapid as glaciers were already at inner-Alpine positions at around 17–18 ka (e.g. Starnberger et al., 2011; Ivy-Ochs et al., 2023). Modern stream level located just above the Neogene bedrock suggests that the incision into sediments that were mainly accumulated during the LGM has largely ceased.

5 Stop 4: Jüngere Deckenschotter – glaciofluvial outwash of the Mindel glaciation (Fig. 5a, b)

Glaciofluvial sediments associated with Mindel glaciation are referred to as Jüngere Deckenschotter. These glaciofluvial gravels often appear as erosional remnants with re-

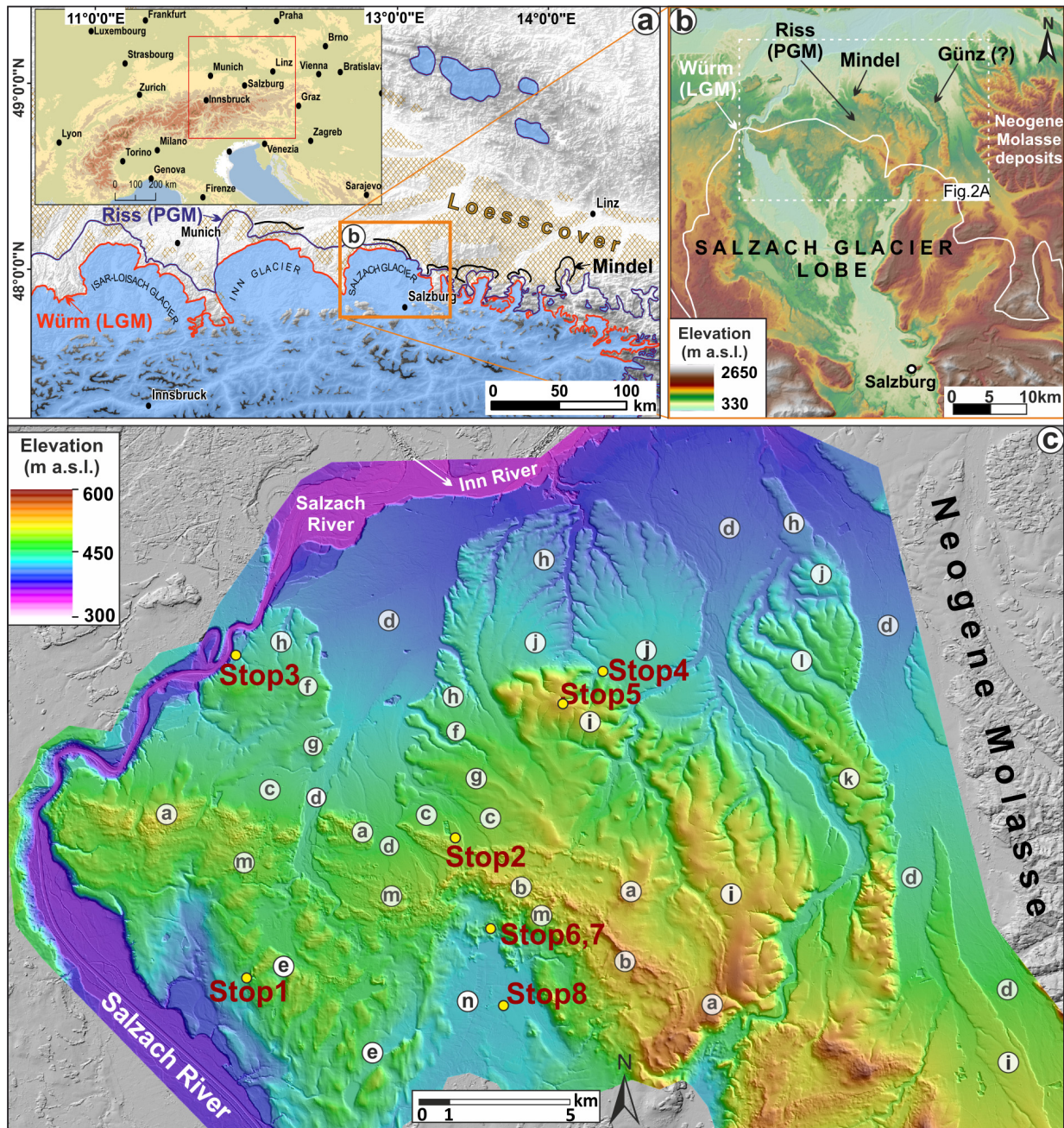


Figure 1. (a) Extent of the Salzach Glacier lobe in the North Alpine Foreland during full-glacial periods of the Last Glacial Maximum (LGM; “Würm”), the penultimate glacial maximum (PGM; “Riss”), and the antepenultimate maximum (“Mindel”, correlated to MIS 12; van Husen and Reitner, 2022). (b) Extent of the Salzach Glacier lobe during different glacial maxima and impact on topography. Miocene sediments preserved east of the major piedmont lobes. DEM bases on NASA’s SRTM (Shuttle Radar Topography Mission, 90 m; for details see Farr and Kobrick, 2000). Modified from Salcher et al. (2015). (c) Topographic overview, landforms, and planned stops in the field trip. Lowercase letters denote Quaternary landforms. (a) LGM (Würm) terminal moraine 1 (max extent). (b) LGM terminal moraine 2. (c) LGM upper outwash terrace “Obere Niederterrasse” (and sub-terrace levels) associated with terminal moraine 1. (d) LGM lower outwash terrace “Untere Niederterrasse” (and sub-terrace levels) associated with terminal moraine 2. (e) Channels of a subglacial drainage system (LGM). (f) Riss terminal moraine 1 (max extent). (g) Riss terminal moraine 2. (h) Riss outwash “Hochterrasse”. (i) Mindel terminal moraine. (j) Mindel outwash terrace “Jüngere Deckenschotter”. (k) Günz terminal moraine. (l) Günz outwash terrace “Ältere Deckenschotter”. (m) LGM ice wastage deposits. (n) Peat bog (Ibmer Moor). DEM resolution is 10 m (resampled from high-resolution airborne lidar; Land Oberösterreich, https://www.data.gv.at/katalog/en/dataset/land-ooe_digitales-gelandemodell-dgm, last access: 6 February 2023; hillshade from <https://www.basemap.at/wmts/1.0.0/WMTSCapabilities.xml> (via WTMS), last access: 1 June 2024). Landforms according to Kolmer et al. (2008) and Salcher et al. (2010).

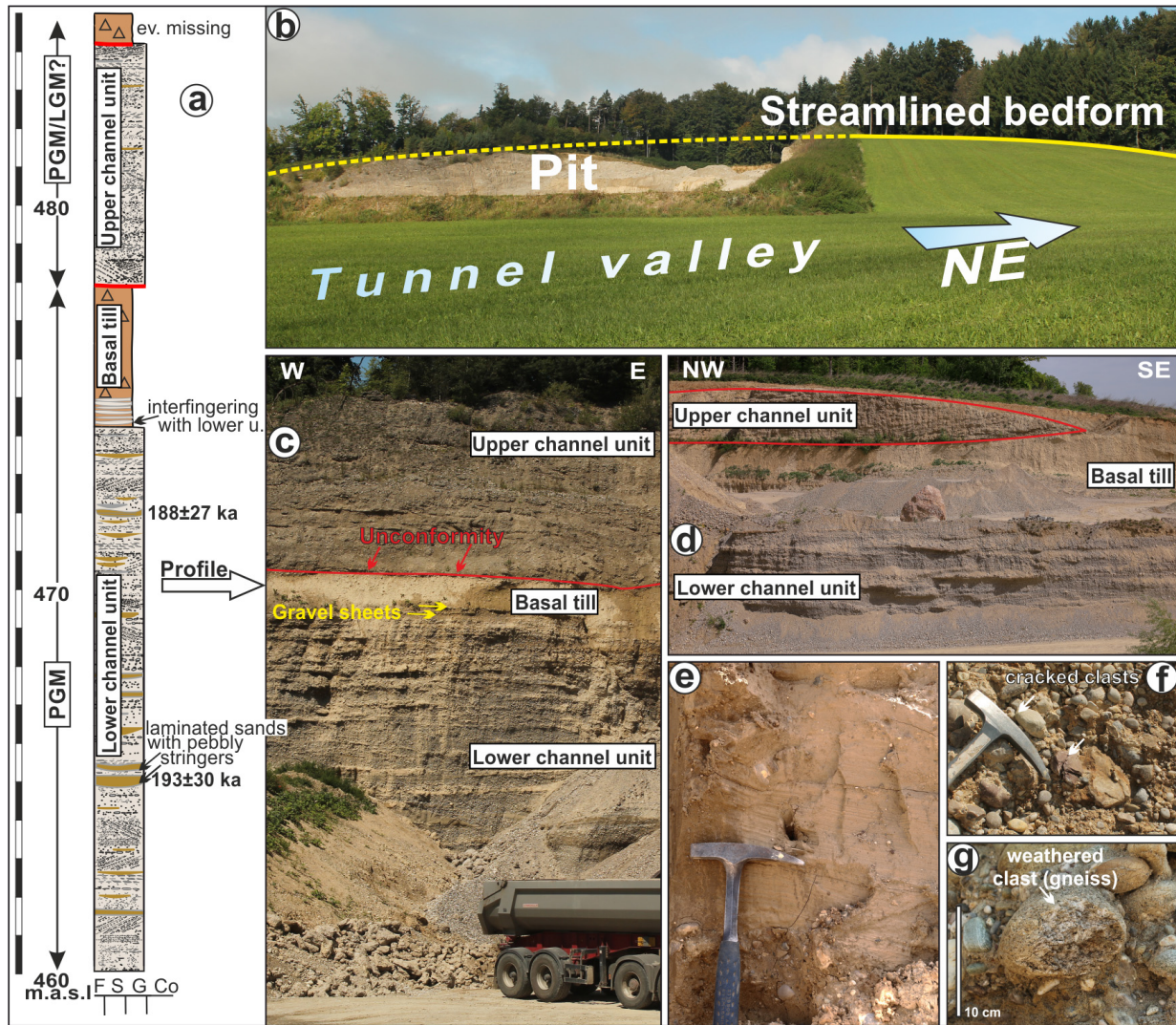


Figure 2. (a) Geological profile showing sediments that represent the advancing stage of the Salzach Glacier. Luminescence ages are indicated (Salcher et al., 2015). (b–d) Glaciofluvial deposits (c, d) are capped by basal till and (b) were streamlined by ice flow. (e) Rare occurrence of laminated fines within basal till may point to uncoupling of the ice from the bed, giving rise to melt-out till formation. (f) Clast supported fluvial sediments are prone to cracking through ice overburden. (g) Relatively high weathering degree of some components is in accordance with depositional ages (PGM). Panels (a) and (b) are modified from Salcher et al. (2015).

stricted spatial extent and are typically characterised by a high degree of cementation (e.g. van Husen, 2000). Pipe-like structures representing zones of focused weathering (“Geologische Orgeln”) are furthermore typical (e.g. Lempe, 2012) but not obvious in this outcrop. Both the high degree of cementation and the intense weathering are a function of time and the relatively high content of carbonate clasts (acting as source of dissolution and subsequent carbonate precipitation). The sedimentary setting reflects a dynamic ice marginal environment with features of the lower- and higher-flow regime. The cave-like appearance of this outcrop seems at least to be partly natural. This is suggested by the recent discovery of a cave (total length of ca. 20 m) by mining activities in the adjacent gravel pit about 200 m to the

west. Radiometric age constraints of Mindel stage deposits are largely absent. Deposits are considered to fall into MIS 12 (van Husen and Reitner, 2011, 2022).

6 Stop 5: Mindel terminal moraine (Fig. 5c)

The Mindel glaciation is considered to reflect the most extensive glaciation in the North Alpine Foreland of the Eastern Alps (Penck and Brückner, 1909). Only a few spots suggest terminal moraines outside of this stage (“Günz”). Terminal moraines of the Mindel glaciation generally exceed the width and height of terminal moraines of other glacial maxima by far.

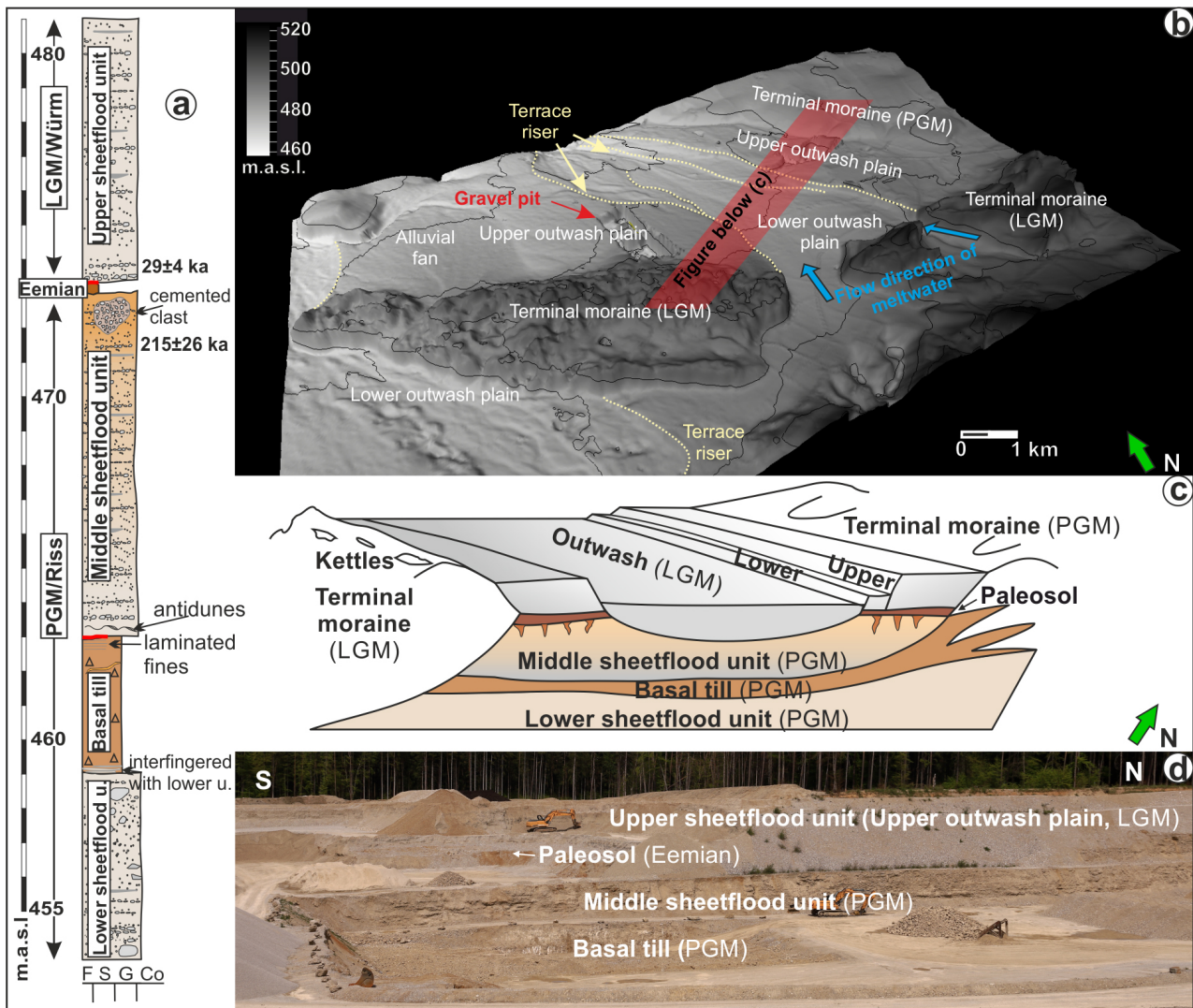


Figure 3. (a) Stratigraphic profile of the outcrop “Pfaffinger” indicating some observed features and the position of derived luminescence data. See (b) for the position. (b) Topography near the terminus of the Salzach Glacier lobe. The gravel pit is located within outwash associated with the terminal moraine of the most extensive position of the LGM (terminal moraine 1; see also Fig. 2). The red bar denotes the geological 3D profile shown in (c). (c) Sketch illustrating the stratigraphy of Würmian (LGM) and Rissian (PGM) deposits. Outwash gravel deposited during the advancing stage of the Riss period was later overridden by the glacier as indicated by the basal till. Later, during ice collapse at the end of the Riss period (Termination II), outwash was deposited on top of the basal till. These sediments were subjected to intense soil-forming processes (last interglacial paleosol) and occasionally covered by loess. The sketch is in good accordance with the glacial-series model of Penck and Brückner (1909). Modified from Salcher et al. (2015). (d) Outcrop overview as of April 2024. DEM resolution is 1 m (Land Oberösterreich, <http://data.ooe.gv.at>, last access: 16 July 2024).

7 Stop 6: Termination I – ice wastage and associated landforms (Fig. 6)

Ice wastage may result in the formation of hummocky moraine and specific landforms like kames or kettle holes comprising a mixture of fluvial, gravitational, and lacustrine deposits. Along the Salzach Glacier lobe, ice wastage deposits are focused in a small area along the former ice margin, commonly not exceeding a width of several hundred metres (cf. Eyles et al., 1999). Glacial recession is often accom-

panied by the formation of short-lived lakes and local kame delta deposition (Fig. 6). Ephemeral lakes may have formed between the ice margin and e.g. the terminal moraine. The top of a delta surface can thereby refer to the altitude of the former lake level. Ice wastage deposits are often characterised by relatively steep surface slopes (Fig. 6c) which are prone to solifluction and slope failure. The characteristic steep topography is therefore not long lived, and landforms can hardly be recognised outside the limits of the LGM.

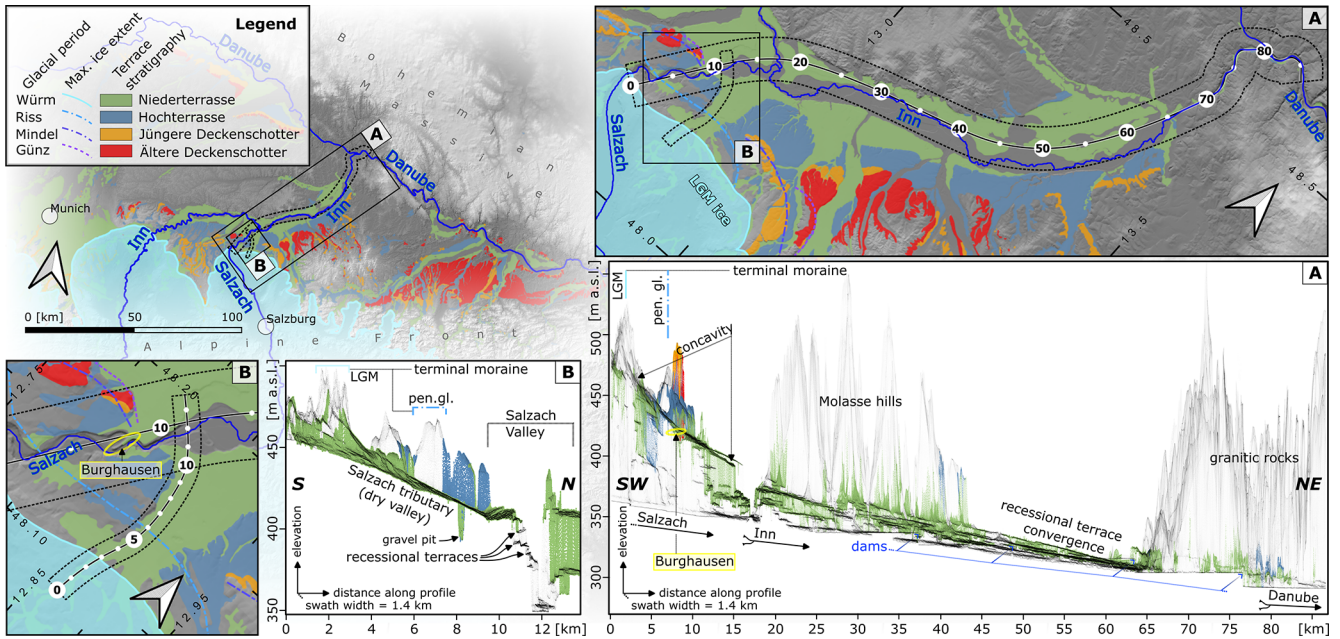


Figure 4. Longitudinal swath profile along the Salzach–Inn (A). Digital topographic data (10 m resolution) are orthogonally projected onto the profile line (black) within the marked swath (dashed black lines; see map views). Fill terraces in glaciofluvial outwash of the LGM (Niederterrasse, green colour) were created during glacier meltdown and the lowering of the outwash source (glacier terminus). Close to the LGM terminal moraine, top slopes reach up to > 10%. Glacier retreat and associated lowering of the glacier terminus led to the decrease in profile slopes. In contrast to terraces of different glacial maxima, recessional levels converge at the same altitude. Profile (B) shows the topography of the main outwash plain, which was active during the full extent of the Salzach Glacier during the LGM (terminal moraine 1, 2). Slightly different outwash slopes reflect different LGM positions. With the onset of deglaciation and glacier recession towards the Salzach valley, this outwash plain got quickly abandoned and laterally cut ca. at kilometre marker 10. DEM resampled from Land Oberösterreich (https://www.data.gv.at/katalog/en/dataset/land-ooe_digitaales-gelandemodell-dgm).

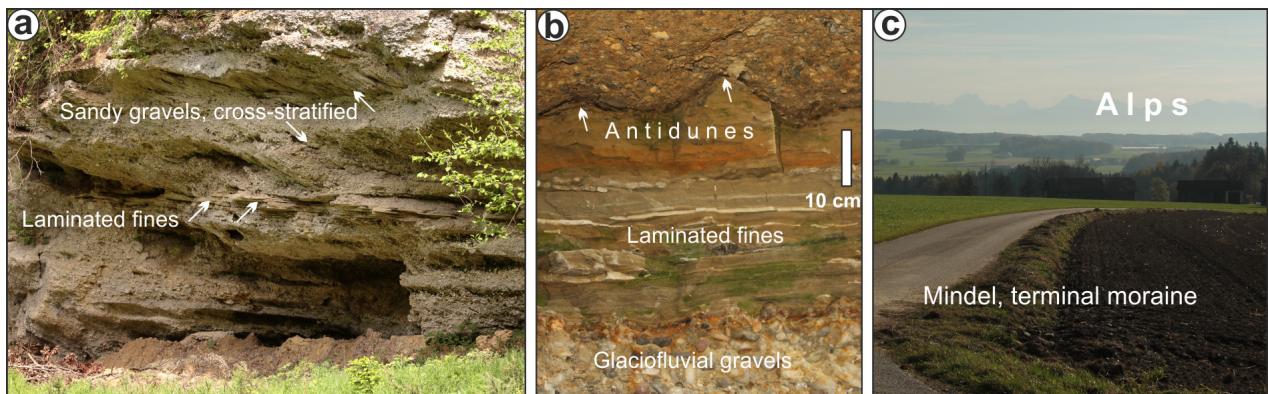


Figure 5. Deposits of the Mindel glaciation. (a) Glaciofluvial gravels (“Höhere Deckenschotter”) associated with the Mindel glaciation show horizontal and cross-bedded strata. A highly dynamic setting (like e.g. an ice marginal fan) is suggested by features of the upper flow regime representing antidunes and upper-stage plane beds (b). (c) View from the Mindel terminal moraine (MIS 12?) towards the Alps.

8 Stop 7: Jackenmoos mire – the formation of kettle holes and its importance for postglacial processes (Fig. 7)

The detachment of ice fragments from the glacier to form dead ice is a common process during meltdown. Sinks or kettle holes can result if dead ice is buried by sediments. They

are typically prevalent in terminal moraines (see Fig. 3) or associated with ice wastage deposits. Kettle holes often appear in larger fields with numerous kettles side by side. Depending on sediment and water inflow, these forms may contain (ephemeral) bodies of standing water. Through horizontal or vertical terrestrialisation (small) lakes may also turn

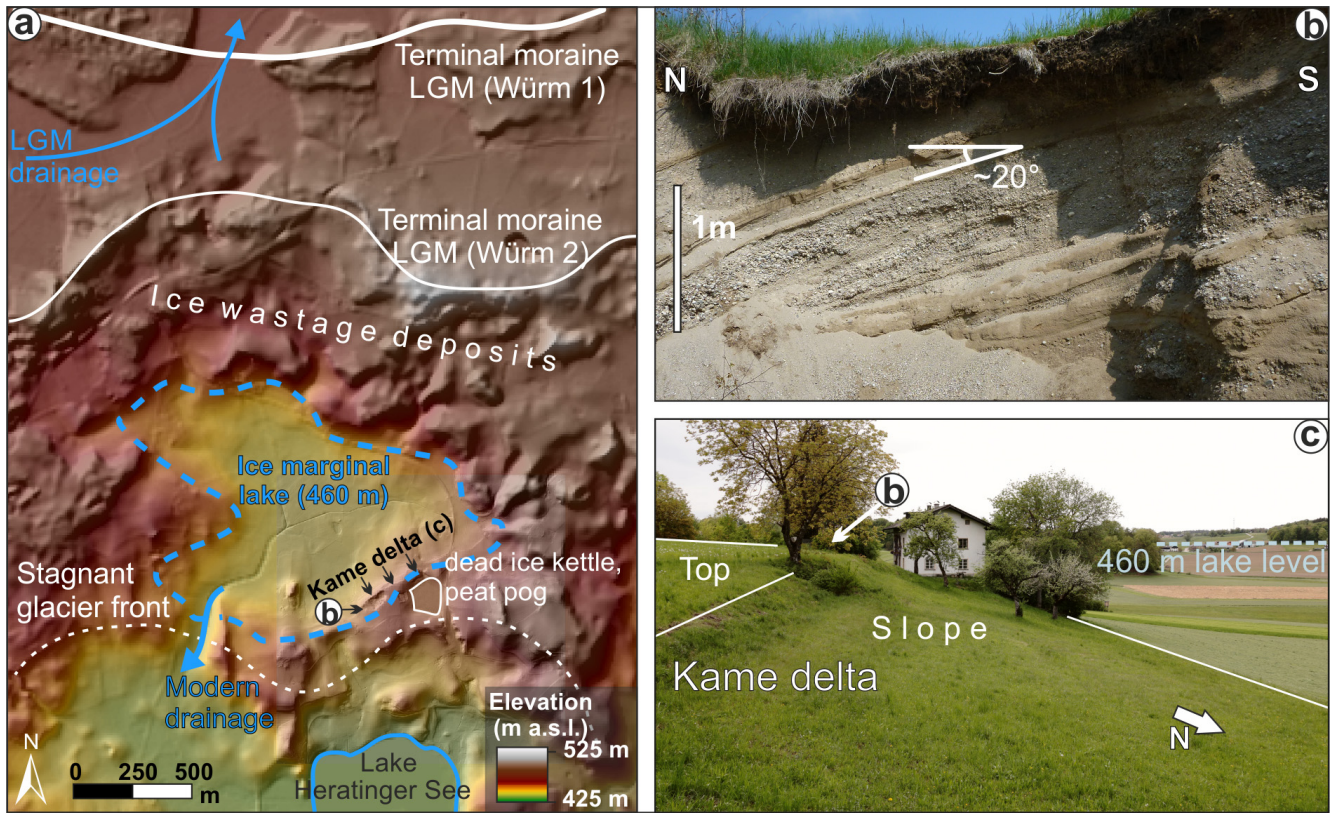


Figure 6. (a) Ice wastage deposits are typically represented by small, steeply sloped landforms near the terminal moraines. DEM from Land Oberösterreich (<http://data.ooe.gv.at>). (b) Foreset of a local kame delta deposit. See (a) for the location. (c) The top of the kame delta marks the former altitude of a short-lived ice marginal lake. The presence of dead ice led to the formation of a large kettle hole. This sink turned into a kettle hole mire (Stop 7).

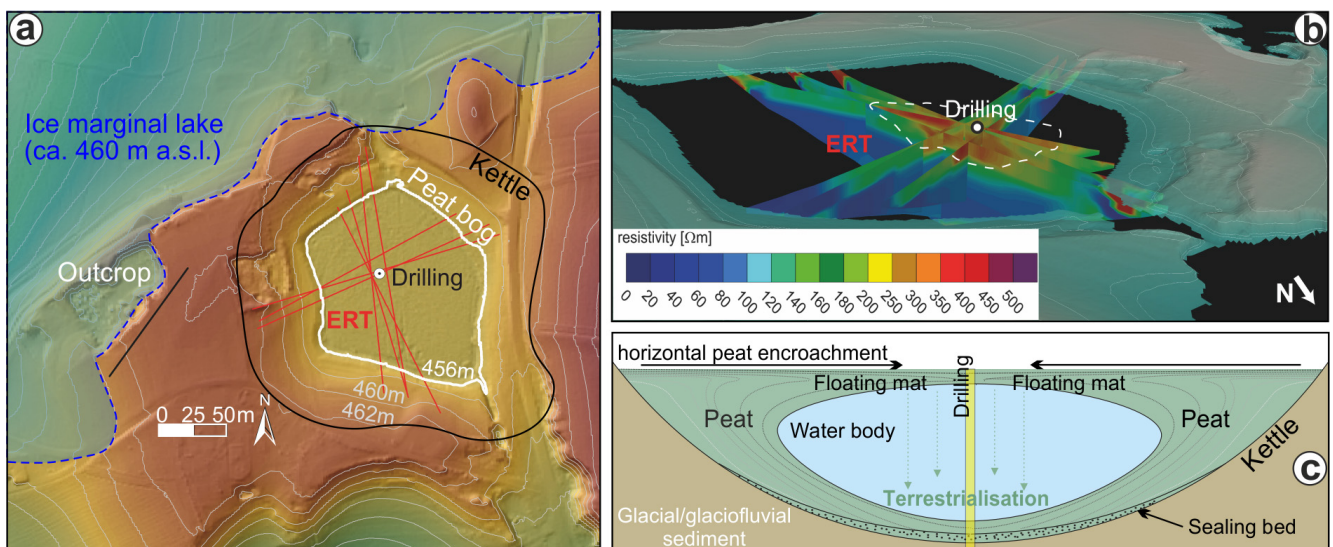


Figure 7. (a) Jackenmoos mire formed in a kettle hole of a kame delta (Fig. 6). (b) Distribution of resistivity within the mire is shown by electrical resistivity tomography (ERT). The waterbody is indicated by values of high resistivity referring to a low degree of mineralisation. (c) Concept of floating-mat terrestrialisation after Gaudig et al. (2006) and Götz et al. (2018). The location of the drill core is highlighted as a yellow bar. DEM from Land Oberösterreich (<http://data.ooe.gv.at>). Modified from Götz et al. (2018).

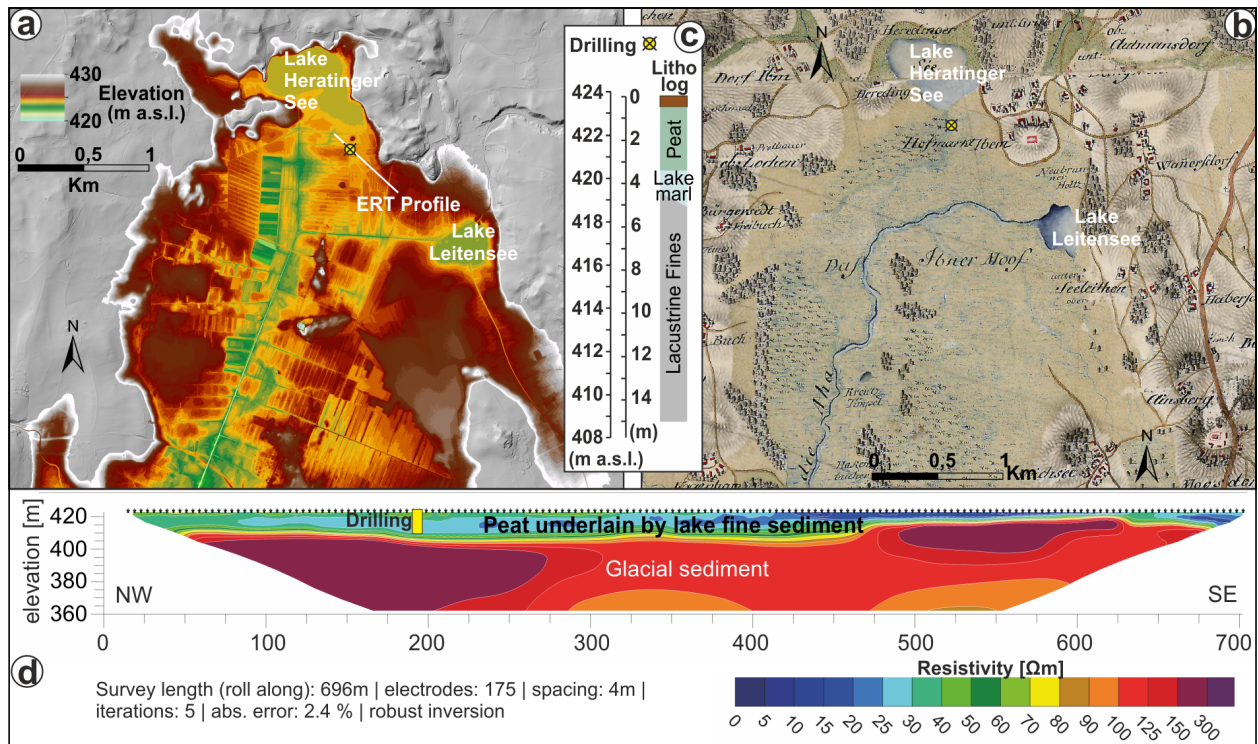


Figure 8. (a) Topography of Austria’s largest peat bog (Ibmer Moor, northern part). DEM with 0.5 m ground resolution (Land Oberösterreich, <http://data.ooe.gv.at>) highlights the major anthropogenic overprint through artificial drainage (long linear features of some 100 m) and peat exploitation (rectangular features). (b) First Military Survey (Josephinische Landesaufnahme; 1775–1777) showing approximately the same area as above (a) but with a largely undisturbed environment. Note the modifications to the drainage system. Map is derived from <http://mapire.eu> (last access: 1 June 2024). (c) Drill log showing the postglacial to Holocene stratigraphy just south of Lake Heratinger See. (d) Electrical resistivity tomography section. Low-resistivity parts (blue–green) indicate the presence of lake fines (clay, lake marls). Higher values (red colours) indicated the presence of coarse-grained glacial sediment. Panel (d) was modified from Götz et al. (2018).

into kettle hole mires (Fig. 7). In the process of terrestrialisation waterbodies can be completely covered by a floating vegetation mat and peat (Fig. 7c). The contrast between the floating mat, the waterbody, the underlying material, and the rim of the kettle can be discriminated by electrical resistivity tomography well (Fig. 7b). The unusual high resistivity of the waterbody is a function of low mineralisation.

9 Stop 8: Ibmer Moor peat bog – natural trail (Fig. 8)

The “Ibmer Moor” is the largest peat bog area in Austria. This stop on the natural trail gives an overview of some relatively undisturbed parts of the peat bog. While the peat bog in the southern part (located in the federal state of Salzburg) was completely exploited (and thus destroyed), the northern, Upper Austrian part remained better preserved. Large parts of the peat bog formed through late-glacial to Holocene terrestrialisation of a lake that had been left after deglaciation. This process was promoted by the water depth of only a few metres. Climate relaxation is indicated by lake marl deposition often present below the peat. Two small residual lakes are

still left from the ongoing process of terrestrialisation (Lake Heratinger See and Lake Leitensee).

Data availability. DEM data can be accessed via https://www.data.gv.at/katalog/de/dataset/land-ooe_digitaales-gelandemodell-dgm (Federal state of Upper Austria, 2024).

Author contributions. BS and RS planned the field trip and the article together. BS made most figures and wrote the major part with contributions from all authors. Figure 4 was entirely made by TP.

Competing interests. At least one of the (co-)authors is a guest member of the editorial board of *DEUQUA Special Publications* for the special issue “Quaternary landscape dynamics in the Eastern Alps: from the highest peaks to the northern foreland basin – a guidebook to field trips”. The peer-review process was guided by an independent editor, and the authors also have no other competing interests to declare.

Disclaimer. Publisher's note: Copernicus Publications remains neutral with regard to jurisdictional claims made in the text, published maps, institutional affiliations, or any other geographical representation in this paper. While Copernicus Publications makes every effort to include appropriate place names, the final responsibility lies with the authors.

Acknowledgements. We highly appreciate Ylvie Aranmanoth's field assistance. Furthermore, we thank Noreen Vielreicher for English language corrections in an earlier version of the paper.

Financial support. This research has been supported by the Paris Lodron University of Salzburg Publication Fund.

References

- Benn, D. I. and Evans, D. J. A.: *Glaciers and Glaciations*, Arnold, London, ISBN 0-340-58431-0, 1998.
- Blair, T. C. and McPherson, J. G.: Alluvial fan processes and their natural distinction from rivers based on morphology, hydraulic processes, sedimentary processes, and facies, *J. Sediment. Res.*, 64A, 450–489, 1994.
- Eyles, N., Boyce, J. I., and Barendregt, R. W.: Hummocky moraine: sedimentary record of stagnant Laurentide Ice Sheet lobes resting on soft beds, *Sediment. Geol.*, 123, 163–174, 1999.
- Farr, T. G. and Kobrick, M.: Shuttle Radar Topography Mission produces a wealth of data, *Eos, Transactions AGU*, 81, 583–583, 2000.
- Federal state of Upper Austria: Digital elevation model of Upper Austria (0.5 m resolution baseing on airborne laserscan missions), Federal state of Upper Austria (Land Oberösterreich), data.gv.at [data set], https://www.data.gv.at/katalog/en/dataset/land-ooe_digitaales-gelandemodell-dgm, last access: 16 July 2024.
- Gaudig, G., Couwenberg, J., and Joosten, H.: Peat accumulation in kettle holes: bottom up or top down?, *Mires Peat.*, 1, 1–16, 2006.
- Götz, J., Salcher, B. C., Starnberger, R., and Krisai, R.: Geophysical, topographic and stratigraphic analyses of perialpine kettles and implications for postglacial mire formation, *Geogr. Ann. A*, 100, 254–271, 2018.
- Ivy-Ochs, S., Monegato, G., and Reitner, J. M.: The Alps: glacial landforms from the Last Glacial Maximum, in: *European Glacial Landscapes*, edited by: Palacios, D., Hughes, P. D., García-Ruiz, J. M., and Andrés, N., Chap. 58, 449–460, Elsevier, Amsterdam, the Netherlands, <https://doi.org/10.1016/B978-0-12-823498-3.00030-3>, 2022a.
- Ivy-Ochs, S., Monegato, G., and Reitner, J. M.: The Alps: glacial landforms prior to the Last Glacial Maximum, in: *European Glacial Landscapes*, edited by: Palacios, D., Hughes, P. D., García-Ruiz, J. M., and Andrés, N., Chap. 39, 283–294, Elsevier, Amsterdam, the Netherlands, <https://doi.org/10.1016/B978-0-12-823498-3.00008-X>, 2022b.
- Ivy-Ochs, S., Monegato, G., and Reitner, J. M.: The Alps: glacial landforms during the deglaciation (18.9–14.6 ka), in: *European Glacial Landscapes*, edited by: Palacios, D., Hughes, P. D., García-Ruiz, J. M., and Andrés, N., Chap. 20, 175–183, Elsevier, Amsterdam, the Netherlands, <https://doi.org/10.1016/B978-0-323-91899-2.00005-X>, 2023.
- Kolmer, C., van Husen, D., and Salcher, B.: *Landschaftsgeschichte und Hydrogeologie der neogenen und quartären Ablagerungen zwischen Mattig und Inn*, Amt der oberösterreichischen Landesregierung, Linz, Austria, 243 pp., 2008.
- Krzyszowski, D. and Zielinski, T.: The Pleistocene end moraine fans: controls on their sedimentation and location, *Sediment. Geol.*, 149, 73–92, 2002.
- Lempe, B.: Die geologischen Verhältnisse auf der GK25 Blatt Nr. 8027 Memmingen unter besonderer Berücksichtigung der Verwitterungserscheinungen in pleistozänen Schmelzwasserschottern und deren Einfluss auf ihre bautechnischen Eigenschaften. Entwicklung einer Verwitterungsklassifizierung, PhD Thesis, Technische Universität München, 224 pp., <http://mediatum.ub.tum.de/node?id=1096718> (last access: 16 May 2024), 2012.
- Miall, A. D.: A review of the braided river depositional environment, *Earth Sci. Rev.*, 13, 1–62, 1977.
- Nemec, W. and Postma, G.: Quaternary alluvial fans in southwestern Crete: sedimentation processes and geomorphic evolution, in: *Alluvial Sedimentation: International Association of Sedimentologists. Special Publication*, edited by: Marzo, M. and Puigdefabrogas, C., Blackwell Science, <https://doi.org/10.13140/2.1.1535.5521>, 1993.
- Penck, A. and Brückner, E.: *Die Alpen im Eiszeitalter*, Tauchnitz, Leipzig, 1909.
- Raymo, M. E.: The timing of major climatic terminations, *Paleoceanography*, 12, 577–585, 1997.
- Salcher, B. C., Hinsch, R., and Wagreich, M.: High-resolution mapping of glacial landforms in the North Alpine Foreland, Austria, *Geomorphology*, 122, 283–293, 2010.
- Salcher, B. C., Starnberger, R., and Götz, J.: The last and penultimate glaciation in the North Alpine Foreland: New stratigraphical and chronological data from the Salzach glacier, *Quatern. Int.*, 338, 218–231, 2015.
- Starnberger, R., Rodnight, H., and Spötl, C.: Chronology of the Last Glacial Maximum in the Salzach Palaeoglacier Area (Eastern Alps), *J. Quaternary Sci.*, 26, 502–510, 2011.
- Todd, S. P.: Stream-driven, high-density gravelly traction carpets: possible deposits in the Trabeg Conglomerate Formation, SW Ireland and some theoretical considerations of their origin, *Sedimentology*, 36, 513–530, <https://doi.org/10.1111/j.1365-3091.1989.tb02083.x>, 1989.
- van Husen, D.: Geological processes during the Quaternary, *Mitteilungen der Österreichische Geologische Gesellschaft*, 92, 135–156, 2000.
- van Husen, D. and Reitner, J. M.: An Outline of the Quaternary Stratigraphy of Austria, *E&G Quaternary Sci. J.*, 60, 24, <https://doi.org/10.3285/eg.60.2-3.09>, 2011.
- van Husen, D. and Reitner, J. M.: Quaternary System, in: *The Lithostratigraphic Units of Austria: Cenozoic Era(them)*, edited by: Piller, W. E., Geological Survey of Austria, Vienna, 240–267, ISBN 978-3-903252-15-8, 2022.
- Weinberger, L.: Ein Rinnensystem im Gebiete des Salzach-Gletschers, *Zeitschrift für Gletscherkunde und Glazialgeologie*, vol. 2, 1952.



Brunhes to burials – loess region of Krems, Lower Austria

Tobias Sprafke^{1,2}, Robert Peticzka³, Christine Thiel⁴, and Birgit Terhorst⁵

¹School of Agronomy, Forestry, and Food Sciences (HAFL), Bern University of Applied Sciences, Länggasse 85, 3052 Zollikofen, Switzerland

²Institute of Geography, University of Bern, Hallerstrasse 12, 3012 Bern, Switzerland

³Department of Geography and Regional Research, University of Vienna, Althanstrasse 14, 1090 Vienna, Austria

⁴Federal Institute for Geosciences and Natural Resources, Stilleweg 2, 30655 Hanover, Germany

⁵Institute of Geography and Geology, University of Würzburg, Am Hubland, 97074 Würzburg, Germany

Correspondence: Tobias Sprafke (tobias.sprafke@bfh.ch)

Relevant dates: Published: 9 September 2024

How to cite: Sprafke, T., Peticzka, R., Thiel, C., and Terhorst, B.: Brunhes to burials – loess region of Krems, Lower Austria, *DEUQUA Spec. Pub.*, 5, 41–54, <https://doi.org/10.5194/deuquasp-5-41-2024>, 2024.

Abstract: This excursion is dedicated to loess–paleosol sequences (LPSs) and the Quaternary research history in the region around Krems an der Donau (Krems a.d. Donau), Austria. The landscape at the eastern exit of the picturesque Wachau valley, carved by the Danube into crystalline basement rocks, is covered by thick loess and has a more than 100-year-long research history. Local Upper Paleolithic findings (e.g., Venus of Willendorf, Fanny of Stratzing, Wachtberg infant burials) are world famous. The outcrops of Paudorf, Göttweig-Furth, and Krems-Schießstätte were type localities of the Quaternary period until the 1970s. Recently, these complex LPSs with discontinuities and polygenetic units were reinvestigated, with a focus on the Middle to Late Pleistocene (Brunhes) record.

1 Introduction

Loess exposures are among the most instructive Quaternary paleoenvironmental archives. Loess–paleosol sequences (LPSs) record phases of morphodynamic activity and stability, mainly driven by climatic variations (Pécsi and Richter, 1996; Rohdenburg, 1970). Sedimentological approaches support paleoenvironmental reconstructions from loess packages (Antoine et al., 2009; Újvári et al., 2016), whereas paleopedological work is required for paleosols, which represent distinct paleoecological conditions of a certain duration (Bronger, 1976; Sprafke, 2016). Hiatuses and polygenetic units complicate paleoclimatic interpretations but add insights into geomorphic evolution (Lehmkuhl et al., 2021, 2016).

The region around Krems an der Donau (Krems a.d. Donau) (Fig. 1) in Lower Austria, at the eastern end of the

Wachau valley, is widely known for thick LPSs (< 40 m) and has a long research tradition (Petschko et al., 2022; Riedl et al., 2022). In the first half of the 20th century, local LPSs provided a stratigraphic framework for enclosed Paleolithic findings, foremost the world-famous Venus of Willendorf (Bayer, 1913, 1909). Important recent discoveries are the Venus of Galgenberg (Neugebauer-Maresch, 1993) and the Wachtberg double infant burial (Einwögerer et al., 2006). Famous loess outcrops in this area are Paudorf, Göttweig, and Krems, which were type localities of the Quaternary (Bayer, 1913; Fink, 1961, 1956; Götzinger, 1936; Kovanda et al., 1995), before the emergence of marine stratigraphy in the 1970s (Emiliani, 1955; Shackleton and Opdyke, 1973).

Local LPSs are mainly located in slope positions; due to erosional and colluvial processes the LPSs contain discontinuities and polygenetic units. Detailed macro- and micromorphological observations coupled with numerical ages

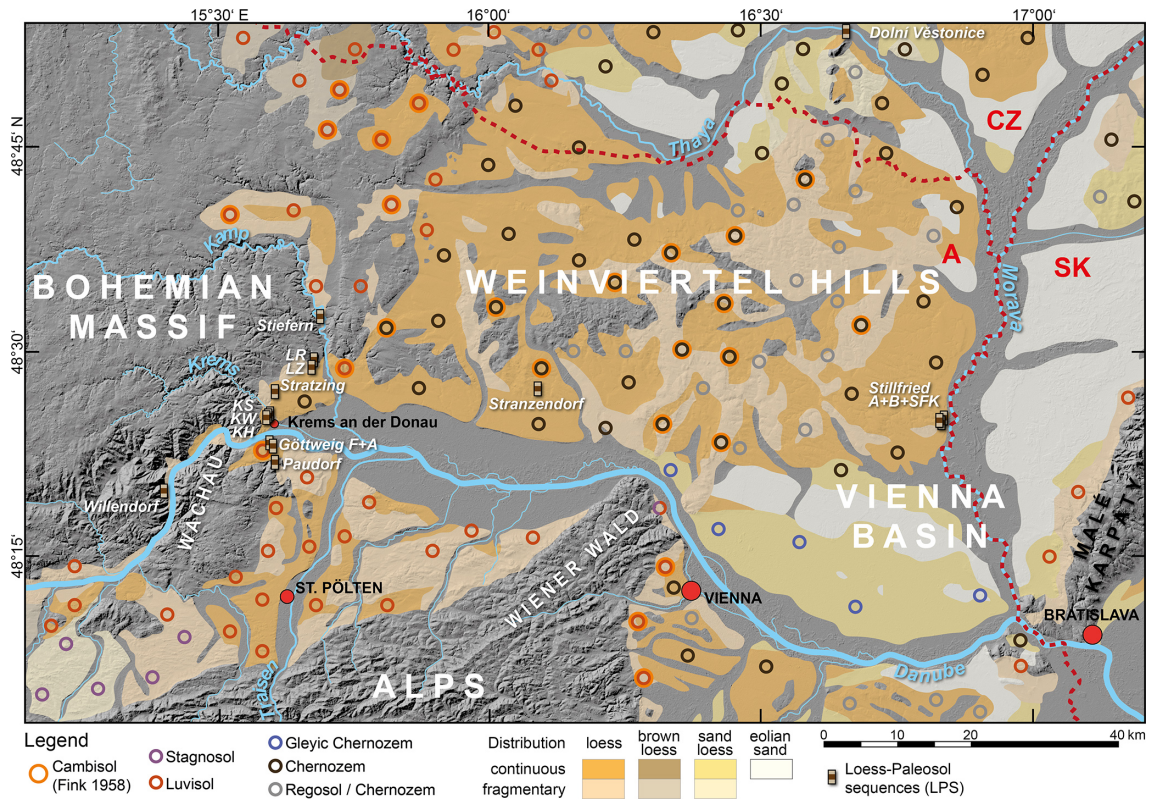


Figure 1. Topography, eolian sediments, soils from loess (soil types tentatively adapted to IUSS Working Group WRB, 2022), and LPSs in northeastern Austria, based on Loishandl and Peticzka (2005), Fink (1958), and Fink and Nagl (1979); hillshade from USGS (2014). Humid loess landscape located around St. Pölten and further west, transition area to the north along the Bohemian Massif eastern margin, and dry loess landscape further east (Fink, 1965). LR, LZ: Langenlois Red Outcrop, Langenlois Ziegelei (brickyard) Kammerer; KS, KW, KH: Krems-Schießstätte, Krems-Wachtberg, Krems-Hundssteig; F+A: Furth and Aigen.

have helped to unravel the formation processes and their timing (Sprafke et al., 2014). Colorimetric and granulometric data from samples taken in high vertical resolution along a continuous column (Antoine et al., 2009) have proven exceptionally useful for stratigraphic differentiation (Sprafke, 2016; Sprafke et al., 2020).

This field trip aims to present concepts and data from the last 15 years of research against the background of more than 100 years of variegated research history. Unless indicated otherwise, figures relate to Sprafke (2016) with modifications.

1.1 Physical geography of the excursion area

The excursion area is located in the surroundings of Krems a.d. Donau in the western part of Lower Austria. The Wachau region and the “Weinviertel” region further east are known for the rather continental, “Pannonian” climate (Nagl, 1983). The considerable climatic gradient between the oceanic northwest (700–900 mm m.a.p.) and the continental northwest (500–600 mm m.a.p.) is related to the Bohemian Massif acting as a barrier for Atlantic moisture brought by the westerlies. This highland (~ 500–1000 m a.s.l.) represents the re-

maining crystalline basement of the Paleozoic Variscan orogen (Matura, 2006). The lowlands (~ 180–500 m a.s.l.) between the Alps and the Bohemian Massif are mainly filled with molasse sediments deposited during the Alpine orogeny. During the late Neogene to the Quaternary the Danube and its tributaries removed a considerable amount of these sediments and left fluvial deposits (Wessely and Draxler, 2006), which are present in terraces of varying altitudes and degrees of preservation. Like the Pleistocene fluvial deposits, the widespread loess cover was deposited during cold stages (Fig. 1). The connection of terraces and loess stratigraphy has remained difficult, due to incomplete records and different tectonic impact (Sprafke, 2021). The present-day soil cover in the loess area reflects climatic differences. Southwest of the Bohemian Massif there are (often Stagnic) Luvisols (Ah–E–Bt–C profile), whereas mainly Chernozems (Ah–C profile) developed on a comparable substrate further east, representing forest and steppe soils, respectively (Fink et al., 1979; IUSS Working Group WRB, 2022).

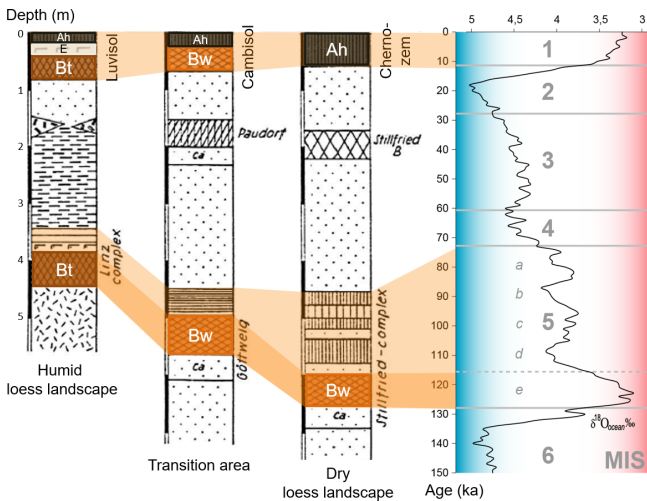


Figure 2. The classic pedostratigraphic model of Austrian LPSs (Fink, 1965) and correlation with the marine oxygen isotope record (Railsback et al., 2015). The proposed chronostratigraphy of the transition area (Fink, 1976) is no longer valid.

1.2 Loess landscapes and paleosols in Austria

Based on the obvious differences in soil cover and observations in the loess record, Fink (1956) postulated a subdivision of the Austrian lowlands into three loess landscapes (Fig. 2). The humid loess landscape (Feuchte Lösslandschaft) west of the Bohemian Massif with Holocene Luvisols from loess also exhibits a Bt horizon representing the last interglacial, which is superimposed by colluvial layers (“Linz complex”). The dry loess landscape (Trockene Lösslandschaft) east of the Bohemian Massif, characterized by Chernozems, hosts a Bw horizon representing the last interglacial, which is superimposed by a stack of humic horizons divided by thin loess layers (“Stillfried complex”). This pedostratigraphic concept basically remains valid until today, whereas the transition area (Übergangsgebiet) in between the humid and dry loess landscape and its pedostratigraphy were the subject of considerable controversies (Fink, 1979b; Sprafke, 2021).

Paudorf, Göttweig, and Krems were established in the 1960s as key units of Quaternary stratigraphy (Fink, 1961, 1965), as the thick LPSs of the transition area are unique for central Europe and were thought to be rather complete. The ~1–2 m thick paleosol Göttinger Verlehmungszone (GVZ) was first thought to represent a warm Aurignacian (early Upper Paleolithic) period, followed by loess deposition during the colder Gravettian (Bayer, 1913); 2 decades later, a ~1 m thick humic, slightly weathered pedocomplex in the upper part of the Paudorf loam pit (Paudorfer Bodenbildung) was attributed to a major interstadial of the last glacial, whereas the 2 m thick pedocomplex in the lower part of the profile was correlated to the GVZ and the last interglacial (Fink, 1956; Göttinger, 1936). Further, in the outcrop of Krems-Schießstätte, a pedocomplex that was thought to represent

the GVZ was recognized (Fink, 1976: KR4 paleosol). A ~3–4 m thick complex of rather strongly weathered soils below KR4 (Kremser Komplex; Fink, 1976: KR7–9) was attributed to a previous long interglacial (Fink, 1961).

However, fundamental revisions had to be accepted in the 1970s in the context of a Czech–Austrian collaboration. Mollusks in the Paudorfer Bodenbildung indicated its formation during the last interglacial, and the Göttinger Verlehmungszone was related to a Middle Pleistocene interglacial (Fink, 1969). As the Matuyama–Brunhes boundary (MBB) was detected in the upper part of Krems Schießstätte, just below KR4, the Kremser Komplex clearly had an Early Pleistocene age (Fink, 1976; Fink and Kukla, 1977). Thermoluminescence ages by Zöllner et al. (1994) supported the main revision of Paudorf and Göttinger. Krems-Schießstätte remained well known for its Early Pleistocene record (Kukla and Čílek, 1996). Noteworthy are works at these type localities in the context of a geological survey in the Weinviertel region (Kovanda et al., 1995).

Recent investigations of still-accessible outcrops in the Krems region started over 15 years ago. Fundamental advances in luminescence dating have allowed for more precise interpretations and correlations for about the last 300 kyr (Terhorst et al., 2011; Thiel et al., 2011a, b, c). Paleo-environmental reconstruction from the polygenetic LPSs of the transition area have focused on the Brunhes record (Sprafke, 2016; Sprafke et al., 2013, 2014). In recent years, the last glacial LPSs have received increasing attention, often related to Upper Paleolithic sites (Groza et al., 2019; Hambach, 2010; Händel et al., 2021; Lomax et al., 2014; Meyer-Heintze et al., 2018; Nigst et al., 2014; Reiss et al., 2022; Sprafke et al., 2020; Terhorst et al., 2015; Zeeden et al., 2015; Zöllner et al., 2014).

2 Krems-Wachtberg: last glacial loess, paleoclimate, and archeology (Stop 1)

The spur between the Krems and Danube rivers in the north of the picturesque city of Krems a.d. Donau is covered by an LPS of up to 37 m thickness, reaching back into the Early Pleistocene, partly exposed at Krems-Schießstätte (Stop 2; Fink, 1976). At the southeast-exposed slope, up to 10 m thick Late Pleistocene loess contains several Upper Paleolithic occupation layers, which have been the subject of excavations for > 100 years (Einwögerer et al., 2009; Neugebauer-Maresch, 2008). From 2005 to 2015, excavations at the site of Krems-Wachtberg (48°24′53.95″ N, 15°35′58.39″ E; no more profiles accessible due to house construction) (Händel et al., 2014) largely focused on archeological horizon (AH) 4, at ~5.5 m depth, dated to ~31.2 ka (Simon et al., 2014), where buried infants were discovered in 2005 (Einwögerer et al., 2006). The adjacent ca. 8 m thick LPS has no major discontinuities and spans a time range from ~20–40 ka (Lomax et al., 2014; Sprafke et al., 2020). Magnetic proxy variations

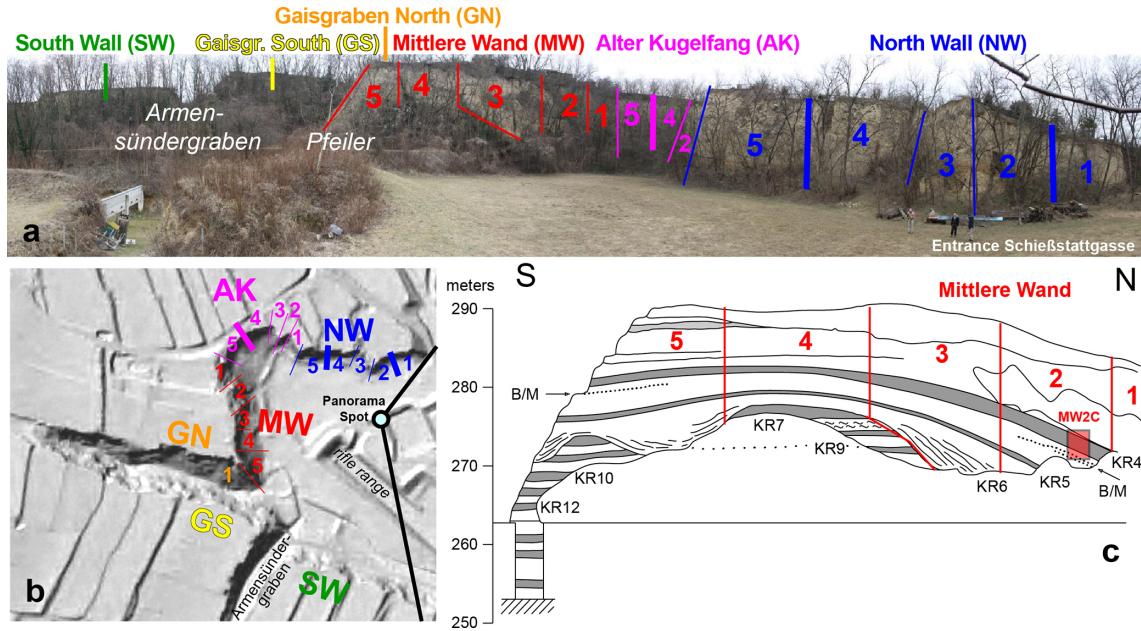


Figure 3. Krems-Schießstätte. (a) Panoramic photo and (b) hillshade with outcrop sectors. (c) Mittlere Wand (Fink, 1979a).

and field stratigraphic units (incipient paleosols, tundra gley soils, reworked units, loess) have been tentatively correlated to the Greenland ice core record (Hambach et al., 2010; Heiri et al., 2014; Terhorst et al., 2014). High-resolution color and grain size analyses and available age information were recently integrated into a unified chronostratigraphic framework, revealing that, contrary to the western central European reference LPS Nussloch, Heinrich events did not result in thick dust accumulation but rather in reworking within a polar desert ecosystem (Sprafke et al., 2020).

3 Krems-Schießstätte: thickest loess of Austria; magnetic reversals (Stop 2)

Krems-Schießstätte (48°25′0.99″ N, 15°35′48.25″ E) is a large outcrop (Fig. 3) that was repeatedly the subject of investigations during the last century. Noteworthy are the joint Czech–Austrian investigations in the late 1960s and early 1970s, taken up in the 1990s (Kovanda et al., 1995). Most work has focused on the Mittlere Wand, where the majority of the paleosols is exposed and the Matuyama–Brunhes boundary (MBB) and older magnetic field reversals were traced (Fink, 1976). The investigations in the late 1960s to 1970s revealed the presence of 16 soil horizons that were labeled from top to bottom in ascending order. KR1 is the recent soil, and KR2 and KR3 are only weakly developed and could not be unambiguously traced in our detailed study of sector GN1. Therefore, KR4 is the only significant pedocomplex above the MBB (Fink and Kukla, 1977). Following these authors, Krems-Schießstätte may complement the Brno Red Hill LPS, which is seen as rather complete record of the

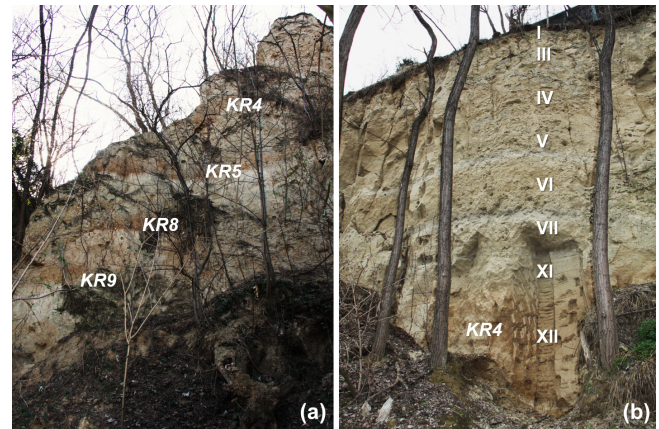


Figure 4. Prominent paleosols in Krems-Schießstätte with KR labels (Fink, 1976; Fink and Kukla, 1977). (a) Sector MW5 with the (invisible) reported MBB between KR4 and KR5, below a major hiatus of KR8 and KR9 (see Fig. 3d). (b) Sector NW2 with the KR4 profile sampled in high resolution and stratigraphic designations by Sprafke (2016).

Brunhes chron (see Sect. 6, Conclusions). A few years later, the Stranzendorf LPS, which is interpreted to reach back to the Pliocene, was used to complement the Red Hill–Krems succession to a whole central European record of glacial–interglacial cycles comparable to the long records of the Chinese Loess Plateau (Kukla and Cílek, 1996). A comprehensive review of these studies is given in Kovanda et al. (1995).

Recent investigations focused on the Brunhes record of Krems-Schießstätte (including KR4), with additional data from KR5 and KR7, both below the MBB. High-resolution

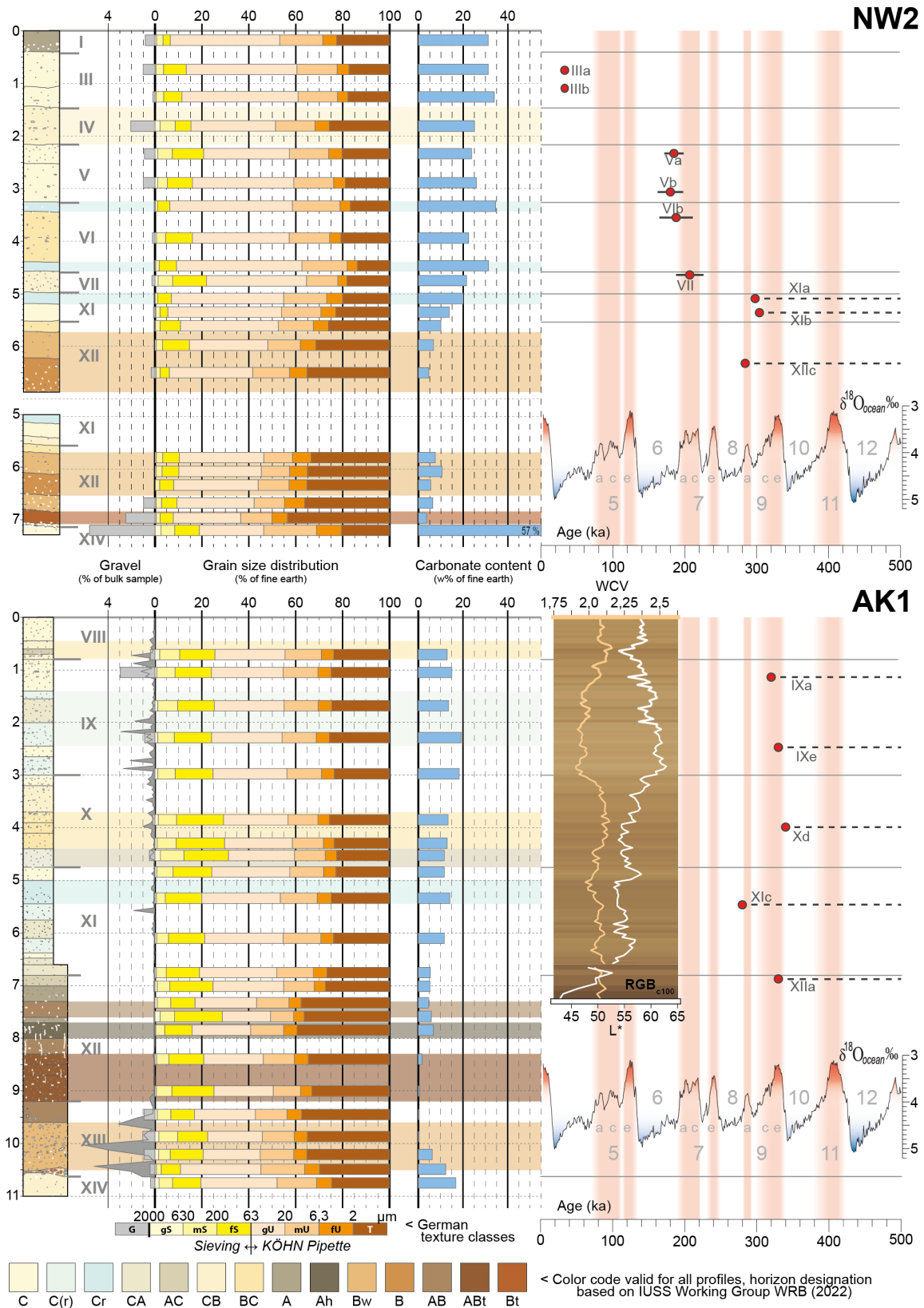


Figure 5. Stratigraphy, granulometry, and carbonate contents of NW2 and AK1; loess colors at AK1 (details in Sect. 3.2); and preliminary luminescence ages against the marine oxygen isotope record (Railsback et al., 2015), adapted from Sprafke (2016).

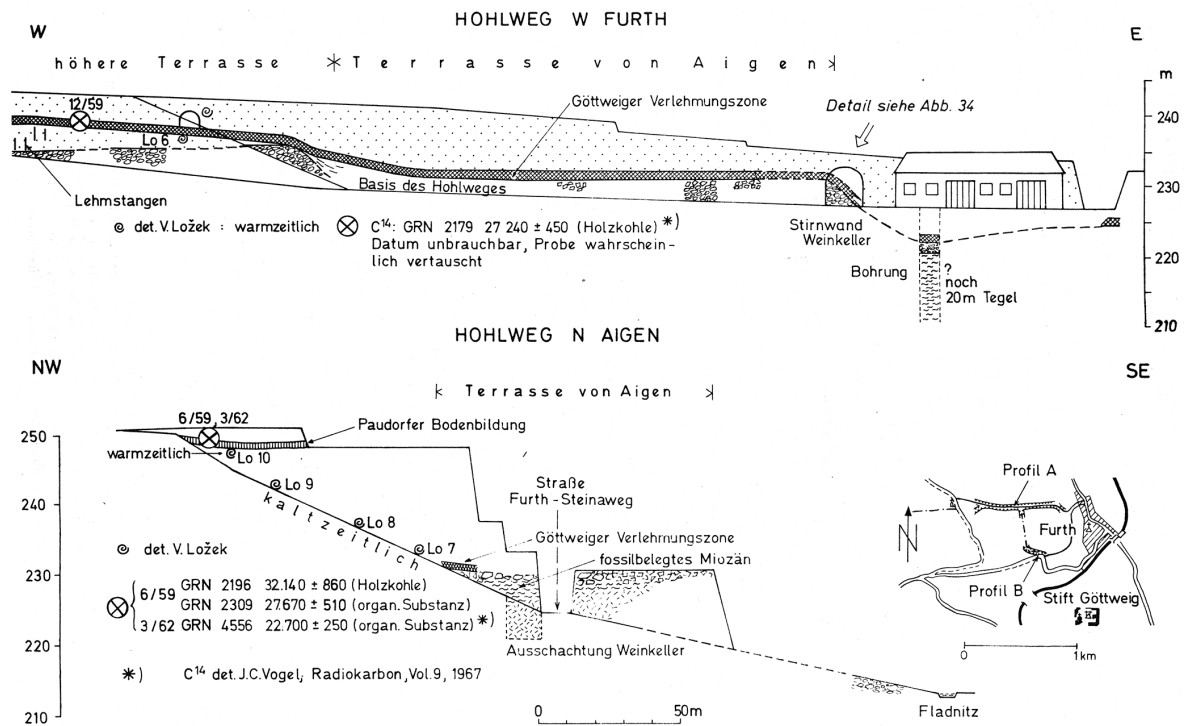


Figure 9. Overview of Göttweig-Furth and Göttweig-Aigen from Fink (1976).

color measurements and mesomorphological studies in representative sections of the wall facilitated the stratigraphic subdivision of the laterally variable outcrop walls. Distinct horizons were investigated in more detail using, e.g., micro-morphology, and for distinct loess packages luminescence ages were determined.

3.1 Sector NW2

Entering the brickyard from the gate at Schießstattgasse, well-differentiated loess sediment above the characteristic KR4 pedocomplex is exposed at the outcrop wall on the right side (Fig. 4). Luminescence ages reveal marked discontinuities in the loess above KR4 (Fig. 5). While the topmost last glacial loess is rather uniform, the penultimate glacial loess consists of brownish loess enriched in coarser material next to pale horizons dominated by silt. The characteristic Unit VI can be traced along the entire outcrop. Below another considerable hiatus KR4 has a rather sharp lower boundary between a Bt and basal Ck horizon. The middle part shows advanced weathering but no signs of clay illuviation. A detailed study of KR4 will be presented in the profile of sector MW2. On the way along the North Wall into the Alter Kugelfang the pedocomplex stays at a comparable altitude, whereas loess between Unit VI and the KR4 pedocomplex strongly increases in thickness.

3.2 Sector AK1

Contrary to the neighboring AK2 and AK3 the profile at AK1 (Fig. 5) does not reach up to Unit VI but through the complete KR4, which is extraordinarily thick here, due to local deposition of soil sediments. Preliminary luminescence data indicate a minimum age of MIS 8 (marine isotope stage) for the succession of partly brownish and bleached loess sediments. The presence of a significant component of coarse material can be interpreted with the polygenetic development in the interplay of eolian sedimentation and in situ and colluvial processes, which is typical of most of the loess sediments of the Krems region. The closely spaced profiles of AK1–3 were compared based on field and sample observations and color data. The latter are measured by a spectrophotometer and allow for a robust subdivision of loess sediments and pedocomplexes. We use the warm–cold value (WCV) as a ratio of warm to cold colors (Sprafke et al. 2013), with L^* indicating luminance, a^* for red (> 0) vs. green (< 0), and b^* for yellow (> 0) vs. blue (< 0); the background shows RGB_{c100} , representing RGB colors with enhanced contrast. A limited profile depth of the outcrop walls below private gardens had an influence on color measurements, rendering a profile correlation based on color data alone challenging for this weakly differentiated material (Sprafke, 2016).

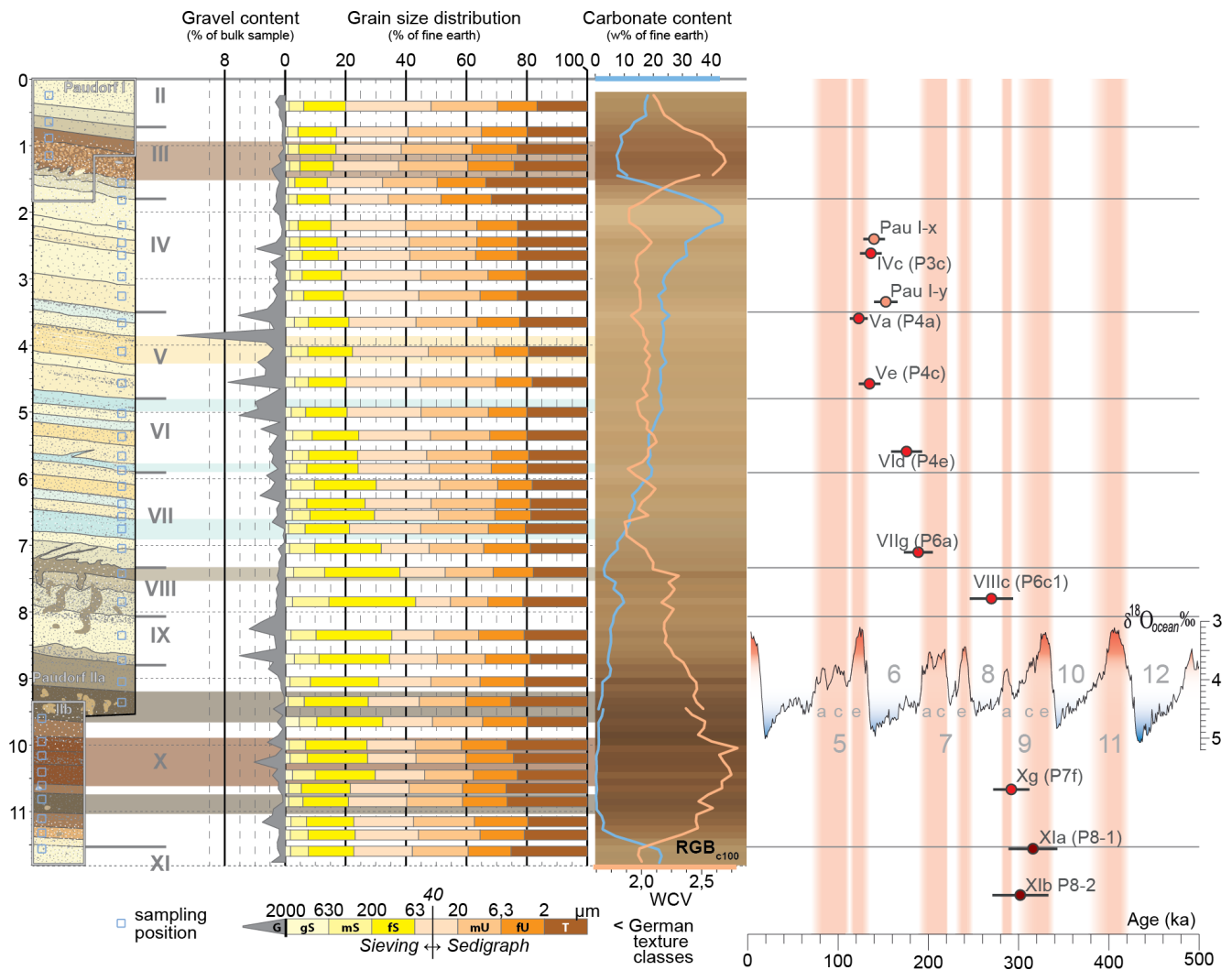


Figure 10. Paudorf LPS (Sprafke, 2016), with grain size, carbonate, and color data from Sprafke et al. (2013). Grain size data from Sprafke et al. (2013). Luminescence ages are shown in the framework of the marine oxygen isotope record (Railsback et al., 2015; Sprafke et al., 2014).

3.3 Sector MW2

The KR4 pedocomplex is best differentiated in MW2, also shown in the standard sequence by Fink (1978). Here, KR4 has a Bt horizon in the bottom and is considerably weathered in the middle part; however, in the upper middle and in the topmost part weathered humic horizons are found. Color data, as presented in the sections before, also support the classification of well-developed soil horizons; oscillations are due to inhomogeneous, aggregated clay-rich material and secondary carbonate (Fig. 6). Semi-quantitative micromorphological analyses of different features following the terminology of Stoops (2003) (Fig. 7) are complemented by the qualitative assessment of feature constellations. Microstructure, primary carbonates, and clay coatings are key to classifying paleosols (Bronger, 2003, 1999) and to reconstructing polygenesis (Sprafke et al., 2014). Phases of pedogenesis

and reworking are linked to paleoenvironmental variations; it is suggested that KR4 formed during up to three glacial interglacial cycles of the early Middle Pleistocene (Fig. 8).

3.4 Sectors MW3–GN1

Sectors MW3–5 provide some insights into the Matuyama record of Krems-Schießstätte Mittlere Wand (Fink, 1976; Fink and Kukla, 1977). At MW3, a strong inclination of paleosols KR4 and KR5 and a colluvium in the basal part are observed. At MW4, the Kremser Komplex (Fink, 1961) is exposed, consisting of KR9, KR8, and KR7, from bottom to top. KR7 is known as Krems soil (Brandtner, 1956) and the most weathered paleosol currently exposed at Krems-Schießstätte; it has a marked petrocalcic horizon at the base. A comparison of the color and micromorphology of KR7, the GVZ, and the basal Bw horizon of the Stillfried complex

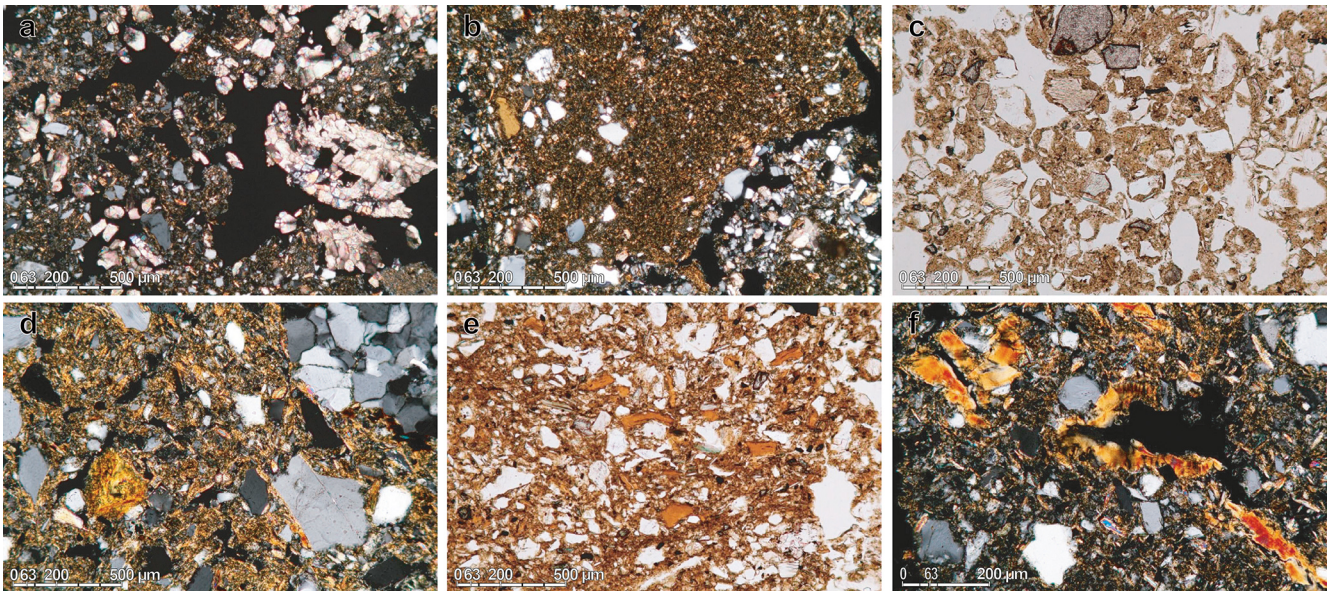


Figure 11. Micromorphology of samples from Paudorf locus typicus. (a) Calcified root cell, partly disturbed by bioturbation (III_d). (b) Bw fragment (III_c). (c) Granular structure (cryo- vs. bioturbation?) (VIII_a). (d) Rolled clay coatings in weathered groundmass (X_d). (e) Fragments of clay coatings (X_{f1}). (f) Clay coatings partly in situ (X_g).

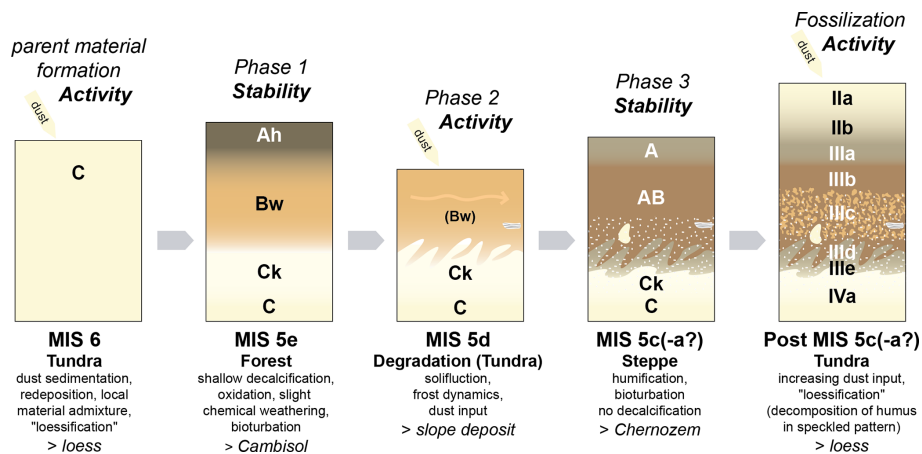


Figure 12. Formation model of the upper pedocomplex (Unit III) at Paudorf during MIS 5, with main processes, tentative chronology in comparison to the MIS 5 pedocomplex at Stillfried, and related paleoenvironments.

(Eemian) indicates overall moderate interglacial weathering intensities in the study area. Finally, at the southern corner of MW5 to GN1 (the Pfeiler), the oldest exposed parts of the whole outcrop are found (Fig. 4).

4 Furth-Zellergraben: Göttweiger Verlehmungszone (Stop 3)

The Göttweiger Verlehmungszone (GVZ; 48°22′30.83″ N, 15°36′13.49″ E) exposed in the Zellergraben near Furth bei Göttweig crosses several terraces and loess sediments (Fig. 9). The GVZ was described over 100 years ago by archeologists, was suggested to represent a warm period of

the Aurignacian (Bayer, 1913), and was later thought to represent an earlier interstadial of the last glacial period (Brandtner, 1956; Gross, 1960, 1956). Fink (1961) established the view that it was the last interglacial paleosol (Fink, 1960, 1956; Göttinger, 1936). The GVZ could not be bracketed by luminescence ages because the sample above already indicates an age older than the possible dating range, i.e., > 350 ka (Thiel et al., 2011b). A formation during MIS 11 and/or older interglacials is likely (Kovanda et al., 1995; Sprafke, 2016). In the upper part of the sequence, a few hundred meters to the south (Aigen), a paleosol comparable to the MIS 5 complex in Paudorf is exposed (Thiel et al., 2011b; Zöllner et al., 1994).

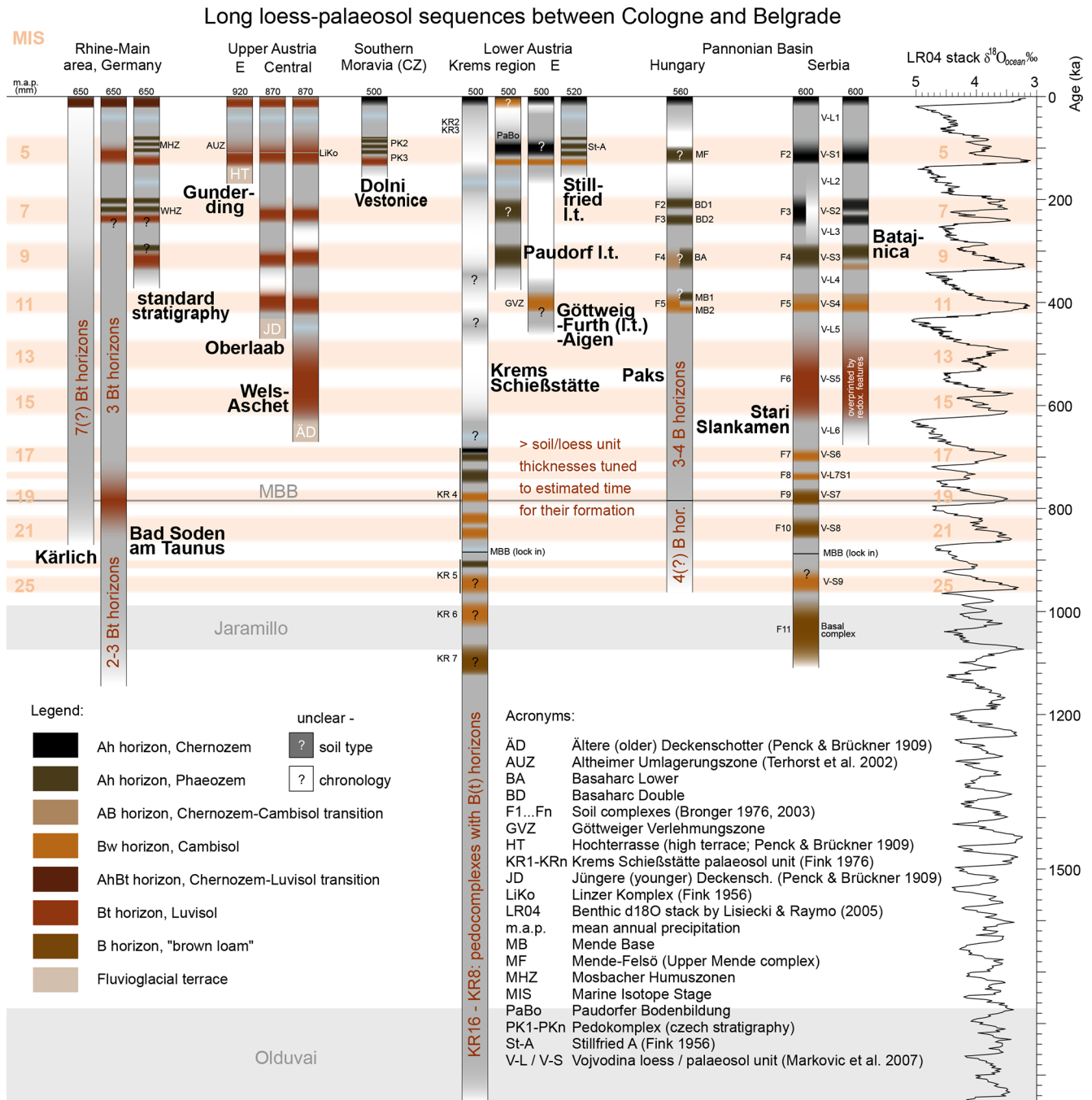


Figure 13. Compilation of paleopedological records in a transect from central to southeastern Europe based on various sources (Antoine et al., 2013; Bibus, 2002; Boenigk and Frechen, 1998; Bronger, 2003; Lisiecki and Raymo, 2005; European Soils Bureau Network, 2005; Marković et al., 2009, 2011; Pécsi and Richter, 1996; Schmidt et al., 2011; Scholger and Terhorst, 2013; Semmel and Fromm, 1976; Terhorst, 2013; Terhorst et al., 2002; Zöllner et al., 1988).

5 Paudorf: polygenetic paleosols and related paleoenvironments (Stop 4)

The loam pit in the northwest of Paudorf (48°21'22.93" N, 15°36'30.00" E), also known as Paudorf locus typicus (Brandtner, 1956; Fink, 1976, 1954, 1965; Göttinger,

1936; Terhorst et al., 2011; Zöllner et al., 1994), is located at ~260 m.a.s.l. at the footslope of the Waxenberg (~500 m.a.s.l.). Two prominent paleosols are visible in the up to 11 m thick LPS (Fig. 10). These were studied in detail by Sprafke et al. (2014); slight modifications in the stratigraphy and pedocomplex evolution by Sprafke (2016) are due

to insights from the Stiefern LPS and Krems-Schießstätte. The penultimate glacial loess of these sites shows interesting similarities, i.e., brownish horizons enriched in coarse material and bleached horizons with dominating silt. Next to eolian deposition and in situ alteration, the influence of slope processes is evident in the evolution of the local loess sediments, provoking questions on the loess definition (Sprafke, 2022; Sprafke and Obrecht, 2016). The complex evolution of enclosed pedocomplexes requires thin-section studies and robust age control (Sprafke et al., 2014) (Figs. 11 and 12).

Based on the semi-quantitative analyses combined with a qualitative investigation, several stages of development were reconstructed for the pedocomplexes. The correlation of different stages for the MIS 5 is based on comparisons with nearby pedocomplexes with similar pedogenic intensities but higher temporal resolution, e.g., the Stillfried complex (Fink, 1954, 1979b; Zöller et al., 1994). For the MIS 9 pedocomplex (not shown), there are no nearby records for comparison; therefore the correlations with the marine isotope substages and reconstructed paleoenvironments are tentative (Sprafke, 2016).

6 Conclusions

The studied Middle to Late Pleistocene LPSs are polygenetic and discontinuous, and age control is limited (luminescence ages to about 300 ka; MBB is ca. 780 ka). However, some general conclusions can be drawn from the presented results if the paleopedological record is considered and combined with the concept of climate-phytomorphic soils (Bronger, 2003, 1976). Absence of significant clay illuviation indicates that during the last 1 Myr interglacial climates in Lower Austria were different than those in western central Europe but more similar to the Pannonian Basin (with minor deviations; Fig. 13). In turn, glacial periods had a central European character, indicated by the presence of tundra gleys. Yet, loess of the last glacial has revealed characteristic differences in landscape response to millennial-scale paleoclimatic fluctuations compared to western central Europe.

Data availability. All data for Sprafke (2016) are available in an open-access manner from the University of Würzburg library repository (<https://doi.org/10.25972/WUP-978-3-95826-039-9>, Sprafke, 2016b).

Author contributions. This work is based on the PhD thesis of TS and was conceptualized and managed by TS (investigation) and BT (supervision, resources) with support from RP and CT. Luminescence data are from CT. TS wrote the text and created the visualizations; all co-authors reviewed and edited the paper.

Competing interests. The contact author has declared that none of the authors has any competing interests.

Disclaimer. Publisher's note: Copernicus Publications remains neutral with regard to jurisdictional claims made in the text, published maps, institutional affiliations, or any other geographical representation in this paper. While Copernicus Publications makes every effort to include appropriate place names, the final responsibility lies with the authors.

Acknowledgements. We thank the Schützenverein Krems 1440 for granting access to the Krems-Schießstätte outcrop. Many thanks go to Simon Meyer-Heintze, Sergey Sedov, and the Österreichische Akademie der Wissenschaften (ÖAW) archeologists for close collaboration and to the many students who worked with us in Krems and surroundings. For detailed acknowledgements, please refer to Sprafke (2016).

Financial support. This open-access publication was funded by the Bern University of Applied Sciences.

References

- Antoine, P., Rousseau, D. D., Moine, O., Kunesch, S., Hatté, C., Lang, A., Tissoux, H., and Zöller, L.: Rapid and cyclic aeolian deposition during the Last Glacial in European loess: a high-resolution record from Nussloch, Germany, *Quaternary Sci. Rev.*, 28, 2955–2973, 2009.
- Antoine, P., Rousseau, D. D., Degeai, J. P., Moine, O., Lagroix, F., Kreutzer, S., Fuchs, M., Hatté, C., Gauthier, C., Svoboda, J., and Lisá, L.: High-resolution record of the environmental response to climatic variations during the Last Interglacial-Glacial cycle in Central Europe: the loess-palaeosol sequence of Dolní Věstonice (Czech Republic), *Quaternary Sci. Rev.*, 67, 17–38, 2013.
- Bayer, J.: Jüngster Löß und paläolithische Kultur in Mitteleuropa, *Jahrbuch für Altertumskunde*, III, 149–160, 1909.
- Bayer, J.: Die Gliederung des Diluviums in Europa, *Mitteilungen der Geologischen Gesellschaft*, 6, 188–196, 1913.
- Bibus, E.: Zum Quartär im mittleren Neckarraum – Reliefentwicklung, Löß/Paläobodensequenzen, Paläoklima, *Tübinger Geowissenschaftliche Arbeiten*, D8, 236 pp., ISBN 3-88121-055-5, 2002.
- Boenigk, W. and Frechen, M.: Zur Geologie der Deckschichten von Kärlich/Mittelrhein, *E&G Quaternary Sci. J.*, 48, 38–49, <https://doi.org/10.3285/eg.48.1.04>, 1998.
- Brandtner, F.: Lößstratigraphie und paläolithische Kulturabfolge in Niederösterreich und den angrenzenden Gebieten (Zugleich ein Beitrag zur Frage der Würmgliederung), *E&G Quaternary Sci. J.*, 7, 127–175, <https://doi.org/10.3285/eg.07.1.13>, 1956.
- Bronger, A.: Zur quartären Klima- und Landschaftsentwicklung des Karpatenbeckens auf (paläo-)pedologischer und bodengeographischer Grundlage, *Kieler Geographische Schriften* 45, Geographisches Institut, Universität Kiel, Kiel, 1976.
- Bronger, A.: Löß-Paläoboden-Sequenzen Zentralasiens als Indikatoren einer globalen Kimageschichte des Quartärs?, *E&G Qua-*

- ternary Sci. J., 49, 35–54, <https://doi.org/10.3285/eg.49.1.03>, 1999.
- Bronger, A.: Correlation of loess-paleosol sequences in East and Central Asia with SE Central Europe: towards a continental Quaternary pedostratigraphy and paleoclimatic history, *Quatern. Int.*, 106, 11–31, 2003.
- Einwögerer, T., Friesinger, H., Händel, M., Neugebauer-Maresch, C., Simon, U., and Teschler-Nicola, M.: Upper Palaeolithic infant burials, *Nature*, 444, 285–285, 2006.
- Einwögerer, T., Händel, M., Neugebauer-Maresch, C., Simon, U., Steier, P., Teschler-Nicola, M., and Wild, E. M.: ^{14}C Dating of the Upper Paleolithic Site at Krems-Wachtberg, Austria, *Radio-carbon*, 51, 847–855, 2009.
- Emiliani, C.: Pleistocene temperatures, *J. Geol.*, 63, 538–578, 1955.
- European Soils Bureau Network: Soil Atlas of Europe, European Commission, Office for Official Publications of the European Communities, Luxembourg, 128 pp., ISBN 92-894-8120-X, 2005.
- Fink, J.: Die fossilen Böden im österreichischen Löß, *Quartär*, 6, 85–108, 1954.
- Fink, J.: Zur Korrelation der Terrassen und Lössen in Österreich, *E&G Quaternary Sci. J.*, 7, 49–77, <https://doi.org/10.3285/eg.07.1.07>, 1956.
- Fink, J.: Die Bodentypen Niederösterreichs 1 : 500.000, in: Atlas von Niederösterreich, Freytag-Berndt & Artaria, Wien, 1958.
- Fink, J.: Leitlinien einer österreichischen Quartärstratigraphie, *Mitteilungen der Geologischen Gesellschaft in Wien*, 53, 249–266, 1960.
- Fink, J.: Die Gliederung des Jungpleistozäns in Oesterreich, *Mitteilungen der Geologischen Gesellschaft in Wien*, 54, 1–25, 1961.
- Fink, J.: The Pleistocene in Eastern Austria, *Geol. S. Am. S.*, 84, 179–199, 1965.
- Fink, J. (Ed.): Le loess en Autriche, in: La Stratigraphie des Loess d'Europe, Supplement au Bulletin de l'AFEQ, N. S., CNRS, Paris, 1969.
- Fink, J.: Exkursion durch den österreichischen Teil des nördlichen Alpenvorlandes und den Donauraum zwischen Krems und der Wiener Pforte, ÖAW, Wien, 1976.
- Fink, J.: Exkursion durch den österreichischen Teil des nördlichen Alpenvorlandes und den Donauraum zwischen Krems und der Wiener Pforte, ÖAW, Wien, 1978.
- Fink, J.: Paleomagnetic research in the northeastern foothills of the Alps and in the Vienna Basin, in: Studies on Loess, edited by: Pécsi, M., Acta Geologica Academiae Scientiarum Hungaricae, 22, Budapest, ISSN 0001-5695, 1979a.
- Fink, J.: Stand und Aufgaben der österreichischen Quartärforschung, *Innsbrucker Geographische Studien*, 5, 79–104, 1979b.
- Fink, J. and Kukla, G. J.: Pleistocene climates in central Europe; at least 17 interglacials after the Olduvai Event, *Quaternary Res.*, 7, 363–371, 1977.
- Fink, J. and Nagl, H.: Quartäre Sedimente und Formen (1 : 1 000 000), in: Österreich Atlas, Freytag-Berndt & Artaria, Wien, 1979.
- Fink, J., Walder, R., and Rerych, W.: Böden und Standortsbewertung 1 : 750 000 (1 Blatt + 1 Legende), in: Österreich Atlas, Freytag-Berndt & Artaria, Wien, 1979.
- Götzinger, G. (Ed.): Das Lößgebiet um Göttweig und Krems an der Donau, in: Führer für die Quartär-Exkursionen in Österreich, Geologische Bundesanstalt, Wien, 1936.
- Gross, H.: Das Göttweiger Interstadial, ein zweiter Leithorizont der letzten Vereisung, *E&G Quaternary Sci. J.*, 7, 87–101, <https://doi.org/10.3285/eg.07.1.09>, 1956.
- Gross, H.: Die Bedeutung des Göttweiger Interstadials im Ablauf der Würm-Eiszeit, *E&G Quaternary Sci. J.*, 11, 99–106, <https://doi.org/10.3285/eg.11.1.11>, 1960.
- Groza, S. M., Hambach, U., Veres, D., Vulpoi, A., Händel, M., Einwögerer, T., Simon, U., Neugebauer-Maresch, C., and Timar-Gabor, A.: Optically stimulated luminescence ages for the Upper Palaeolithic site Krems-Wachtberg, Austria, *Quat. Geochronol.*, 49, 242–248, 2019.
- Hambach, U.: Palaeoclimatic and stratigraphic implications of high resolution magnetic susceptibility logging of Würmian loess at the Krems-Wachtberg Upper-Palaeolithic site, in: New Aspects of the Central and Eastern European Upper Palaeolithic – methods, chronology, technology and subsistence, edited by: Neugebauer-Maresch, C. and Owen, L. R., *Mitteilungen der Prähistorischen Kommission*, 72, Österreichische Akademie der Wissenschaften, Wien, <https://doi.org/10.1553/0x0022e03c>, 2010.
- Hambach, U., Marković, S. B., and Zöller, L.: A continuous record of Pleistocene palaeoclimate; the loess sequences of the Vojvodina, north Serbia, *Schriftenreihe der Deutschen Gesellschaft fuer Geowissenschaften*, 68, 222–223, 2010.
- Händel, M., Einwögerer, T., Simon, U., and Neugebauer-Maresch, C.: Krems-Wachtberg excavations 2005–12: Main profiles, sampling, stratigraphy, and site formation, *Quatern. Int.*, 351, 38–49, 2014.
- Händel, M., Thomas, R., Sprafke, T., Schulte, P., Brandl, M., Simon, U., and Einwögerer, T.: Using archaeological data and sediment parameters to review the formation of the Gravettian layers at Krems-Wachtberg, *J. Quaternary Sci.*, 36, 1397–1413, 2021.
- Heiri, O., Koinig, K. A., Spötl, C., Barrett, S., Brauer, A., Drescher-Schneider, R., Gaar, D., Ivy-Ochs, S., Kerschner, H., Luetscher, M., Moran, A., Nicolussi, K., Preusser, F., Schmidt, R., Schoenich, P., Schwörer, C., Sprafke, T., Terhorst, B., and Tinner, W.: Palaeoclimate records 60–8 ka in the Austrian and Swiss Alps and their forelands, *Quaternary Sci. Rev.*, 106, 186–205, 2014.
- IUSS Working Group WRB: World Reference Base for Soil Resources, International soil classification system for naming soils and creating legends for soil maps, 4th edn., International Union of Soil Sciences (IUSS), Vienna, Austria, ISBN 979-8-9862451-1-9, 2022.
- Kovanda, J., Smolíková, L., and Horáček, I.: New data on four classic loess sequences in Lower Austria, *Sborník Geologických Věd. Antropozoikum*, 22, 63–85, 1995.
- Kukla, G. J. and Cílek, V.: Plio-pleistocene megacycles: Record of climate and tectonics, *Palaeogeogr. Palaeoclimatol.*, 120, 171–194, 1996.
- Lehmkuhl, F., Zens, J., Krauss, L., Schulte, P., and Kels, H.: Loess-paleosol sequences at the northern European loess belt in Germany: Distribution, geomorphology and stratigraphy, *Quaternary Sci. Rev.*, 153, 11–30, 2016.
- Lehmkuhl, F., Nett, J. J., Pötter, S., Schulte, P., Sprafke, T., Jary, Z., Antoine, P., Wacha, L., Wolf, D., Zerboni, A., Hošek, J., Marković, S. B., Obrecht, I., Sümegi, P., Veres, D., Zeeden,

- C., Boemke, B. J., Schaubert, V., Viehweger, J., and Hambach, U.: Loess landscapes of Europe – Mapping, geomorphology, and zonal differentiation, *Earth-Sci. Rev.*, 215, 103496, <https://doi.org/10.1016/j.earscirev.2020.103496>, 2021.
- Lisiecki, L. E. and Raymo, M. E.: A Pliocene-Pleistocene stack of 57 globally distributed benthic $\delta^{18}\text{O}$ records, *Paleoceanography*, 20, PA1003, <https://doi.org/10.1029/2004PA001071>, 2005.
- Loishandl, H. and Peticzka, R.: Vom Winde verweht. Die Sedimente und Böden im Verbreitungsgebiet der niederösterreichischen Kreisgrabenanlagen, in: *Geheimnisvolle Kreisgräben*, edited by: Daim, F. and Neubauer, W., Verlag Berger, Wien, ISSN 0506-919X, 2005.
- Lomax, J., Fuchs, M., Preusser, F., and Fiebig, M.: Luminescence based loess chronostratigraphy of the Upper Palaeolithic site Krems-Wachtberg, Austria, *Quatern. Int.*, 351, 88–97, 2014.
- Marković, S. B., Bokhorst, M. P., Vandenberghe, J., McCoy, W. D., Oches, E. A., Hambach, U., Gaudenyi, T., Jovanović, M., Zöller, L., Stevens, T. and Machalett, B.: Late Pleistocene loess-palaeosol sequences in the Vojvodina region, north Serbia, *J. Quaternary Sci.*, 23, 73–84, 2007.
- Marković, S. B., Hambach, U., Catto, N., Jovanović, M., Buggle, B., Machalett, B., Zöller, L., Glaser, B., and Frechen, M.: Middle and Late Pleistocene loess sequences at Batajnica, Vojvodina, Serbia, *Quatern. Int.*, 198, 255–266, 2009.
- Marković, S. B., Hambach, U., Stevens, T., Kukla, G. J., Heller, F., McCoy, W. D., Oches, E. A., Buggle, B., and Zöller, L.: The last million years recorded at the Stari Slankamen (Northern Serbia) loess-palaeosol sequence: revised chronostratigraphy and long-term environmental trends, *Quaternary Sci. Rev.*, 30, 1142–1154, 2011.
- Matura, A.: Böhmisches Masse, in: *Niederösterreich*, edited by: Wessely, G., Geologie der Österreichischen Bundesländer, ISBN 3-85316-23-9, 2006.
- Meyer-Heintze, S., Sprafke, T., Schulte, P., Terhorst, B., Lomax, J., Fuchs, M., Lehmkuhl, F., Neugebauer-Maresch, C., Einwögerer, T., Händel, M., Simon, U., and Solís Castillo, B.: The MIS 3/2 transition in a new loess profile at Krems-Wachtberg East – A multi-methodological approach, *Quatern. Int.*, 464, 370–385, 2018.
- Nagl, H.: Klima- und Wasserbilanztypen Österreichs – Versuch einer regionalen Gliederung mit besonderer Berücksichtigung des außeralpinen Raumes, *Geographischer Jahresbericht aus Österreich*, 40, 50–72, 1983.
- Neugebauer-Maresch, C.: Zur altsteinzeitlichen Besiedlungsgeschichte des Galgenberges von Stratzing/Krems-Rehberg, *Archäologie Österreichs*, 4, 10–19, 1993.
- Neugebauer-Maresch, C. (Ed.): *Krems-Hundssteig – Mammutjägerlager der Eiszeit. Ein Nutzungsareal paläolithischer Jäger- und Sammler(innen) vor 41.000–27.000 Jahren*, ÖAW, Wien, <https://doi.org/10.1553/0x0018c38e>, 2008.
- Nigst, P. R., Haesaerts, P., Dambon, F., Frank-Fellner, C., Malloy, C., Viola, B., Götzinger, M., Niven, L., and Hublin, J. J.: Early modern human settlement of Europe north of the Alps occurred 43 500 years ago in a cold steppe-type environment, *P. Natl. Acad. Sci. USA*, 111, 14394–14399, 2014.
- Pécsi, M. and Richter, G.: *Löss: Herkunft – Gliederung – Landschaften*, Bornträger, Berlin & Stuttgart, ISBN 978-3-443-21098-4, 1996.
- Penck, A. and Brückner, E.: *Die Eiszeiten in den nördlichen Ostalpen*, *Die Alpen im Eiszeitalter Band 1*, Tauchnitz, Leipzig, 393 pp., 1909.
- Petschko, H., Sprafke, T., Peticzka, R., and Wiesbauer, H.: *Sunken Roads and Palaeosols in Loess Areas in Lower Austria: Landform Development and Cultural Importance*, in: *Landscapes and Landforms of Austria*, edited by: Embleton-Hamann, C., Springer International Publishing, Cham, https://doi.org/10.1007/978-3-030-92815-5_11, 2022.
- Railsback, L. B., Gibbard, P. L., Head, M. J., Voarintsoa, N. R. G., and Toucanne, S.: An optimized scheme of lettered marine isotope substages for the last 1.0 million years, and the climatostratigraphic nature of isotope stages and substages, *Quaternary Sci. Rev.*, 111, 94–106, 2015.
- Reiss, L., Stüwe, C., Einwögerer, T., Händel, M., Maier, A., Meng, S., Pasda, K., Simon, U., Zolitschka, B., and Mayr, C.: Evaluation of geochemical proxies and radiocarbon data from a loess record of the Upper Palaeolithic site Kammern-Grubgraben, Lower Austria, *E&G Quaternary Sci. J.*, 71, 23–43, <https://doi.org/10.5194/egqsj-71-23-2022>, 2022.
- Riedl, D., Roetzel, R., Pöpl, R. E., and Sprafke, T.: *Wachau World Heritage Site: A Diverse Riverine Landscape*, in: *Landscapes and Landforms of Austria*, edited by: Embleton-Hamann, C., Springer International Publishing, Cham, https://doi.org/10.1007/978-3-030-92815-5_10, 2022.
- Rohdenburg, H.: Morphodynamische Aktivitäts- und Stabilitätszeiten statt Pluvial- und Interpluvialzeiten, *E&G Quaternary Sci. J.*, 21, 81–96, <https://doi.org/10.3285/eg.21.1.07>, 1970.
- Schmidt, E. D., Semmel, A., and Frechen, M.: Luminescence dating of the loess/palaeosol sequence at the gravel quarry Gaul/Weilbach, Southern Hesse (Germany), *E&G Quaternary Sci. J.*, 60, 9, <https://doi.org/10.3285/eg.60.1.08>, 2011.
- Scholger, R. and Terhorst, B.: Magnetic excursions recorded in the Middle to Upper Pleistocene loess/palaeosol sequence Wels-Aschet (Austria), *E&G Quaternary Sci. J.*, 62, 14–21, <https://doi.org/10.3285/eg.62.1.02>, 2013.
- Semmel, A. and Fromm, K.: Ergebnisse paläomagnetischer Untersuchungen an quartären Sedimenten des Rhein-Main-Gebiets, *E&G Quaternary Sci. J.*, 27, 18–25, <https://doi.org/10.3285/eg.27.1.02>, 1976.
- Shackleton, N. J. and Opdyke, N. D.: Oxygen isotope and paleomagnetic stratigraphy of equatorial Pacific core V28-238: oxygen isotope temperature and ice volumes on a 10^5 year to 10^6 year scale, *Quaternary Res.*, 3, 39–55, [https://doi.org/10.1016/0033-5894\(73\)90052-5](https://doi.org/10.1016/0033-5894(73)90052-5), 1973.
- Simon, U., Händel, M., Einwögerer, T., and Neugebauer-Maresch, C.: The archaeological record of the Gravettian open air site Krems-Wachtberg, *Quatern. Int.*, 351, 5–13, 2014.
- Sprafke, T.: *Löss in Niederösterreich – Archiv quartärer Klima- und Landschaftsveränderungen*, Würzburg University Press, Würzburg, https://opus.bibliothek.uni-wuerzburg.de/files/12778/978-3-95826-039-9_Sprafke_Tobias_OPUS_12778.pdf (last access: 6 July 2024), 2016a.
- Sprafke, T.: *Löss in Niederösterreich – Archiv quartärer Klima- und Landschaftsveränderungen*, *Sprafke_Tobias_OPUS_12778_Anhang*, Excel file, Würzburg University Press, Würzburg [data set], <https://doi.org/10.25972/WUP-978-3-95826-039-9>, 2016b.

- Sprafke, T.: A tribute to Fink (1956): On the correlation of terraces and loesses in Austria, *E&G Quaternary Sci. J.*, 70, 221–224, <https://doi.org/10.5194/egqsj-70-221-2021>, 2021.
- Sprafke, T.: Parent materials: Loess., in: *Encyclopedia of Soils in the Environment*, 2nd edn., edited by: Goss, M. J. and Oliver, M., Academic Press, Oxford, <https://doi.org/10.1016/B978-0-12-822974-3.00016-1>, 2022.
- Sprafke, T. and Obrecht, I.: Loess: Rock, sediment or soil – What is missing for its definition?, *Quatern. Int.*, 399, 198–207, 2016.
- Sprafke, T., Terhorst, B., Peticzka, R., and Thiel, C.: Paudorf locus typicus (Lower Austria) revisited: The potential of the classic loess outcrop for Middle to Late Pleistocene landscape reconstructions, *E&G Quaternary Sci. J.*, 62, 59–72, <https://doi.org/10.3285/eg.62.1.06>, 2013.
- Sprafke, T., Thiel, C., and Terhorst, B.: From micromorphology to palaeoenvironment: The MIS 10 to MIS 5 record in Paudorf (Lower Austria), *Catena*, 117, 60–72, 2014.
- Sprafke, T., Schulte, P., Meyer-Heintze, S., Händel, M., Einwögerer, T., Simon, U., Peticzka, R., Schäfer, C., Lehmkuhl, F., and Terhorst, B.: Palaeoenvironments from robust loess stratigraphy using high-resolution color and grain-size data of the last glacial Krems-Wachtberg record (NE Austria), *Quaternary Sci. Rev.*, 248, 106602, <https://doi.org/10.1016/j.quascirev.2020.106602>, 2020.
- Stoops, G.: *Guidelines for analysis and description of soil and regolith thin sections*, Soil Science Society of America, Madison, Wisconsin, ISBN 0891188428, 2003.
- Terhorst, B.: A stratigraphic concept for Middle Pleistocene Quaternary sequences in Upper Austria, *E&G Quaternary Sci. J.*, 62, 4–13, <https://doi.org/10.3285/eg.62.1.01>, 2013.
- Terhorst, B., Frechen, M., and Reitner, J.: Chronostratigraphische Ergebnisse aus Lößprofilen der Inn- und Traun-Hochterrassen in Oberösterreich, *Z. Geomorphol., Supplementband*, 127, 213–232, 2002.
- Terhorst, B., Thiel, C., Peticzka, R., Sprafke, T., Frechen, M., Fladerer, F. A., Roetzel, R., and Neugebauer-Maresch, C.: Casting new light on the chronology of the loess/paleosol sequences in Lower Austria, *E&G Quaternary Sci. J.*, 60, 19, <https://doi.org/10.3285/eg.60.2-3.04>, 2011.
- Terhorst, B., Kühn, P., Damm, B., Hambach, U., Meyer-Heintze, S., and Sedov, S.: Palaeoenvironmental fluctuations as recorded in the loess-paleosol sequence of the Upper Paleolithic site Krems-Wachtberg, *Quatern. Int.*, 351, 67–82, 2014.
- Terhorst, B., Sedov, S., Sprafke, T., Peticzka, R., Meyer-Heintze, S., Kühn, P., and Solleiro Rebollo, E.: Austrian MIS 3/2 loess-paleosol records – Key sites along a west–east transect, *Palaeogeogr. Palaeoclimatol.*, 418, 43–56, 2015.
- Thiel, C., Buylaert, J. P., Murray, A. S., Terhorst, B., Hofer, I., Tsukamoto, S., and Frechen, M.: Luminescence dating of the Stratzing loess profile (Austria) – Testing the potential of an elevated temperature post-IR IRSL protocol, *Quatern. Int.*, 234, 23–31, 2011a.
- Thiel, C., Buylaert, J.-P., Murray, A. S., Terhorst, B., Tsukamoto, S., Frechen, M., and Sprafke, T.: Investigating the chronostratigraphy of prominent palaeosols in Lower Austria using post-IR IRSL dating, *E&G Quaternary Sci. J.*, 60, 11, <https://doi.org/10.3285/eg.60.1.10>, 2011b.
- Thiel, C., Terhorst, B., Jaburova, I., Buylaert, J. P., Murray, A. S., Fladerer, F. A., Damm, B., Frechen, M., and Ottner, F.: Sedimentation and erosion processes in Middle to Late Pleistocene sequences exposed in the brickyard of Langenlois/Lower Austria, *Geomorphology*, 135, 295–307, 2011c.
- Újvári, G., Kok, J. F., Varga, G., and Kovács, J.: The physics of wind-blown loess: Implications for grain size proxy interpretations in Quaternary paleoclimate studies, *Earth-Sci. Rev.*, 154, 247–278, 2016.
- USGS (United States Geological Survey): Shuttle Radar Topography Mission, 1 Arc Second Non Void Filled (~30 m resolution), United States Geological Survey, <http://earthexplorer.usgs.gov/> (last access: 6 July 2024), 2014.
- Wessely, G. and Draxler, I.: *Pliozän und Quartär*, in: *Niederösterreich*, edited by: Wessely, G., *Geologie der Österreichischen Bundesländer*, ISBN 3-85316-23-9, 2006.
- Zeeden, C., Hambach, U., and Händel, M.: Loess magnetic fabric of the Krems-Wachtberg archaeological site, *Quatern. Int.*, 372, 188–194, 2015.
- Zöller, L., Stremme, H. E., and Wagner, G. A.: Thermolumineszenz-Datierung an Löß-Paläoboden-Sequenzen von Nieder-, Mittel- und Oberrhein, *Chem. Geol.*, 73, 39–62, 1988.
- Zöller, L., Oches, E. A., and McCoy, W. D.: Towards a revised chronostratigraphy of loess in Austria with respect to key sections in the Czech Republic and in Hungary, *Quaternary Sci. Rev.*, 13, 465–472, [https://doi.org/10.1016/0277-3791\(94\)90059-0](https://doi.org/10.1016/0277-3791(94)90059-0), 1994.
- Zöller, L., Richter, D., Blanchard, H., Einwögerer, T., Händel, M., and Neugebauer-Maresch, C.: Our oldest children: Age constraints for the Krems-Wachtberg site obtained from various thermoluminescence dating approaches, *Quatern. Int.*, 351, 83–87, 2014.

B. Salcher

Preface: Quaternary landscape dynamics in the Eastern Alps, from the highest peaks to the North Alpine Foreland – a guidebook to field trips
1

**I. Hartmeyer and
J.-C. Otto**

Rockfall, glacier recession, and permafrost degradation: long-term monitoring of climate change impacts at the Open-Air-Lab Kitzsteinhorn, Hohe Tauern
3

**J. M. Reitner and
M. Steinbichler**

Glaciers and mass movements in the Hüttwinkl Valley (Hohe Tauern range): from the Last Glacial Maximum [LGM] until now
13

B. Salcher et al.

Sediment dynamics of a major piedmont glacier: the Salzach Glacier in the North Alpine Foreland
31

T. Sprafke et al.

Brunhes to burials – loess region of Krems, Lower Austria
41